

**ATTACHMENT 3**  
**U.S. Department of Energy**  
**FEDERAL ASSISTANCE REPORTING CHECKLIST**  
**AND INSTRUCTIONS**

1. Identification Number: <b>DE-FE0002056</b>	2. Program/Project Title: <b>Modeling CO2 Sequestration in Saline Aquifer and Depleted Oil Reservoir to Evaluate Regional CO2 Sequestration Potential of Ozark Plateau Aquifer System, South-Central Kansas</b>														
3. Recipient: University of Kansas Center for Research															
4. Reporting Requirements:  <b>A. MANAGEMENT REPORTING</b> <input checked="" type="checkbox"/> Progress Report <input checked="" type="checkbox"/> Special Status Report  <b>B. SCIENTIFIC/TECHNICAL REPORTING *</b> (Reports/Products must be submitted with appropriate DOE F 241. The 241 forms are available at <a href="https://www.osti.gov/clink">https://www.osti.gov/clink</a> )  <table style="width: 100%; border-collapse: collapse;"> <thead> <tr> <th style="text-align: left; border-bottom: 1px solid black;">Report/Product</th> <th style="text-align: left; border-bottom: 1px solid black;">Form</th> </tr> </thead> <tbody> <tr> <td><input checked="" type="checkbox"/> Final Scientific/Technical Report</td> <td>DOE F 241.3</td> </tr> <tr> <td><input checked="" type="checkbox"/> Conference papers/proceedings/etc.*</td> <td>DOE F 241.3</td> </tr> <tr> <td><input type="checkbox"/> Software/Manual</td> <td>DOE F 241.4</td> </tr> <tr> <td><input checked="" type="checkbox"/> Other (see special instructions)</td> <td></td> </tr> <tr> <td style="padding-left: 20px;">Topical</td> <td>DOE F 241.3</td> </tr> </tbody> </table> <p><i>* Scientific/technical conferences only</i></p> <b>C. FINANCIAL REPORTING</b> <input checked="" type="checkbox"/> SF-425, Federal Financial Report  <b>D. CLOSEOUT REPORTING</b> <input type="checkbox"/> Patent Certification <input type="checkbox"/> Property Certificate <input type="checkbox"/> Other  <b>E. OTHER REPORTING</b> <input checked="" type="checkbox"/> Annual Indirect Cost Proposal <input checked="" type="checkbox"/> Annual Inventory Report of Federally Owned Property, if any <input type="checkbox"/> Other  <b>F. AMERICAN RECOVERY AND REINVESTMENT ACT REPORTING</b> <input type="checkbox"/> Reporting and Registration Requirements	Report/Product	Form	<input checked="" type="checkbox"/> Final Scientific/Technical Report	DOE F 241.3	<input checked="" type="checkbox"/> Conference papers/proceedings/etc.*	DOE F 241.3	<input type="checkbox"/> Software/Manual	DOE F 241.4	<input checked="" type="checkbox"/> Other (see special instructions)		Topical	DOE F 241.3	Frequency	No. of Copies	Addresses
Report/Product	Form														
<input checked="" type="checkbox"/> Final Scientific/Technical Report	DOE F 241.3														
<input checked="" type="checkbox"/> Conference papers/proceedings/etc.*	DOE F 241.3														
<input type="checkbox"/> Software/Manual	DOE F 241.4														
<input checked="" type="checkbox"/> Other (see special instructions)															
Topical	DOE F 241.3														
<b>FREQUENCY CODES AND DUE DATES:</b> A - As required; see attached text for applicability. FG - Final; within ninety (90) calendar days after the project period ends. FC - Final - End of Effort. Q - Quarterly; within thirty (30) calendar days after end of the calendar quarter or portion thereof. S - Semiannually; within thirty (30) calendar days after end of project year and project half-year. YF - Yearly; 90 calendar days after the end of project year. YP - Yearly Property - due 15 days after period ending 9/30.															

## **QUARTERLY PROGRESS REPORT**

**Award Number: DE-FE0002056**

**Recipient: University of Kansas Center for Research &  
Kansas Geological Survey  
1930 Constant Avenue  
Lawrence, KS 66047**

**“Modeling CO<sub>2</sub> Sequestration in Saline Aquifer and Depleted Oil Reservoir  
To Evaluate Regional CO<sub>2</sub> Sequestration Potential of Ozark Plateau Aquifer System,  
South-Central Kansas”**

**Project Director/Principal Investigator: W. Lynn Watney**

**Principal Investigator: Jason Rush**

**Eighteenth Quarter Progress Report**

**Date of Report: 5-8-14**

**Period Covered by the Report: January 1, 2014 to March 31, 2014**

**Contributors to this Report: Brent Campbell, Saugata Datta, John Doveton,  
Mina Fazelalavi, Yousuf Fadolalkarem, David Fowle, Dennis Hedke, Eugene Holubnayak,  
Christa Jackson, Jennifer Raney, Clyde Redger, Jennifer Roberts, Jason Rush,  
George Tsoflias Michael Vega, John Victorine, Lynn Watney**

## EXECUTIVE SUMMARY

The project “Modeling CO<sub>2</sub> Sequestration in Saline Aquifer and Depleted Oil Reservoir to Evaluate Regional CO<sub>2</sub> Sequestration Potential of Ozark Plateau Aquifer System, South-Central Kansas” is focused on the Paleozoic-age Ozark Plateau Aquifer System (OPAS) in southern Kansas. OPAS is comprised of the thick and deeply buried Arbuckle Group saline aquifer and the overlying Mississippian carbonates that contain large oil and gas reservoirs. The study is collaboration between the KGS, Geology Departments at Kansas State University and The University of Kansas, BEREXCO, INC., Bittersweet Energy, Inc. Hedke-Saenger Geoscience, Ltd., Improved Hydrocarbon Recovery (IHR), Anadarko, Cimarex, Merit Energy, GloriOil, and Cisco.

The project has three areas of focus, 1) a field-scale study at Wellington Field, Sumner County, Kansas, 2) 25,000 square mile regional study of a 33-county area in southern Kansas, and 3) selection and modeling of a depleting oil field in the Chester/Morrow sandstone play in southwest Kansas to evaluate feasibility for CO<sub>2</sub>-EOR and sequestration capacity in the underlying Arbuckle saline aquifer. Activities at Wellington Field are carried out through BEREXCO, a subcontractor on the project who is assisting in acquiring seismic, geologic, and engineering data for analysis. Evaluation of Wellington Field will assess miscible CO<sub>2</sub>-EOR potential in the Mississippian tripolitic chert reservoir and CO<sub>2</sub> sequestration potential in the underlying Arbuckle Group saline aquifer. Activities in the regional study are carried out through Bittersweet Energy. They are characterizing the Arbuckle Group (saline) aquifer in southern Kansas to estimate regional CO<sub>2</sub> sequestration capacity. Supplemental funding has expanded the project area to all of southwest Kansas referred to as the Western Annex. IHR is managing the Chester/Morrow play for CO<sub>2</sub>-EOR in the western Annex while Bittersweet will use new core and log data from basement test and over 200 mi<sup>2</sup> of donated 3D seismic. IHR is managing the industrial partnership including Anadarko Petroleum Corporation, Cimarex Energy Company, Cisco Energy LLC, Glori Oil Ltd., and Merit Energy Company. Project is also supported by Sunflower Electric Power Corporation.

## PROJECT STATUS

Task Name	Planned Start Date	Actual Start Date	Planned Finish Date	Actual Finish Date	% Complete
-----------	--------------------	-------------------	---------------------	--------------------	------------

1.0 Project Management & Planning	12/8/2009	12/08/09	2/7/2014		90%
2.0 Characterize the OPAS (Ozark Plateau Aquifer System)	1/1/2010	01/01/10	9/30/2013		95%
3.0 Initial geomodel of Mississippian Chat & Arbuckle Group - Wellington field	1/1/2010	01/01/10	9/30/2010	09/30/10	100%
4.0 Preparation, Drilling, Data Collection, and Analysis - Well #1	9/15/2010	12/15/10	3/31/2011	08/30/11	100%
5.0 Preparation, Drilling, Data Collection and Analysis - Well #2	1/1/2011	02/20/11	6/30/2011	08/30/11	100%
6.0 Update Geomodels	5/1/2011	05/01/11	9/30/2011	10/31/12	100%
7.0 Evaluate CO2 Sequestration Potential in Arbuckle Group Saline Aquifer	8/1/2011	08/01/11	12/31/2011	10/31/12	100%
8.0 Evaluate CO2 Sequestration Potential in Depleted Wellington field	10/15/2011	10/15/11	7/30/2013	+++	90%
9.0 Characterize leakage pathways - risk assessment area	1/1/2010	01/01/10	6/30/2012	10/31/12	100%
10.0 Risk Assessment related to CO2-EOR and CO2 Sequestration in saline aquifer	6/1/2012	06/01/12	9/30/2013	**	95%
11.0 Produced water and wellbore management plans - Risk assessment area	1/1/2012	01/01/12	7/30/2013		98%
12.0 Regional CO2 sequestration potential in OPAS	8/1/2012	02/01/12	9/30/2013	***	92%
13.0 Regional source sink relationship	1/1/2010	1/1//2010	9/30/2013	****	97%
14.0 Technology Transfer	1/1/2010	01/01/10	2/7/1014		90%

Milestone	Planned Completion Date	Actual Completion Date	Validation
HQ Milestone: Kick-off Meeting Held	3/31/2010	03/31/10	Completed
HQ Milestone: Begin collection of formation information from geologic surveys and private vendors	6/30/2010	01/01/10	Completed
HQ Milestone: Semi-Annual Progress Report on data availability and field contractors	9/30/2010	07/30/10	Submitted to Project manager
HQ Milestone: Establish database links to NATCARB and Regional Partnerships	12/31/2010	12/31/10	Completed
HQ Milestone: Annual Review Meeting attended	3/31/2011	10/05/10	Completed
		Note: This milestone was met collectively by all projects. No one project was held accountable to the milestone.	
HQ Milestone: Complete major field activities, such as drilling or seismic surveys at several characterization sites	6/30/2011		Completed
HQ Milestone: Semi-Annual Progress Report (i.e. Quarterly Report ending June 30, 2011)	9/30/2011	09/30/11	Completed
HQ Milestone: Yearly Review Meeting of all recipients; opportunities for information exchange and collaboration	12/31/2011	11/15/11	Attended meeting
HQ Milestone: Complete at least one major field activity such as well drilling, 2-D or 3-D seismic survey, or well logging	3/31/2012	08/15/12	Completed 3D seismic Cutter competed
HQ Milestone: Complete at least one major field activity such as well drilling, 2-D or 3-D seismic survey, or well logging	6/30/2012	10/09/12	Completed cutter well reach TD
HQ Milestone: Semi-annual report (i.e. Quarterly Report ending June 30, 2012) on project activities summarizing major milestones and costs for the project 9/30/2012	9/30/2012	09/30/12	Completed
FOA Milestone: Updated Project Management Plan	3/31/2010	03/31/10	
FOA Milestone: Submit Site Characterization Plan	5/28/2010		Completed
FOA Milestone: Notification to Project Manager that reservoir data collection has been initiated	9/15/2010	01/01/10	Completed
FOA Milestone: Notification to Project Manager that subcontractors have been identified for drilling/field service operations	7/30/2010	01/01/10	Completed
FOA Milestone: Notification to Project Manager that field service operations have begun at the project site	7/1/2010	01/01/10	Completed
FOA Milestone: Notification to Project Manager that characterization wells have been drilled	6/3/2011	03/09/11	Completed
FOA Milestone: Notification to Project Manager that well logging has been completed	6/3/2011	03/09/11	Completed
FOA Milestone: Notification to Project Manager that activities on the lessons learned document on site characterization have been initiated	7/15/2012		Completed
FOA Milestone: Notification to Project Manager that activities to populate database with geologic characterization data has begun	12/31/2010	12/31/10	Completed, email summary
KGS Milestone 1.1: Hire geology consultants for OPAS modeling	3/31/2010	03/31/10	Completed
KGS Milestone 1.2: Acquire/analyze seismic, geologic and engineering data - Wellington field	6/30/2010	06/30/10	Completed, quarterly rpt
KGS Milestone 1.3: Develop initial geomodel for Wellington field	9/30/2010	09/30/10	Completed, email summary
KGS Milestone 1.4: Locate and initiate drilling of Well #1 at Wellington field	12/31/2010	12/25/10	Completed, email summary
KGS Milestone 2.1: Complete Well#1 at Wellington - DST, core, log, case, perforate, test zones	3/31/2011	08/30/11	Completed, email summary
KGS Milestone 2.2: Complete Well#2 at Wellington - Drill, DST, log, case, perforate, test zones	6/30/2011	08/30/11	Completed, email summary
KGS Milestone 2.3: Update Wellington geomodels - Arbuckle & Mississippian	9/30/2011	10/31/12	completed
KGS Milestone 2.4: Evaluate CO2 Sequestration Potential of Arbuckle Group Saline Aquifer - Wellington field	12/31/2011	10/31/12	Completed
KGS Milestone 3.1: CO2 sequestration & EOR potential - Wellington field	3/31/2012		90% complete
KGS Milestone 3.2: Characterize leakage pathways - Risk assessment area	6/30/2012	10/31/12	Completed
KGS Milestone 3.3: Risk assessment related to CO2-EOR and CO2-sequestration	9/30/2012		95% complete
KGS Milestone 3.4: Regional CO2 Sequestration Potential in OPAS - 17 Counties	12/7/2012		90% complete
		Note: This milestone was met collectively by all projects. No one project was held accountable to the milestone.	
HQ Milestone: Make data set from one site characterization project publicly available.	12/31/12		
		Note: This milestone was met collectively by all projects. No one project was held accountable to the milestone.	
HQ Milestone: Complete one major field activity to collect additional characterization data from well drilling, 2-D or 3-D seismic surveys, or well logging/testing.	03/31/13		
		Note: This milestone was met collectively by all projects. No one project was held accountable to the milestone.	
HQ Milestone: Complete, at a minimum, planning for one major field activity, such as well drilling, 2-D or 3-D seismic surveys, or well logging/testing.	06/30/13		
HQ Milestone: Yearly Review Meeting of active projects; opportunities for information exchange and collaboration	09/30/13	Attended Annual Review meeting in August	100% complete
HQ Milestone: Complete one field activity to collect characterization data from well drilling, 2-D or 3-D seismic surveys or well logging/testing.	12/31/13		
HQ Milestone: Complete analysis of field activity in project-related reservoirs to validate additional storage potential.	03/31/14		
HQ Milestone: Semi-annual progress reports for active projects (i.e. Quarterly Report ending March 31, 2014).	06/30/14		
HQ Milestone: Yearly Review Meeting of active projects; opportunities for information exchange and collaboration	09/30/14		

## **TASK SUMMARY IN PREPARATION FOR COMPLETION OF THE PROJECT**

This quarterly report includes all of the tasks and subtasks with dialog pertaining to activities conducted in this quarter or comments related to the completion of the tasks by the end of the project.

### **Task 1: Program Management and Reporting (PMP)**

### **Task 2. Characterize the OPAS**

**Subtask 2.1. Acquire geologic, seismic and engineering data**

**Subtask 2.2. Develop regional correlation framework and integrated geomodel**

**Subtask 2.3. Subsurface fluid chemistry and flow regime analysis**

**Subtask 2.4. Gather and interpret KGS's gravity and magnetic data**

**Subtask 2.5. Remote sensing analysis for lineaments**

Data associated with Task 2 have been being compiled and are being using to establish the final regional storage assessment. Information will be uploaded to the interactive mapper and NATCARB. The latest versions of the structure, isopach, and fault maps are available, but have yet to be uploaded to the interactive mapper (**Figure 1**). The recent seismicity in southern Kansas and Oklahoma has led to a closer inspection of our assembled subsurface data, in particular, structural maps. We will confirm accuracy and consistency in mapping known and indicated faults from which will make our final interpretations.

A simpler web address for our interactive mapper is now being used -- <http://maps.kgs.ku.edu/co2>. The digital type logs in the project will be reviewed in the next quarter before the project is completed. Similarly, stratigraphic correlations will be reviewed. Additional digital deep wells will be inventoried in the study area due the recent increase in drilling in southern Kansas and operators increasing the submission rate for digital (LAS).

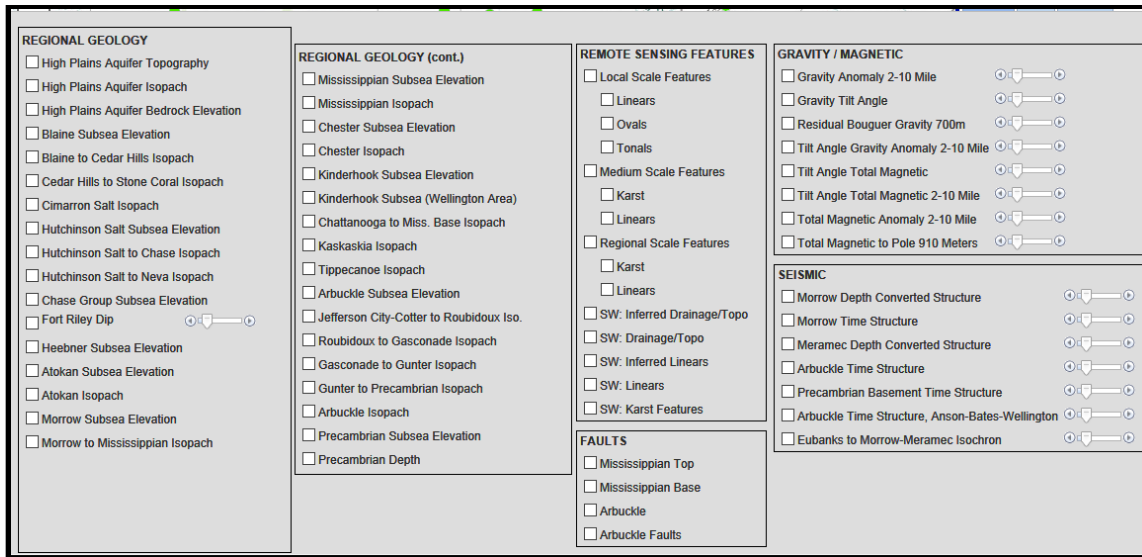


**Figure 1. Latest version of the dropdown menu showing map layers currently present for the project interactive mapper -- <http://maps.kgs.ku.edu/co2>**

### **Task 3. Geomodel of Mississippian Chat & Arbuckle Group - Wellington field.**

**Subtask 3.1. Collect geologic & engineering data**

**Subtask 3.2. Collect 3D seismic data**

**Subtask 3.3. Process 3D seismic data**

**Subtask 3.4. Collect gravity and magnetic data**

**Subtask 3.5. Interpret seismic, gravimetric, and magnetic data**

**Subtask 3.6. Initial geomodel - Wellington**

A field-wide geomodel for the Mississippian oil reservoir will be completed in the final two quarters.

The Arbuckle geomodel has been completed and utilized in the Class VI application of DE-FE0006821. The seismic data needed for the model has been processed and interpreted, but student thesis work funded by other means continues to refine the interpretation including petrographic analysis of the Mississippian reservoir at Wellington Field by Montalvo summarized in **Appendix A -- Diagenesis and distribution of diagenetic facies in the Mississippian of south-central Kansas.**

### **Task 4: Preparation, Drilling, Data Collection and Analysis – Test Borehole #1**

**Subtask 4.1. Locate Test Borehole #1**

**Subtask 4.2. Permitting for Test Borehole #1**

**Subtask 4.3. Drill, retrieve core, and run DST – Test Borehole #1**

**Subtask 4.4. Openhole Wireline Logging – Test Borehole #1**

- Subtask 4.5. Wellbore Completion – Test Borehole #1**
- Subtask 4.6. Analyze wireline log - Test Borehole #1**
- Subtask 4.7. Test and sample fluids (water) from select intervals – Test Borehole #1**
- Subtask 4.8. Analyze Arbuckle core from Test Borehole #1**
- Subtask 4.9. Analyze Mississippian core from Test Borehole #1**
- Subtask 4.10. PVT analysis of oil and water from Mississippian chat reservoir**
- Subtask 4.11. Analyze water samples from Test Borehole #1**
- Subtask 4.12. Microbiological studies on produced water**
- Subtask 4.13. Correlate log and core properties**
- Subtask 4.14. Examine diagenetic history of fracture fill**

Subtasks 4.1 focused on the geochemical and microbiological aspects of CO<sub>2</sub> interaction with the rock continues to be addressed. Work is summarized by Christa Jackson, M.S. candidate at KU in **Appendix B – “Geological and Microbiological Influences on Reservoir and Seal Material During Exposure to Supercritical CO<sub>2</sub>, Arbuckle Group, Kansas”**. This work is supported by both DOE-NETL and The Petroleum Research Fund.

#### **Task 5. Preparation, Drilling, Data Collection, and Analysis - Test Borehole #2**

- Subtask 5.1. Locate Test Borehole #2**
- SubTask 5.2. Permitting for Test Borehole #2**
- Subtask 5.3. Drill, and run DST – Test Borehole #2**
- Subtask 5.4. Openhole wireline logging - Test Borehole #2**
- Subtask 5.5. Complete well and perforate selectively to test and sample fluids – Test Borehole #2**
- Subtask 5.6. Analyze wireline log – Test Borehole #2**

#### **Task 6. Update Geomodels**

- Subtask 6.1. Hydrogeologic studies**
- Subtask 6.2. 2D shear wave survey**
- Subtask 6.3. Process & interpret 2D shear**
- Subtask 6.4. Revise 3D seismic interpretation**
- Subtask 6.5. Update geomodel - Arbuckle & Miss**

Yousuf Fadolalkarem is working with the Wellington 2D and 3D seismic data in a thesis titled, “Pre-stack Seismic Attribute Analysis of the Mississippian Chert and the Arbuckle at the Wellington Field, South-central Kansas”. This study is examining the pre-stack 3D seismic data attribute analysis and inversion to predict reservoir properties of the Mississippian cherty dolomite and the Arbuckle Group. Synthetic wedge modeling of pre-stack seismic is being used to examine relationships between reservoir thicknesses and AVO impedance inversion techniques that will be applied to 3D pre-stack field seismic data using the Hampson-Russell software. These techniques are P- and S-impedance inversion, Lambda-mu-rho inversion and Elastic Impedance inversion. Predictions from the pre-stack analysis will be compared to well data and post-stack analysis results.

This work will help define the relationships between seismic data attributes and properties of the Mississippian reservoir and Arbuckle aquifers at the Wellington and will help advance the understanding of capabilities and limitations of pre-stack seismic methods for predicting reliably reservoir thickness and porosity. The final full-field reservoir models of the Mississippian and Arbuckle will utilize these results as possible in the timeframe available before the final report is completed. This work is leveraging the DOE-NETL funding with support from the Kansas Interdisciplinary Carbonate Consortium (KICC).

An update of the Mississippian geomodel in Wellington Field was made by J. Rush. The focus of the latest work was directed to further resolve the stratigraphy and structure using the 3D seismic survey. The well log-based structure on the top of the Mississippian for the combined Anson-Bates and Wellington Fields show the broad structural high over the Wellington Field (Figure 2). This is compared to the area of higher relief in the Anson-Bates area to the northwest.

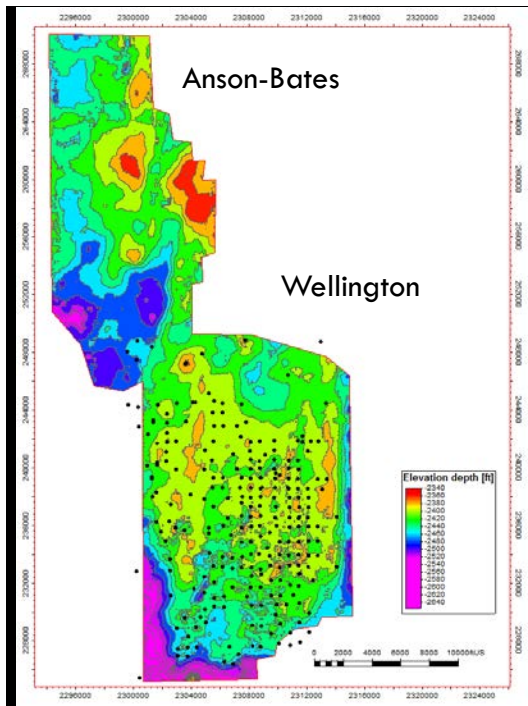


**Figure 2. Structure top of Mississippian with elevations derived from well log data.**

A west-to-east well log (gamma ray and porosity) cross section across the field delimits the higher porosity at the top of the Mississippian interval (**Figure 3**). These well data serve as the calibration for resolving the internal seismic stratigraphy shown in subsequent figures. A Petrel layering model of the Mississippian in **Figure 4** shows three major internal divisions of the Mississippian. The light blue colored basal Pierson (lower “Cowley facies”) is classified as a transgressive systems tract (TST). These layers thicken to the east (landward) and notably thin basinward to the west. The basal strata also onlap an underlying erosional surface.

The darker blue middle Mississippian strata step basinward, west of the location of toplap truncation (Figure 4). There also appears to be erosion of the topset strata that is interpreted to have occurred during a sea level lowstand. This internally consistent and correlatable layer model also suggests that the structural high is persistently positive during the Mississippian, supporting earlier work suggesting the same. The red colored thin upper Mississippian is the residual cherty interval that appears to be concentrated over the structural high, likely reflecting the more intense weathering on the crest (Figure 4).

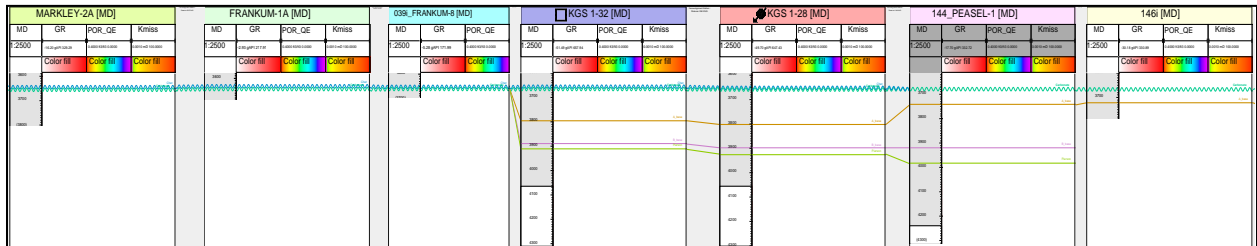


**Figure 3. West-to-east cross section including #1-32 and #1-28. Higher porosity reservoir interval is located on top of the Mississippian. Internal stratal markers are shown by correlations lines.**

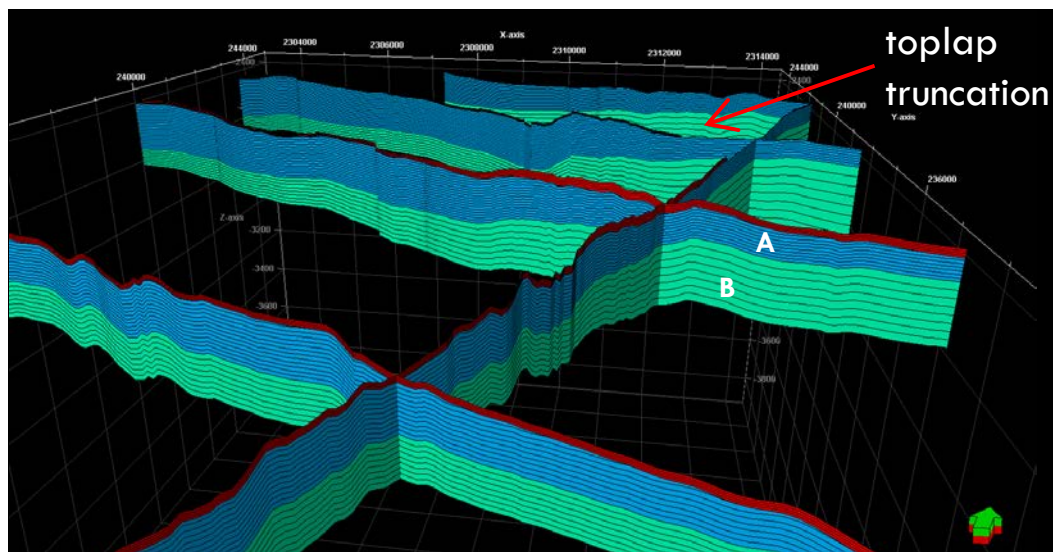


**Figure 4. Petrel layering based on correlation of logs and seismic data.**

**Figure 5** illustrates the structural elements that have been clarified with the depth-converted systems. As indicated in **Figure 4**, the Mississippian reveals set patterns of internal strata geometries. These strata are slightly interrupted by local structure, but show the downlap and onlap quite clearly on the 3D seismic (**Figure 5**). The basal Mississippian is quite irregular (yellow line) overlapping a local structural high at #1-32 where the Chattanooga Shale has been previously eroded prior to the Mississippian transgression. Moreover, the seismic discontinuities

bounding it on west and east sides suggest faulting to form a horst that was present at least until the upper Mississippian.

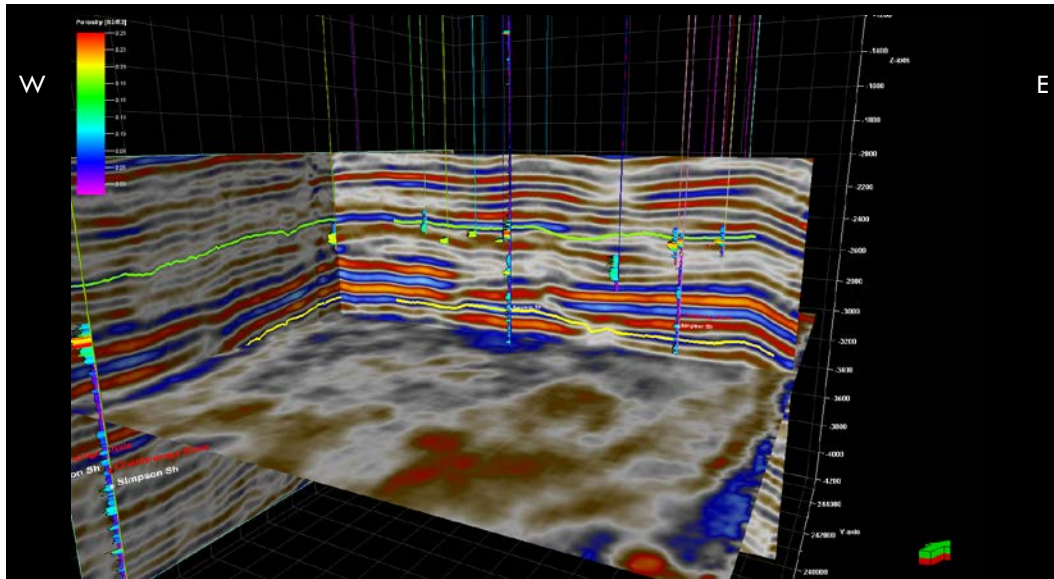


**Figure 5. Faults, grabens, and Mississippian onlap are key structural and depositional features recognized on this inline-cross line extract of the 3D seismic volume at Wellington Field. The top of Mississippian is bright green line and the base of the Mississippian is the yellow line. This visualization is in depth. Deep wells #1-32 and #1-28 are shown along W-E crossline.**

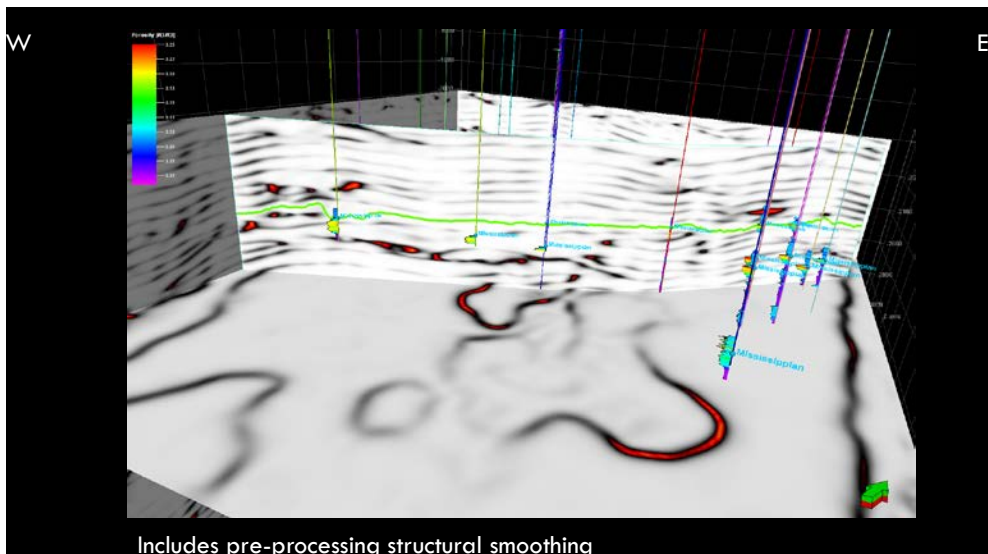


**Figure 6. Wellington Field seismic showing variance attribute on PSDM.**

The prestack depth migration was used to show a variance attribute that helped to further delimit the likely faults at the base of the Mississippian (**Figure 6**). The red wavy lines are the likely

faults developed near the crest of the structural high. Note their location and the configuration of the top for the Mississippian, again indicating the possible diminished offset on the faults the higher in the Mississippian. A key point is that the structure continues to be active current with deposition, preceding the major tectonic activity at the end of the Mississippian.

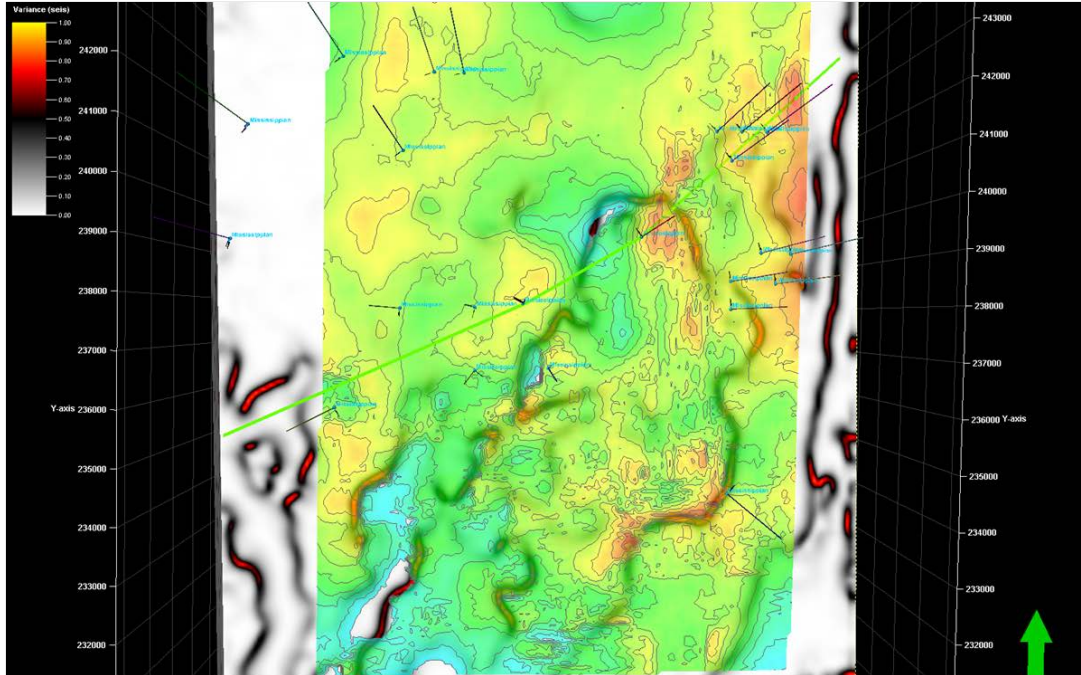


**Figure 7. Wellington Field seismic structure co-rendered with Variance Attribute (PSDM).**

The map view of the Variance Attribute shown in **Figure 7** at the base of the Mississippian indicates the southeast portion of Wellington Field is outlined by a fault that closely outlines the highest portion of the structure. Well #1-32 is on the west side, outside of the area within the faulted (horst) volume. The structural offset across the faults is relatively low, <50 ft, but is also accompanied by drape/flexure beyond the fault itself.

The structural activity that was concurrent with deposition persists to through the Upper Pennsylvanian where the thick (100 ft) Oread Limestone on the east side of Wellington Field thins dramatically to the west (**Figure 8**). The paleotopography is representative of a regional change from shelf to basin for the Oread Limestone, basin to the west-southwest and landward east and north.

Fault interpretation with the variance attribute is confirmed as illustrated by the anomaly intersecting with the cross line profile of the seismic amplitude (**Figure 9**).

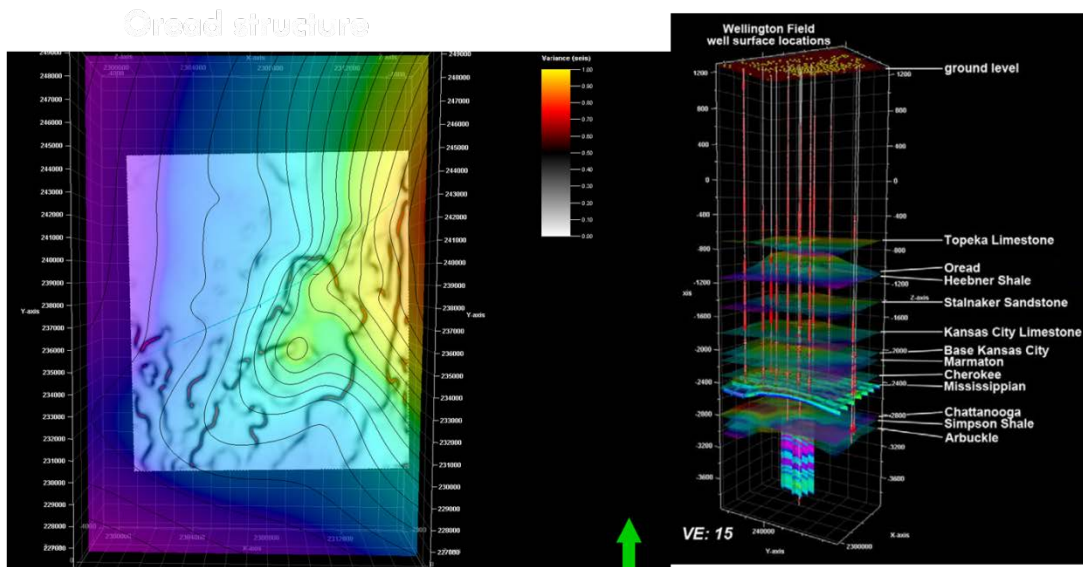


**Figure 8. Oread shelf edge closely corresponds to the underlying NE-trending fault.**

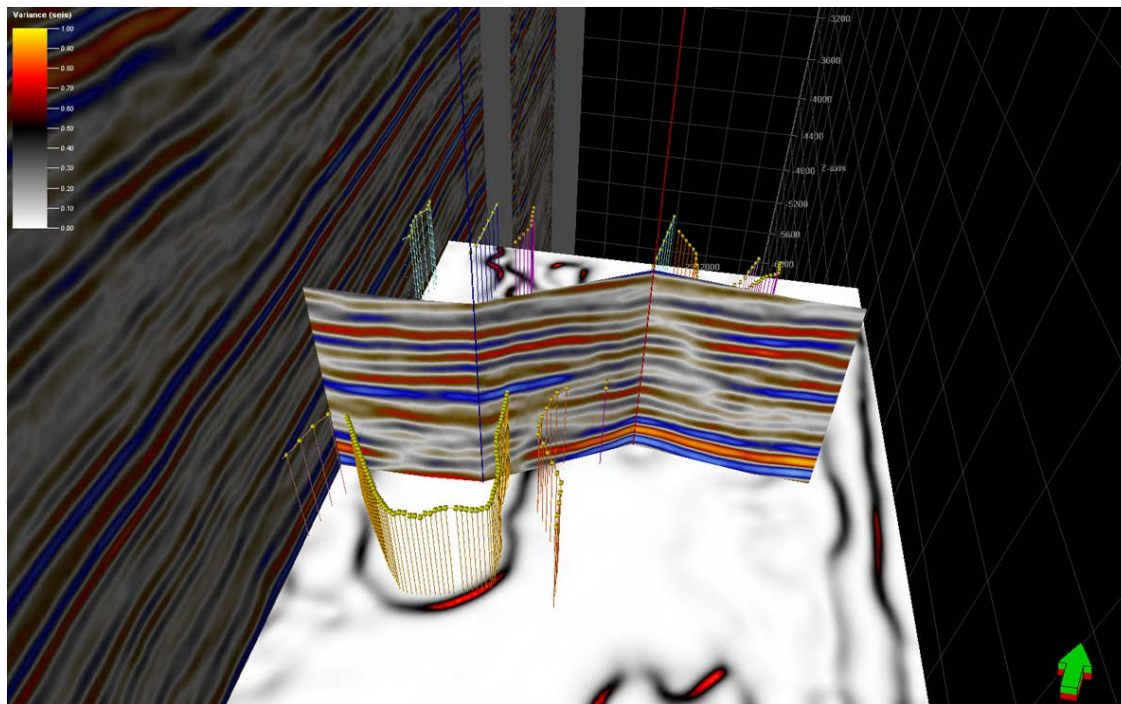


**Figure 9. Wellington Field, fault model and variance.**

The volumetric curvature (VC) was previously used to define discontinuities in the seismic until it was realized that the data seemed to be too noisy (**Figure 10**). The pattern of the VC at this stage of the processing also suggested an artifact from the acquisition “footprint”. More work on the use of VC is needed, particularly; looking at different resolutions, before move convincing

results can be obtained as noted in another DOE supported study at Bemis-Shutts Field in Kansas.

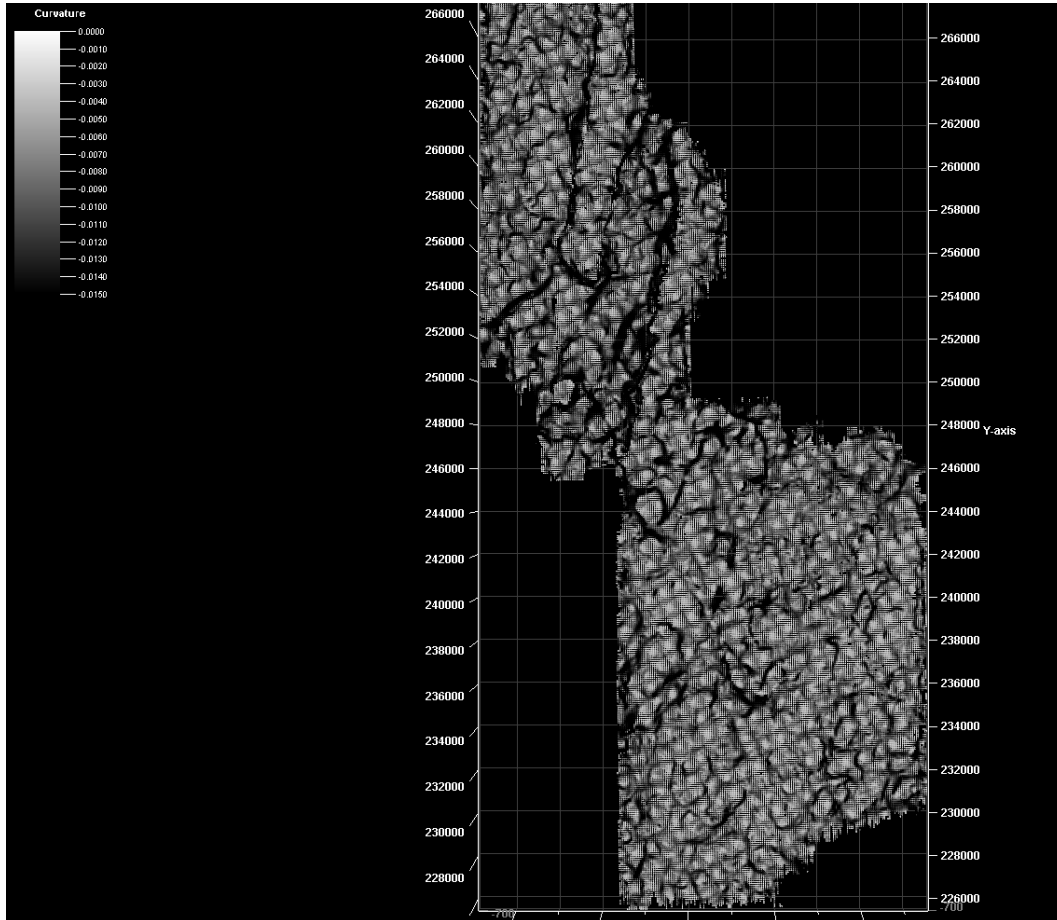


**Figure 10. Volumetric Curvature -- Too noisy? Need to QC using different lateral resolutions. More convincing results were found for the Bemis-Shutts project.**

The Petrel-based genetic inversion of the 3D volume to obtain the porosity for the layered Mississippian model is shown in **Figure 11**. The more continuous porosity is noted on the west side of the field corresponding the portion of the middle portion of the Mississippian before it toplaps to the east.

A detailed layer-based porosity model of the entire Mississippian in **Figure 12** further shows the toplap of the layers and porosity to the east and the downlap to the west. The layers clearly show the progradational packages, even at this reservoir scale.

The porosity log used in the gridding that is displayed in **Figure 12** was smoothed. This log porosity profile is compared with the seismically derived porosity from the genetic inversion in **Figure 13**. The resampling to the 3-D grid uses exact transform seismic porosity to log values

during SGS. The porosity model uses SGS & the seismic porosity attribute. There is an excellent correlation between the logs and the log-seismic integrated model.

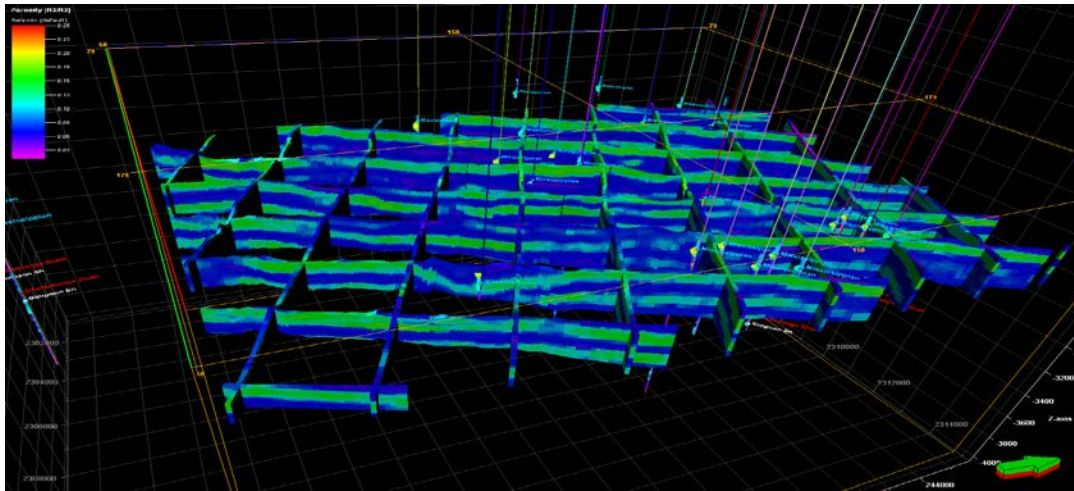


**Figure 11. Genetic Inversion sampled to 3-D Grid for the Mississippian reservoir.**

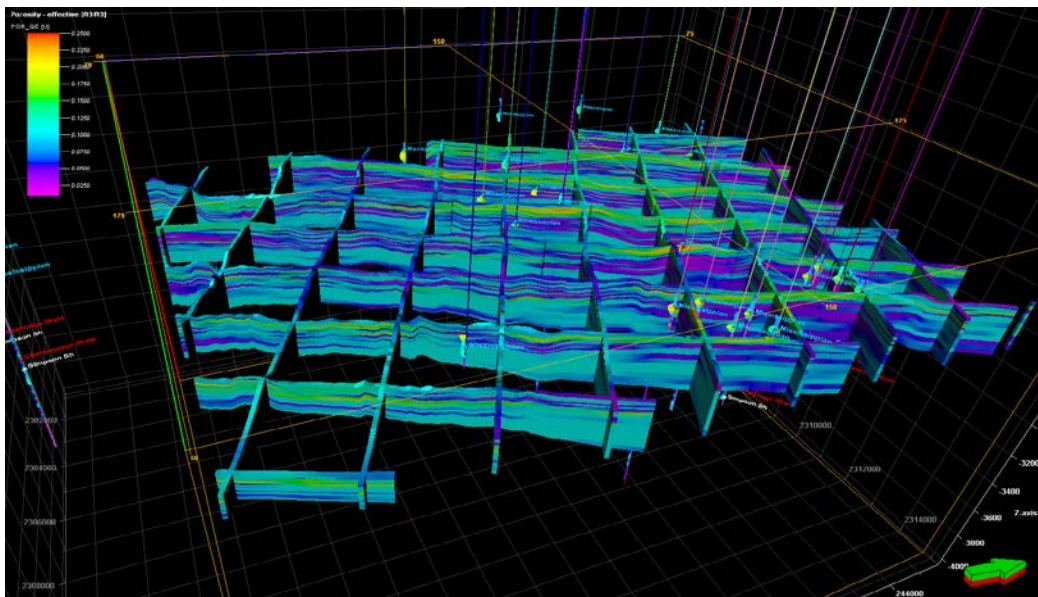


**Figure 12. Porosity Model using SGS & Seismic Porosity Attribute. The seismic porosity attribute distribution is normalized to upscaled porosity values.**

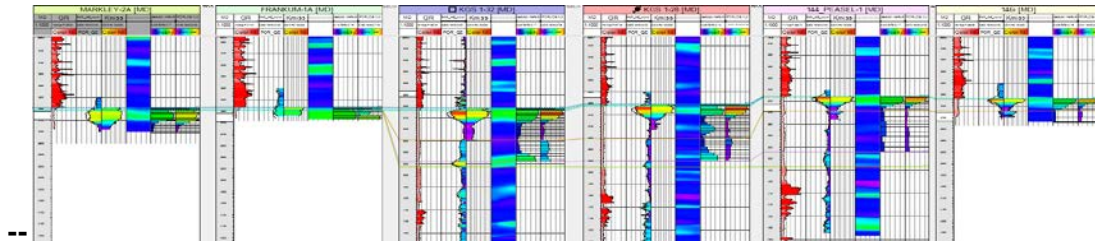


**Figure 13. Seismic porosity attribute and upscaling results along west-east well cross section.**

The interim conclusions from revisiting and updating the geomodel of the Mississippian reservoir at Wellington include:

1. Conductive fractures dominate fluid flow into wellbore (PLT) in low K reservoirs. The Mississippian has both high and low permeability facies, thus fracture modeling is very important. CO<sub>2</sub> injection will likely be affected by the fractures presenting themselves as either conduits or barriers to the CO<sub>2</sub>.
2. Mississippian has similar tight basinal expressed as the “lower Cowley facies” that are part of the TST. These facies thicken unto the Wellington structure while the reservoir facies undergo toplap and truncation from west to east across the field.
3. Seismic attributes aid *comprehensive* characterization, particularly to delimit high angle fractures and faults that do not intersect the wellbores and have smaller offsets that are usually attributed to flexure.
4. Production decline can be overcome or injection of fluids like CO<sub>2</sub> can be tailored when fractures and faults are considered in the geomodeling and simulation activities.

**Task 7. Evaluate CO<sub>2</sub> Sequestration Potential in Arbuckle Group Saline Aquifer - Wellington field**

- Subtask 7.1. CO<sub>2</sub> sequestration potential**
- Subtask 7.2. Long-term effectiveness of cap rock**
- Subtask 7.3. CO<sub>2</sub> sequestered in brine**
- Subtask 7.4. CO<sub>2</sub> sequestered as residual gas**
- Subtask 7.5. CO<sub>2</sub> sequestered by mineralization**
- Subtask 7.6. Field management - max CO<sub>2</sub> entrapment**
- Subtask 7.7. Monte Carlo - total CO<sub>2</sub> seq capacity**

The geomodel and simulation studies used in the Class VI application for project DE-FE0006821 were completed in this quarter. The Wellington data in particular are being used to calibrate the type logs for the regional study area using a neural network. The approach is described later under Task 12 -- **Regional CO<sub>2</sub> Sequestration Potential in OPAS - 17 Counties.**

The Class VI application used a permeability model that is admittedly biased to the matrix pores with the whole core analyses and nuclear magnetic resonance tool. DST's and variable rate pulse

test were used to scale the results to these measurements to adjust the permeability as used in the simulation for the Class VI permit application (**Figure 14**). The 50 ft flexure noted to the immediate west of #1-28 corresponds with the fault suggested in recent work described above (**Figures 7, 8, and 9**). The fault also cuts into the Mississippian and at least flexure continuing to affect the Upper Pennsylvanian Oread Limestone thickness shown in **Figure 8**.

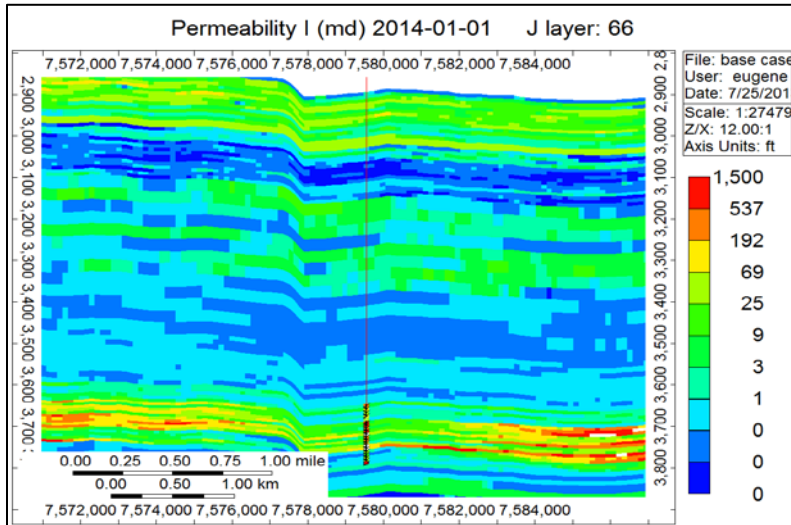


**Figure 14. A west to east permeability profile of the Arbuckle crossing the location of the proposed injection well #1-28.**

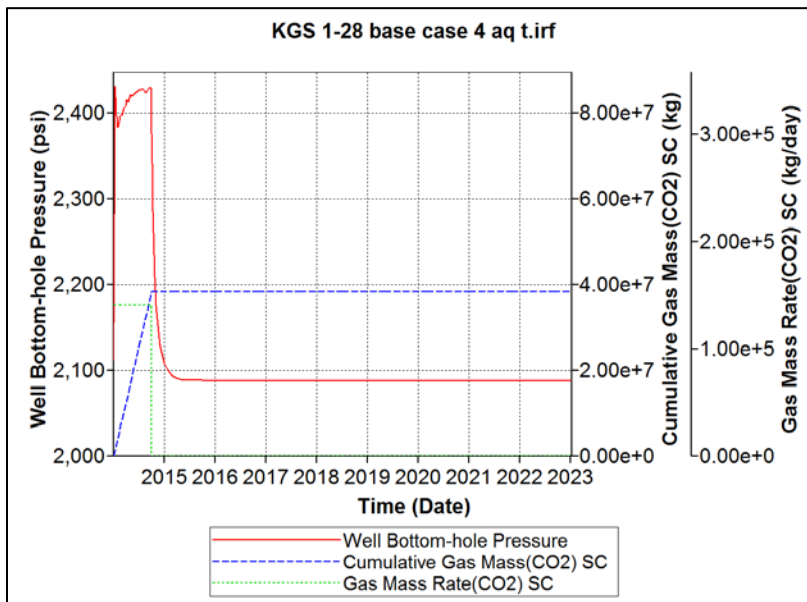


**Figure 15. Simulated bottom hole pressure, 325 psi max. (0.485 psi/ft) 120 tonne/day, 40,000 tonne total CO<sub>2</sub>.**

The maximum simulated bottom hole pressure with this modeling used for the Class VI application is close to what the pressure would be under hydrostatic conditions (**Figure 15**). This conservative pressure would permit the injection of 40,000 tonnes of CO<sub>2</sub> over ~9 months.

The size of the resulting CO<sub>2</sub> plume with free phase gas saturations varying from nearly zero to one spans a diameter of ~2000 ft (**Figure 16**). The nearly 100% free phase CO<sub>2</sub> portion of the plume should intersect the observation well #2-28.

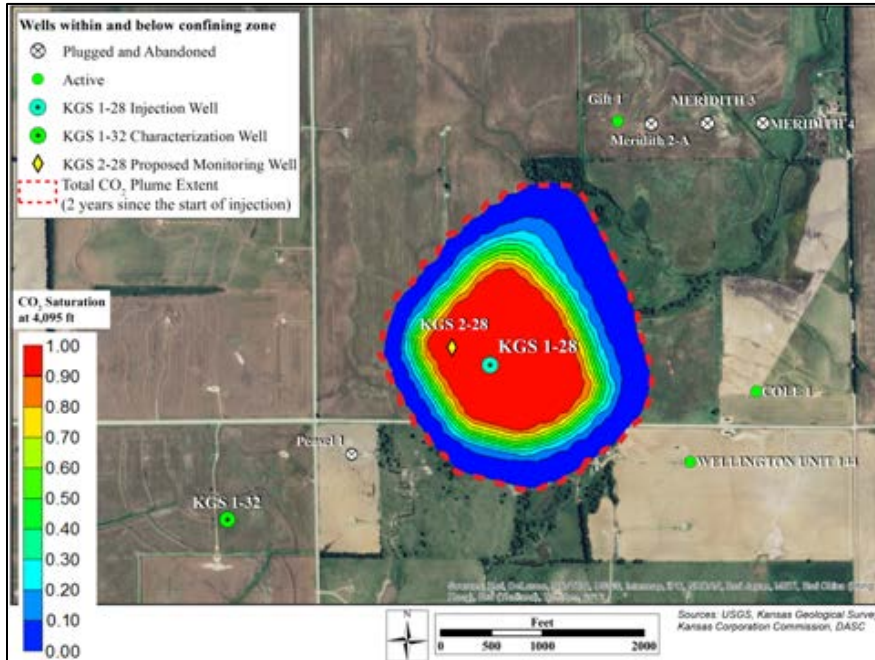


**Figure 16. Simulated CO<sub>2</sub> plume with pressure, volume, and time described in Figure 15.**

### **Task 8. Evaluate CO<sub>2</sub> Sequestration Potential by CO<sub>2</sub>-EOR in Depleted Wellington field**

- Subtask 8.1. CO<sub>2</sub>-EOR potential
- Subtask 8.2. Long-term effectiveness of cap rock
- Subtask 8.3. CO<sub>2</sub> sequestered in brine and residual gas
- Subtask 8.4. CO<sub>2</sub> sequestered by mineralization
- Subtask 8.5. Field management - optimize CO<sub>2</sub>-EOR
- Subtask 8.6. Monte Carlo - total CO<sub>2</sub> seq capacity

The full-field simulation has yet to be completed. As described above the field-wide geomodel for the Mississippian is underway.

### **Task 9. Characterize leakage pathways - Risk assessment area**

- Subtask 9.1. Collect reservoir characterization data - external sources
- Subtask 9.2. Map fracture-fault network
- Subtask 9.3. Verify seal continuity and integrity
- Subtask 9.4. Inventory well status
- Subtask 9.5. Gather expert advice on well integrity

Wells have been inventoried and well integrity has been defined. The newest geomodel will be used to further model the fractures and faults that are now being resolved as previously described above.

**Task 10: Risk Assessment Related to CO<sub>2</sub>-EOR in Mississippian Chat Reservoir and CO<sub>2</sub> Sequestration in Arbuckle Aquifers**

- Subtask 10.1. Model CO<sub>2</sub> plume for 100, 1000, and 5000 yrs after injection stops**
- Subtask 10.2. Model plume attenuation during and after injection**
- Subtask 10.3. Model effects of natural aquifer flow on CO<sub>2</sub> plume**
- Subtask 10.4. Estimate time frame for free phase CO<sub>2</sub> to become negligible**
- Subtask 10.5. Model effectiveness of cap rocks to contain leakage**
- Subtask 10.6. Leakage modeling through abandoned wells**
- Subtask 10.7. Model worst-case CO<sub>2</sub> leakage scenario**
- Subtask 10.8. Estimate surface environmental effects due to leakage**

Simulations with leakage has been examined, but will be updated using the final geomodel.

**Task 11: Produced Water and Wellbore Management Plans**

- Subtask 11.1. Identify at-risk wells in Wellington Field**
- Subtask 11.2. Outline Best Practices and well recompletion plans for at-risk wells**
- Subtask 11.3. Outline Best practices and well completion plans for new CO<sub>2</sub> injector wells**
- Subtask 11.4. Summarize practices in place for disposal of produced water**

Wells have been examined for at-risk characteristics. Steps will be taken to plug a well in close proximity to the CO<sub>2</sub> plume generated by the small scale injection test. Other wells lie significantly beyond this area that would need to be addressed if larger scale disposal would be considered. The criteria followed in this assessment will become the best practice. If there is any doubt, remedial action will be necessary.

**Task 12. Regional CO<sub>2</sub> Sequestration Potential in OPAS - 17 Counties**

- Subtask 12.1. Map reservoir compartments in Arbuckle aquifer in a regional context**
- Subtask 12.2. Coarse grid simulation over select OPAS areas to estimate regional CO<sub>2</sub> sequestration potential**
- Subtask 12.3. Generalized estimates of miscible CO<sub>2</sub>-EOR in similar and larger oil fields in approximately 17 counties**
- Subtask 12.4. Estimate regional CO<sub>2</sub> sequestration potential of OPAS**

The regional assessment of CO<sub>2</sub> storage potential in southern Kansas has undergone a year long process of refining estimates of key variables that are essential in accurate reporting. It has been previously shown how the original estimates were made based on average properties and assumptions. The work progressed in this quarter set on a course of providing the best realization of permeability both K<sub>v</sub> and K<sub>h</sub>, capillary pressure, and estimates of reaction rates to provide

reliable storage numbers. The calibration wells #1-28 and #1-32 at Wellington and the Cutter KGS #1 were used in this analysis. The geomodels are being constructed for the 10 regional simulation sites that are analogous to the Wellington and Cutter fields with structural closure and overlying oil field (**Figure 17**).

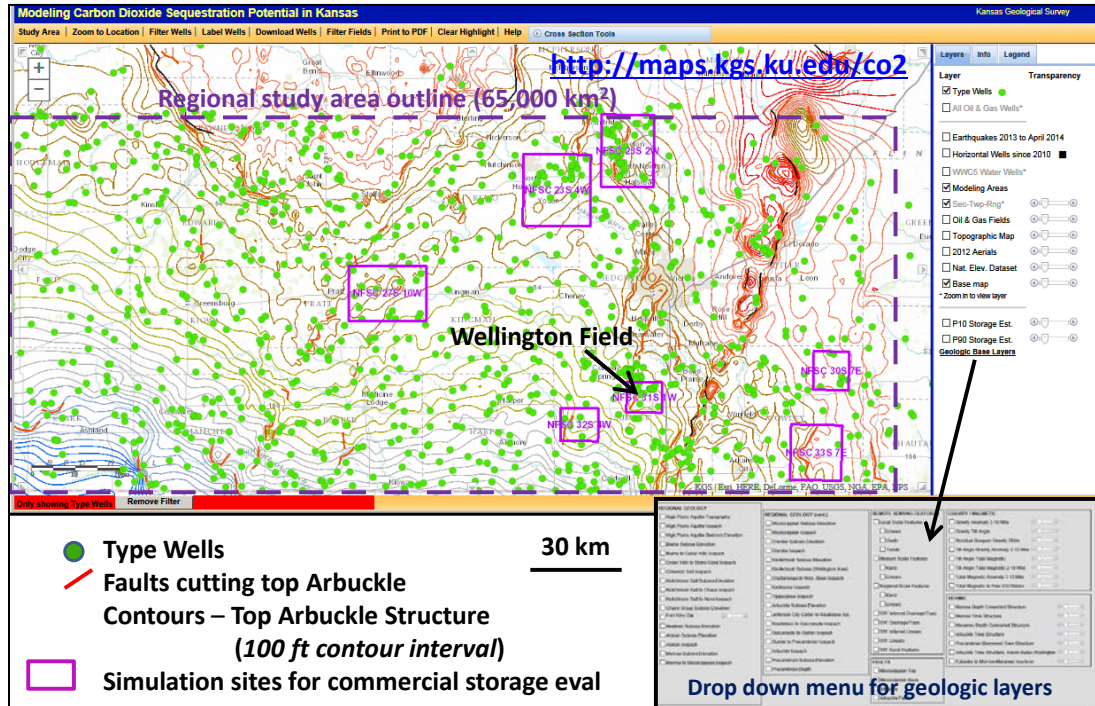


**Figure 17. Interactive mapper showing the eastern 7 regional modeling sites, Wellington Field, and the type wells and faults on a structure map of the top of the Arbuckle.**

The oil fields play an important role in making the economics of capturing the anthropogenic by utilizing for CO<sub>2</sub>-EOR (**Figure 18**). Screening of oil fields for suitability for CO<sub>2</sub>-EOR has been implemented on the interactive mapper including producing zone, depth, and cumulative production. API gravity will be used as a proxy for estimating minimum miscibility pressure.

The permeability prediction for use in the regional modeling and storage assessment has been a difficult exercise when we moved beyond the cored and fully logged calibration wells in Wellington and Cutter Fields. However, a consensus was reached on the realizations that are being generated to and complete the sequestration potential task.

The key decision was to move to a neural network solution after having examined many alternatives. That testing of the latter proved troublesome even though in concept, the originally looked quite promising, e.g., fuzzy logic. The neural net is being validated with the calibration wells. The input variables include the well logs that have been digitized in the regional study



to be thoroughly established. The uncertainty will be introduced from studies of the outcomes when computed injectivity can be compared with observed results.

RHO<sub>maa</sub> and U<sub>maa</sub> were not found to contribute significantly to permeability prediction, although they suggest that chertier dolomites tend to be more permeable than dolomites. However, gamma-ray, porosity, resistivity were useful as predictors, and so the model input requirements are from a basic triple combo well log suite common in Type Well Database:

1. GR (Gamma-ray, API units)
2. PHIt (volumetric porosity%)
3. PHIr ( connected porosity estimated from resistivity log %)

$$PHIDensity[] = (2.71 - RHOB[]) / (2.71 - 1)$$

$$Rwa[] = (((PHID[] + PHIN[]) / 2)^2) * (ResDeep[] / 1)$$

$$PHIr[] = (Rwa[] / ResDeep[])^{.5}$$

Doveton, KGS

**Figure 19. Input variables for the neutral network solution to estimate permeability.**

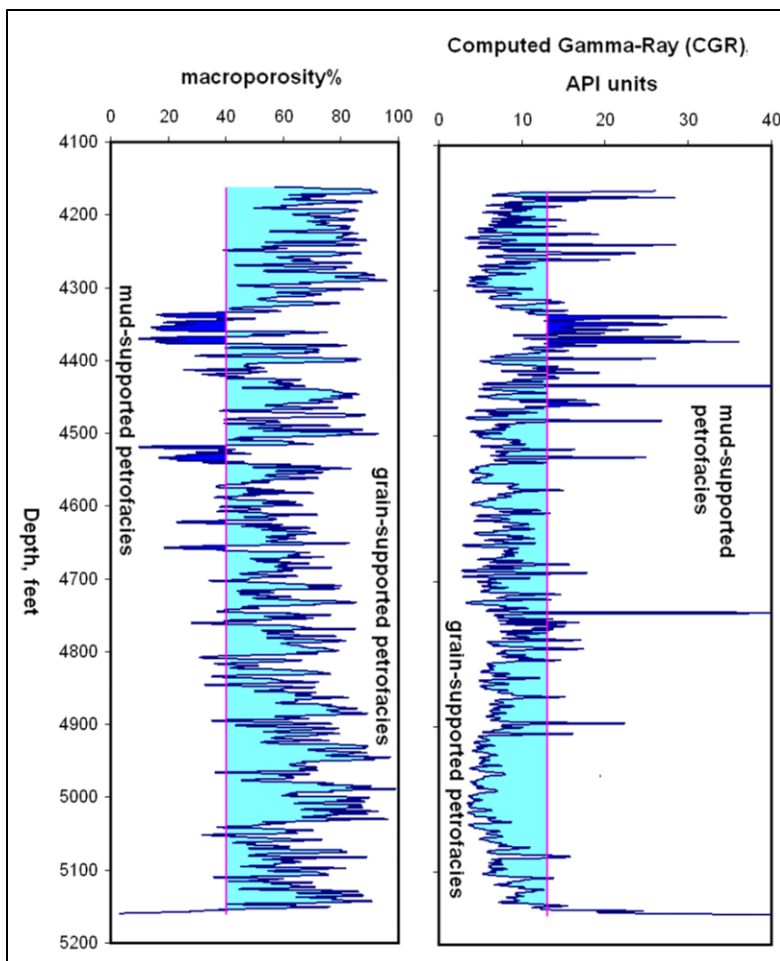


**Figure 20. The CGR (K+Th) shows good distinction between more permeable grainstones and less permeable mudstones. Complication: Standard gamma-ray logs include uranium, which may bias grainstones towards mudstones**

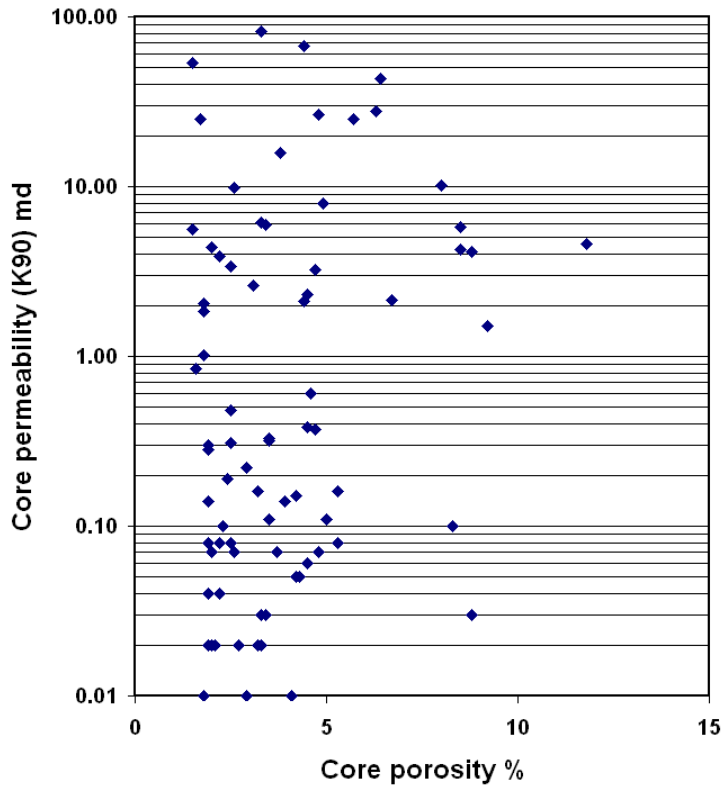


Figure 21. PHIt (volumetric porosity%). There must be some relationship between porosity and permeability.

From the first Archie equation for carbonates:

$$F = \frac{R_o}{R_w} = \frac{1}{\Phi_R^2}$$

where  $\Phi_R$  is the electrically connected porosity.

So,

$$\Phi_R = \sqrt{\frac{R_w}{R_o}}$$

Complication:  $R_w$  is significantly higher in the top of the Arbuckle than in the middle and this variability needs to be accommodated in the calculation of PHIt

Figure 22. Connected porosity is estimated from resistivity logs when  $R_w$  is known. (Hint: the connected porosity should not exceed the total porosity.)

## Formation Resistivity Factor (FF, m)

- Only channel pores participate actively in the flow of electric current. Traps are neutral.
- In viscous flow traps are not neutral – Viscous forces promote the transfer of fluids from traps to flowing pores

**That is why FRF may not always be correlated to Perm**

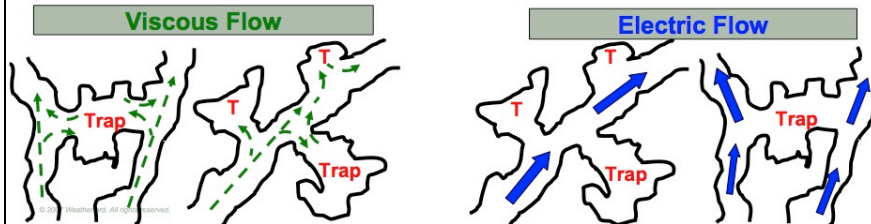


Figure 23. Weatherford warns that electrical connectivity does not necessarily mimic fluid connectivity, but they imply that it is worth trying.

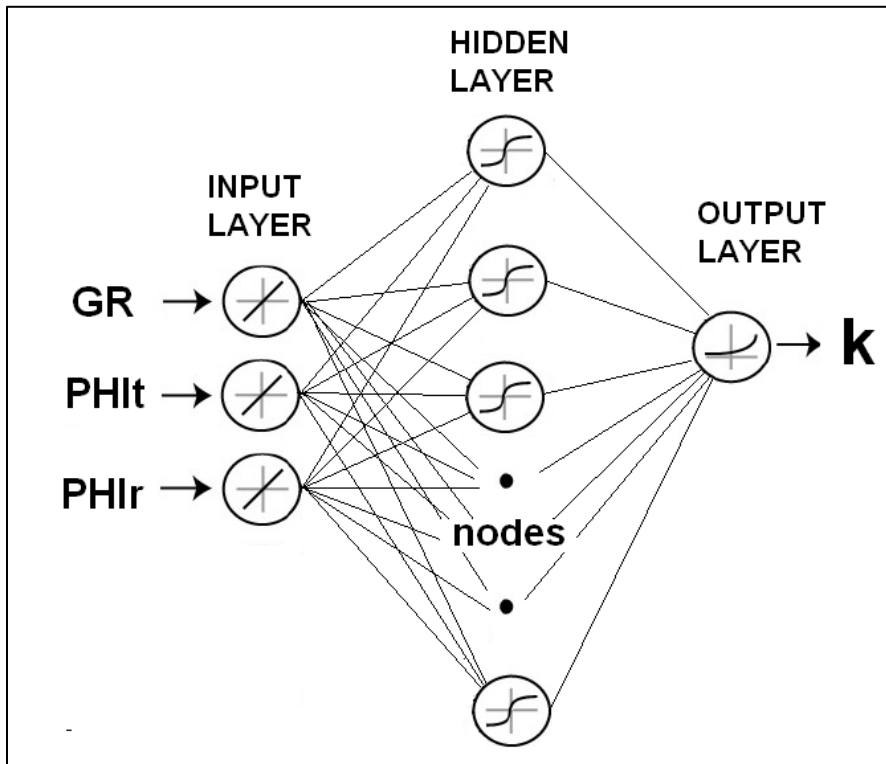
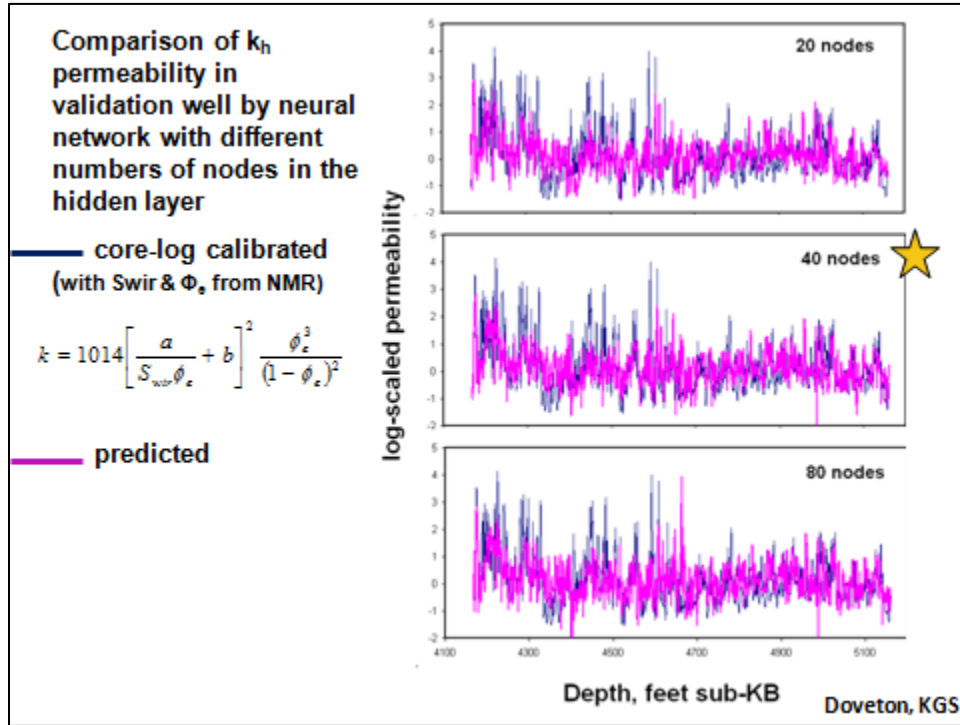


Figure 24. Neural network (NN) prediction of Arbuckle permeability from logs

Results of permeability estimated from the neural network compared with actual permeability indicate that the dynamic range is quite good compared to trials with other methods. The 40-node model was selected for use in creating the permeability realizations for the type wells (**Figure 25**). While the R-squared is below 21% for the 40-mode neural network, it is the best result in the trial and error process that was pursued over the past year (**Figure 26**).



**Figure 25. Prediction of permeability in the Arbuckle of the validation well Wellington #1-28 from regression analysis of calibration well #1-32 based on gamma-ray, porosity, and electrically connected porosity.**

The need to establish an  $R_w$  to determine connected porosity is a matter of fitting a  $R_o$  line on a Pickett plot, iteratively fitting the  $R_t$  with the  $R_o$  line to solve for  $R_w$ , or plot a  $R_{wa}$  vs depth.

The resulting  $R_w$  generally varies with depth in the Arbuckle and once that trend is established, the  $R_w$  can be extrapolated as is being done in this neural network methodology (**Figure 28**).

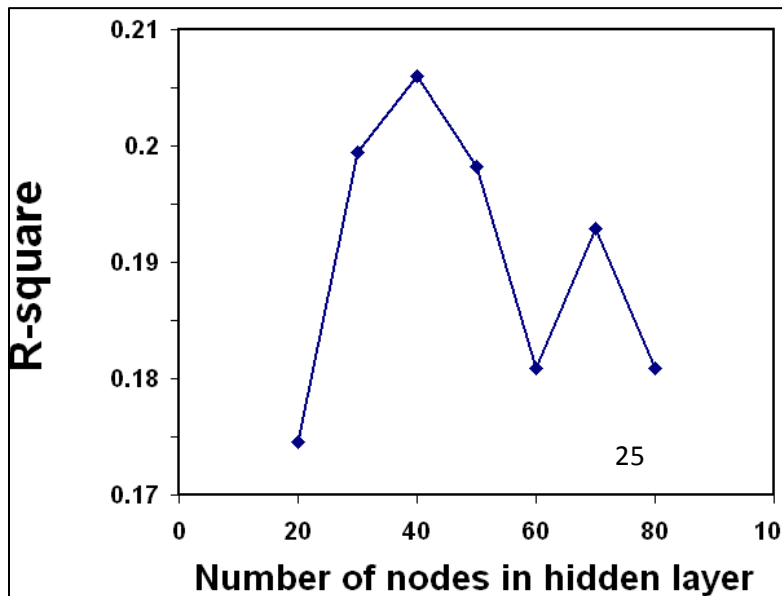


**Figure 26. R-square of NN predictions of permeability with actual permeabilities in validation well #1-28 for different number of nodes in the hidden layer.**

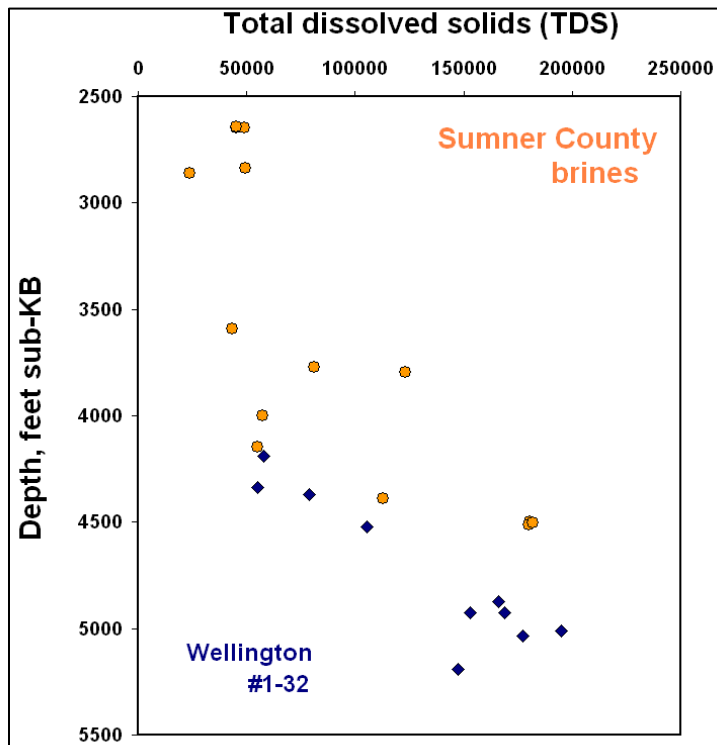
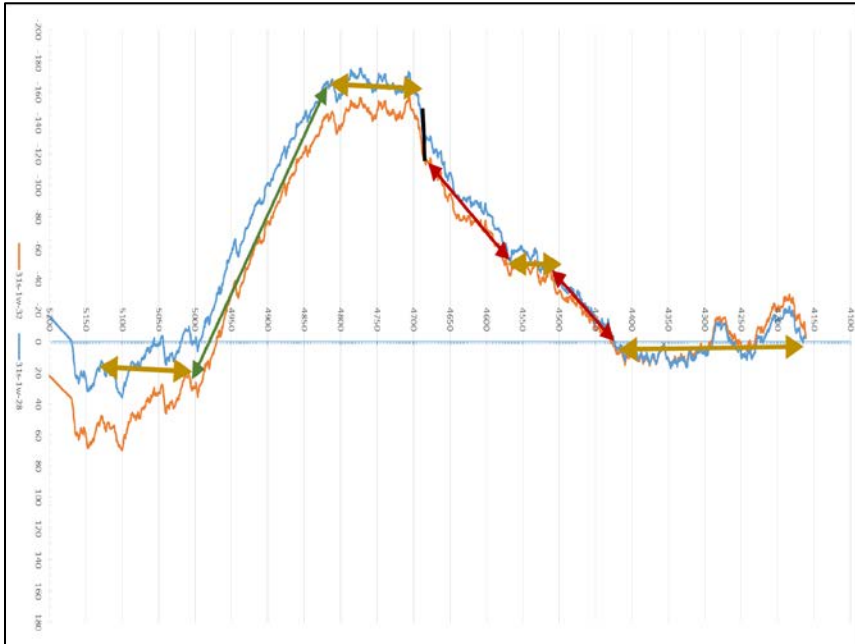


**Figure 28. Use catalog salinities for validation purposes and estimate  $R_w$  from Pickett plot and/or  $R_{wa}$  versus depth.**

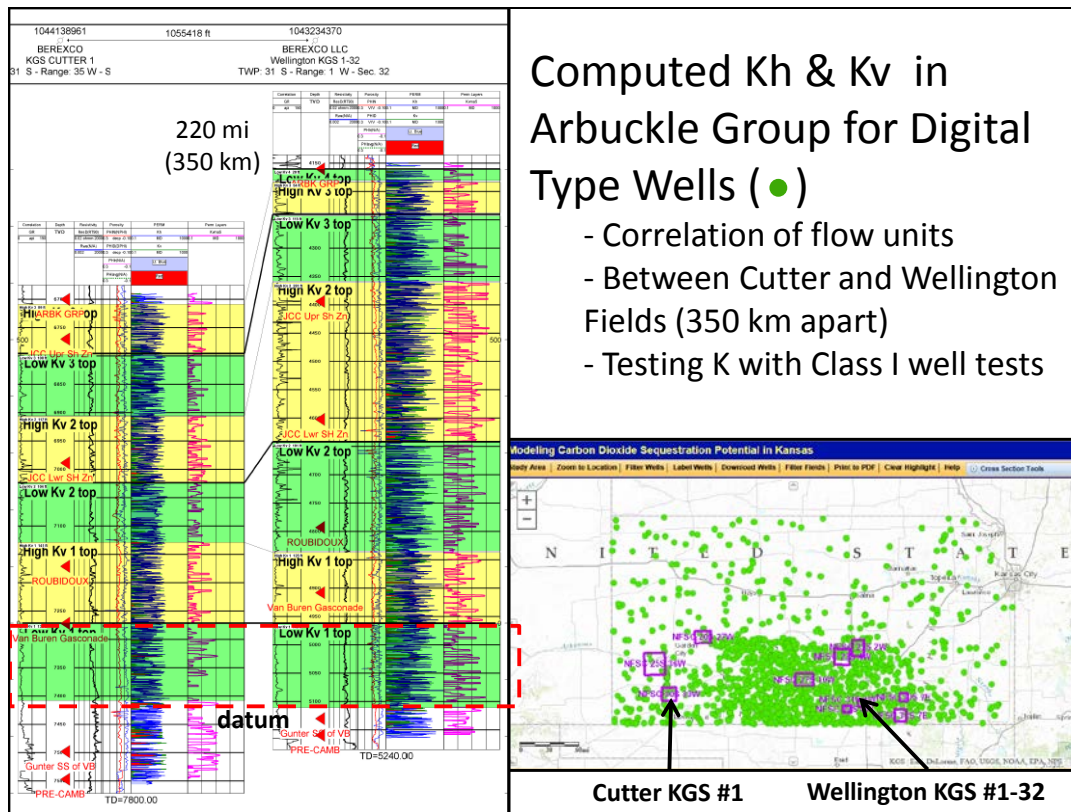
Once the permeability is established and distributed to the wells, the next steps include estimating the vertical permeability and defining the flow units. Considerations were given to the use of “Fisher Plots” as shown in **Figure 29** for the wells #1-32 and #1-28. This methodology includes 1) use the log of  $K_h$ , 2) determine the mean – using only depths where  $K_h$  is provided, 3) at each depth calculate the deviation of the  $\text{Log}(K_h)$  at that depth from the mean  $\text{Log}(K_h)$ , 4) plot the cumulative deviation vs depth where continual changes in direction indicate a zone of commonality (**Figure 29**). While this approach was considered, a visual correlation of flow units based on a combination of plots of  $K_h$  and  $K_v$  was defined to establish a reliable, regional correlation of flow units (**Figures 30 and 32**). Since the pore types and abundance are closely linked to lithofacies and stratigraphy, this is a satisfying outcome.

The flow units have been extended to all the wells that have penetrated the Arbuckle interval and structure and isopachous maps have been constructed for each flow unit (Figure 33). The flow units and their attributes will initially be used to simulate commercial scale  $\text{CO}_2$  injection at the

10 regional sites (Figure 33). Since the permeability ( $K_h$  and  $K_v$ ) and porosity are reported for every half foot, the data will be upscaled to accommodate the large volume of the model.



**Figure 29. Flow unit Fisher Plot – Cumulative deviation of the log kh from the mean log Kh versus depth for Wellington KGS #1-28 and #1-32. Arrows indicate zones of commonality where cumulative permeability increases at various rates.**



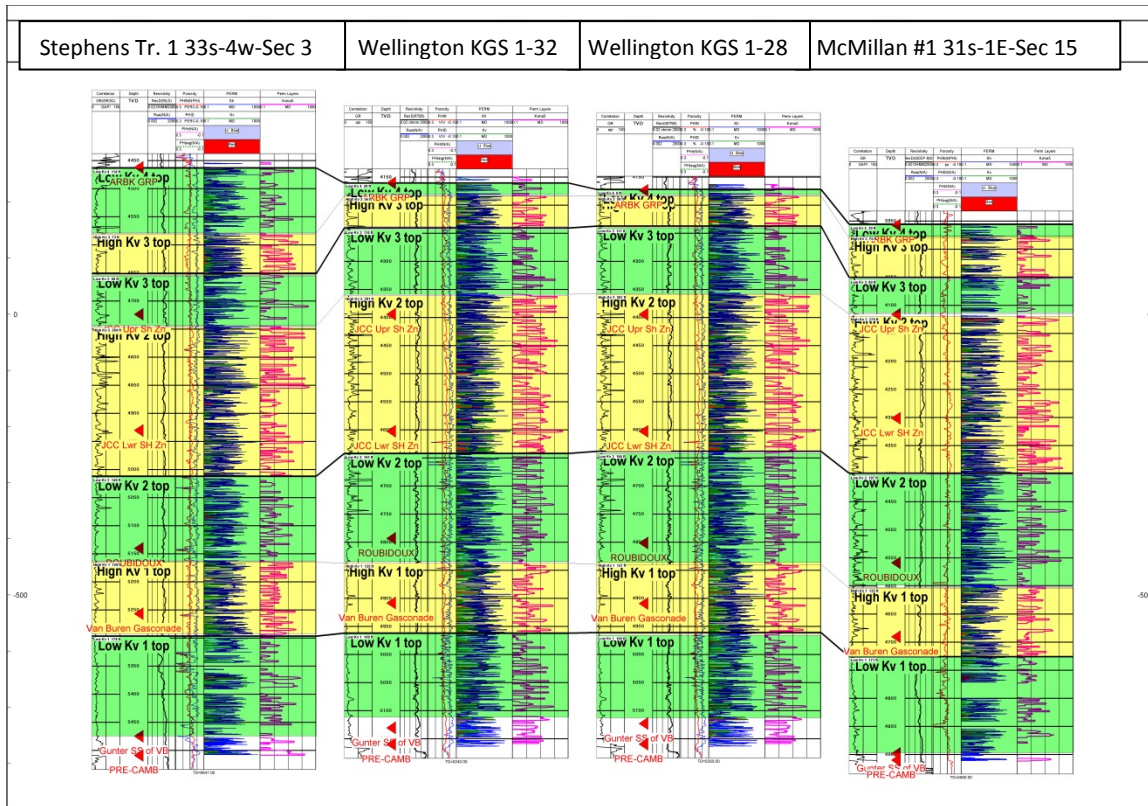


**Figure 31. SW-NE cross section illustrating correlation of flow units in the Arbuckle in the vicinity of Wellington Field.**

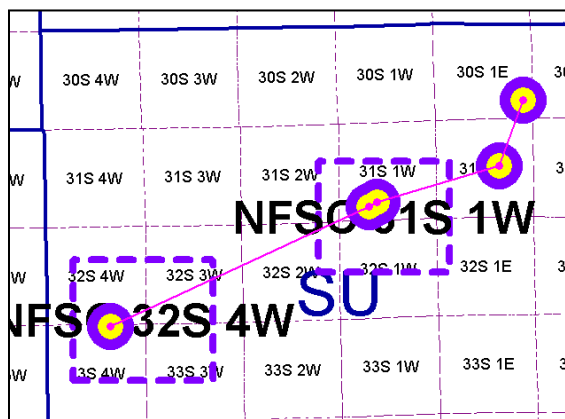


**Figure 32. Cross section index for cross section shown in Figure 31.**

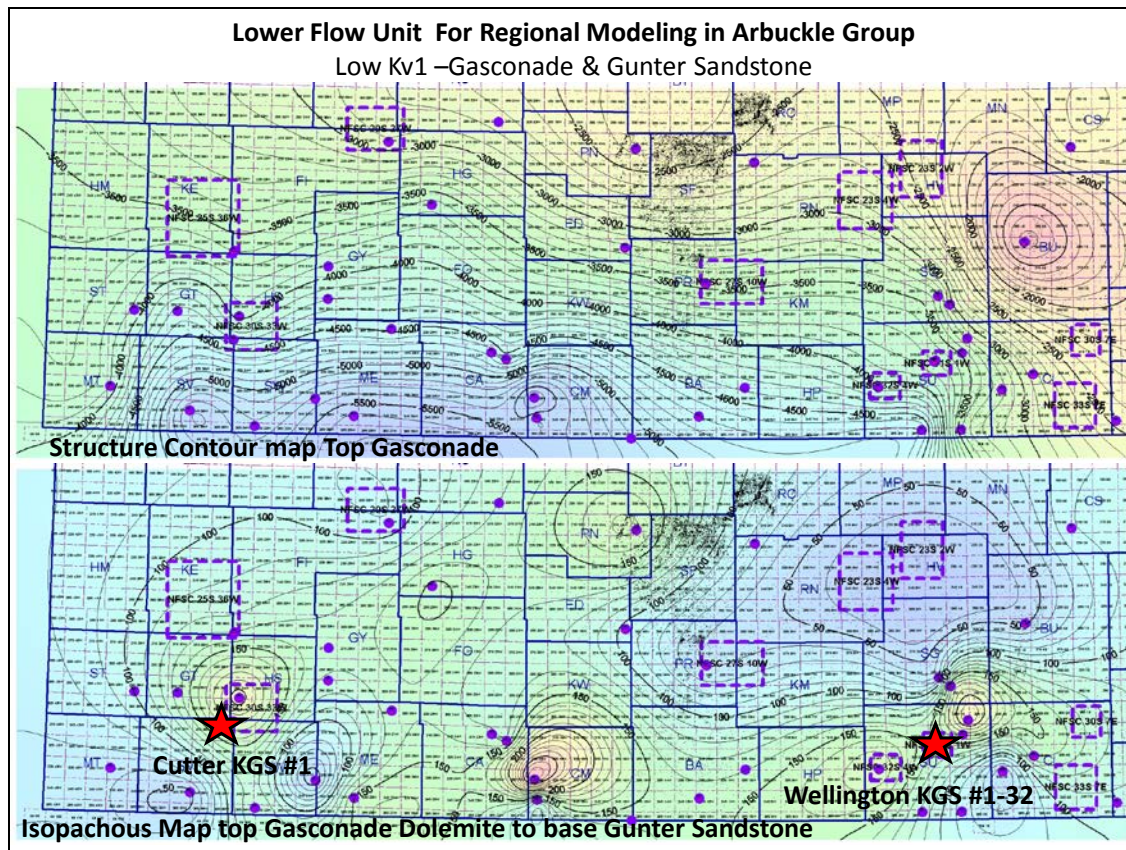


**Figure 33. Structure and isopachous maps of the lower flow unit of the Arbuckle for the southern Kansas study area. Purple boxes identify the locations of regional simulations.**

Simulations and estimates of CO<sub>2</sub> storage capacity will also utilize the capillary pressure to account for an important trapping mechanism of CO<sub>2</sub> (**Figure 34**). The standard capillary tables will be used as input into the simulations. It has been previously demonstrated that considerable amounts of microporosity exist in the Arbuckle, including the injection interval, that would contribute to trapping CO<sub>2</sub> (**Figure 35**).

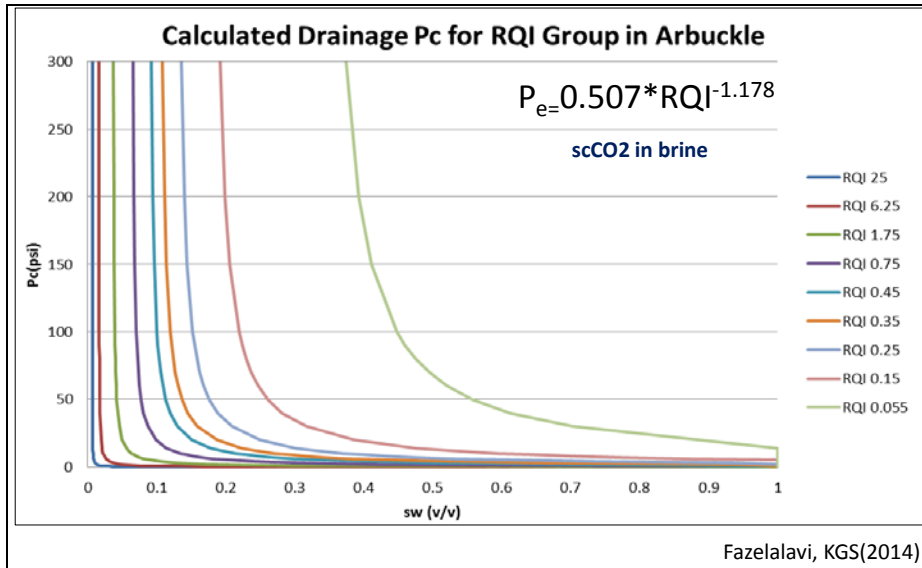


Figure 34. Range of pore types in Arbuckle Group quantified by reservoir quality index (RQI).

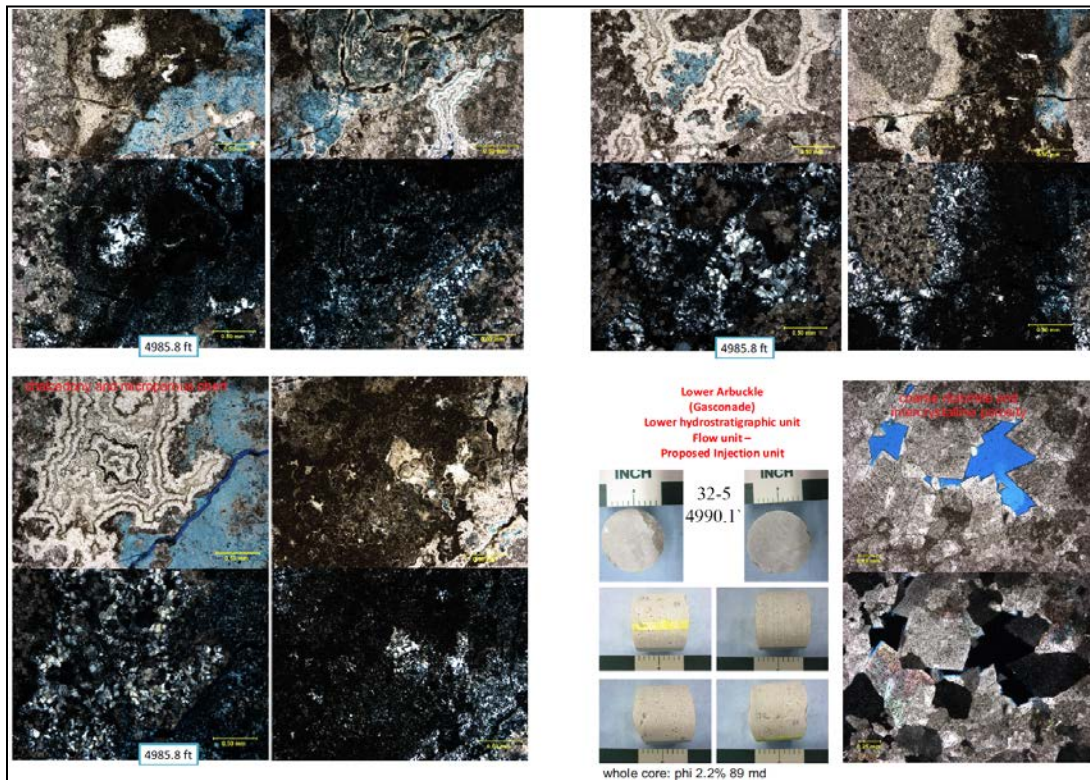


Figure 35. Microporosity is abundant, even in the lower Arbuckle injection zone that would be important for capillary trapping (imbibition) of CO<sub>2</sub>.

## **Java Web Application Update**

The analysis and visualization of the petrophysical data used in the regional assessments and interpretations is facilitated by the Java web applications tools, available as standalone <http://www.kgs.ku.edu/Gemini/Tools/Tools.html> or accessible via the interactive mapper.

## **New Database Connection to Retrieve Data**

A new database connection was developed to retrieve data that is now common to all of the web apps. Eventually, all GEMINI Tools will be combined into one directory structure to facilitate access and use of all (12 and counting) of the apps including passing information from one application to another. This integration will also facilitate updates to the software since one change can then be compiled for all 12 web apps instead of making 12 changes and recompiling, thus minimizing the chances for mistakes.

## **Type Log Applet Update**

TYPE LOG APPLLET is a vital means to keep the stratigraphic nomenclature and classification current and will be available to revise and refine the stratigraphic units (top picks) for the 502 type logs currently available for the state of Kansas. The application allows the user to add, modify, or verify existing stratigraphic units (tops). A stratigraphic committee will review the type logs and test the application before the completion of the project.

The procedure has been simplified with basic testing completed.

Step 1: Login to Enable Image Map:

Enter your email address into the text field and select the "Login" Button.

The "Display Wells in County Map" Button will turn Yellow, meaning it is selected.

Step 2: Choose Button to Display Wells by County or by Area:

Step 3: Click on Map to Plot Wells on a Township-Range-Section (TRS) Grid County Map or Area Map.

Step 4: User would review wells in assigned area containing "skeleton" stratigraphic units (top picks).

Step 5: User can agree with picks (top depths) or not. If you select one of the units, a dialog will appear identifying the owner of the top and asking you to "Agree" or "Disagree". If you do not agree with picks you need to enter a different depth, and then select the "Disagree" Button.

Step 6: If you enter a NEW Stratigraphic Unit (top pick) for a well, a top that is not already created, you become the owner for that top for that well. All other users can agree or disagree, if they disagree PLEASE put a depth you feel the top should be at.

- Only the owner of the top pick within a specific well will be allowed to change the depth. When you select the top a dialog will appear with the owner at the top of the dialog.
- For Each Top Pick within each well must have at least 3 people agreeing with the depth for the
  - top to be accepted as "GOLD". The goodness of a top pick has 4 levels as follows,
  - Lowest Level: "LEAD" The user creates a top within a well.
  - "COPPER" At least ONE Person agrees with your depth for the top pick.
  - "SILVER" At least TWO People agree with your depth for the top pick.
  - Highest Level: "GOLD" At least THREE People agree with your depth for the top pick.

NOTE: you can have any number disagreeing with your pick, but you only need three to agree to make it "GOLD".

Step 7: The Well is considered "COMPLETE" when at least 95% to 100% (100% is better) of the top picks are "GOLD". Mission accomplished.

User will be able to examine correlations in cross sections at assist in making refinements (Figure 36).

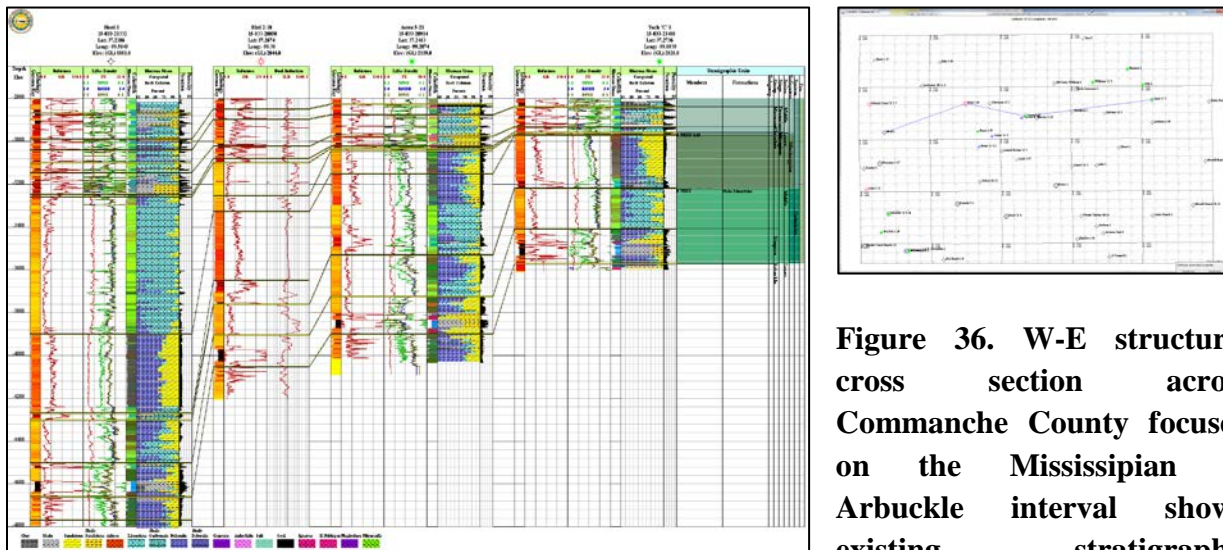


**Figure 36. W-E structural cross section across Commanche County focused on the Mississippian to Arbuckle interval shown existing stratigraphic**

**correlations and lithologic variability that will provide useful in establishing the correlations.**

## GEMINI Source Directory Update

All the web apps are now part of GEMINI after merging the Kimeleon Source Code. Presently the following web apps are part of the GEMINI Source Directory,

- Drill Stem Test (DST) Data Entry & Quantitative Analysis
- PFEFFER-java
- Hingle & Pickett Plots
- Kimeleon
- Zone Kluster (Zeke) - A Depth Constrained Cluster Analysis
- Profile (Expanded LAS File Viewer)

Specifically the primary source code that is common to all the above web apps are the Input-Output (I/O) Java Files. Read & Write Log ASCII Standard (LAS) files, Read Comma-separated values (CSV) files specifically for Tops, Core, although geologist report is included. Also the Kansas Geological Survey (KGS) well data download specifically LAS Files and Image Files and KGS Database downloads, i.e., Core Data, Tops Data, Perforation Data & DST Data. The following web apps still need to be added to the GEMINI Directory Structure,

- Synthetic Seismic Profile Plot
- 3D & 2D Cross Plots
- KGS Well Data Web Site - specifically the "Display Using Gemini" (LAS) Applet.

Production Plot & Decline Curve Analysis does not really have any common java source files so it will not be included in the GEMINI Java Source Directory. Cross Section may ultimately be separate from GEMINI because of the plot tracks and how they are handled, but the I/O is the same as above. There are a few of web apps that also need to be considered for inclusion in GEMINI,

- LAS File Viewer, which is really a subset of the Profile web app
- LAS File Viewer with Wavelet Analysis.
- Digitize Electric Well Log (E-Log) Images (Digitizer)

Finally, the LAS File Viewer may be replaced by using Profile and removing the input dialogs and allowing the user read in their data by the I/O Java classes. This decision will be made before the completion of the project. Current GEMINI app directory is shown in **Figure 37**.

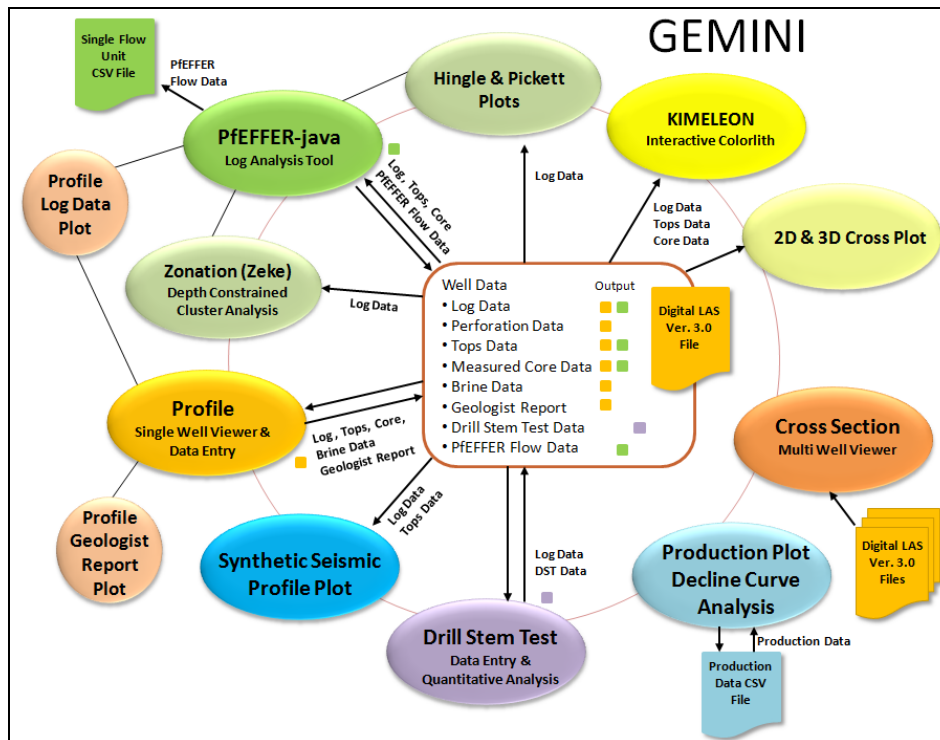


Figure 37. Gemini Directory of Java Apps

## Java Commonality

The Gemini Java File Matrix provides commonality of the files with each web app. There is also an I/O web app that is on both files, which identifies the base Input-Output (I/O) Java files that are basically common to all the web apps. The I/O web app only reads in the well data and writes the data to a Log ASCII Standard (LAS) version 3.0 file.

The I/O Java Files composed of the following,

- Read Log ASCII Standard (LAS) version 2.0 & version 3.0 Files
- Write Log ASCII Standard (LAS) version 3.0 File
- Read Comma-separated Values (CSV) Files
- Read Extensible Markup Language (XML) generated in the Kansas Geological Survey (KGS) ORACLE PL/SQL Stored Procedures.

## Improve Structure and Coding of Java-Applications Toward Commercialization

A proposal was prepared for an internal completion at KU to acquire funds that directed toward the commercialization of the Java web applications used to manage and view the data. The essence of this application is included in **Appendix F**.

**Task 13: Regional Source-Sink Relationships in approximately 17 Counties in South-Central Kansas**

**Subtask 13.1. Map major point CO<sub>2</sub> sources in Kansas**

**Subtask 13.2. Map major CO<sub>2</sub> sinks in Kansas**

The practical and economic linkage of the CO<sub>2</sub> source and sinks has been taken up with the Kansas Governor's Office and the Department of Commerce. See **Appendix E**.

**Task 14: Technology Transfer**

**Subtask 14.1. Build and maintain project website with interactive access to data and analyses via graphic display and analytical web tools**

**Subtask 14.2. Link project web-site to relevant DOE databases**

**Subtask 14.3 Submit project results to peer reviewed journals for publication**

**Task 15: Extend Regional Study of Ozark Plateau Aquifer System (OPAS) to the Western Border of Kansas – “Western Annex” and extend the type log database to include the whole state of Kansas to address fluid flow under commercial scale CO<sub>2</sub> sequestration.**

**Subtask 15.1. Extend regional study by evaluating CO<sub>2</sub> sequestration potential in 5000 mi<sup>2</sup> area west of the existing 17+ county area and extend the type log database to the whole state of Kansas to address fluid flow under commercial scale CO<sub>2</sub> sequestration.**

**Subtask 15.2. Create consortium of companies**

**Subtask 15.3. Encourage development of business plan to sequester emitted CO<sub>2</sub>**

**Task 16: Collect and Analyze Existing Data for Developing Regional Geomodel for Arbuckle Group Saline Aquifer in Western Annex**

**Subtask 16.1. Assemble, reprocess, and interpret existing 3D seismic and other data**

**Subtask 16.2. Analysis of KGS's gravity and magnetic data**

**Subtask 16.3. Remote sensing analysis**

**Task 17. Acquire (New) Data at a Select Chester/Morrow Field to Model CO<sub>2</sub> sequestration Potential in the Western Annex**

**Subtask 17.1. Collect existing seismic, geologic, and engineering data – Chester/Morrow fields**

**Subtask 17.2. Select Chester/Morrow field to acquire new data**

**Subtask 17.3. Collect new multicomponent 3D seismic survey**

**Subtask 17.4. Process multi-component 3D seismic survey**

## Subtask 17.5. Develop initial geomodel for the selected Chester/Morrow field

### Cutter and Eubanks Seismic Processing and Interpretation

The focus for the seismic interpretation using the p- and s-wave Cutter and Eubanks fields has been the lithological classification of the oil reservoir is via Hampson-Russell software. Useful results appear to be coming from both post-stack and pre-stack inversion. The pre-stack inversion results are then theoretically useable for a further classification to discriminate sand/shale/carbonate, etc. This is also done inside Hampson-Russell. It is clear that inversion alone moves us to a significantly greater understanding of the broad lithological context.

green = mostly shale  
yellow-orange = mostly sand  
blue-magenta = mostly carbonate

Several preliminary examples are shown from Cutter (**Figure 38**) and Eubank

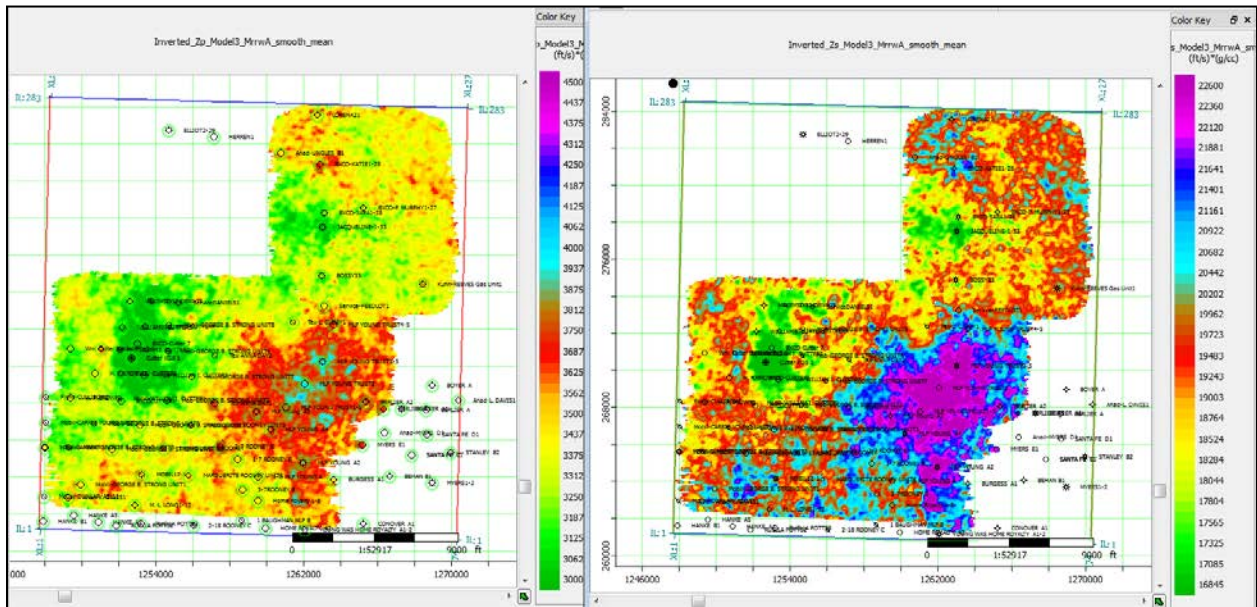


**Figure 38. Preliminary velocity\*density inversions in the Morrow Shale interval in Cutter Field.**

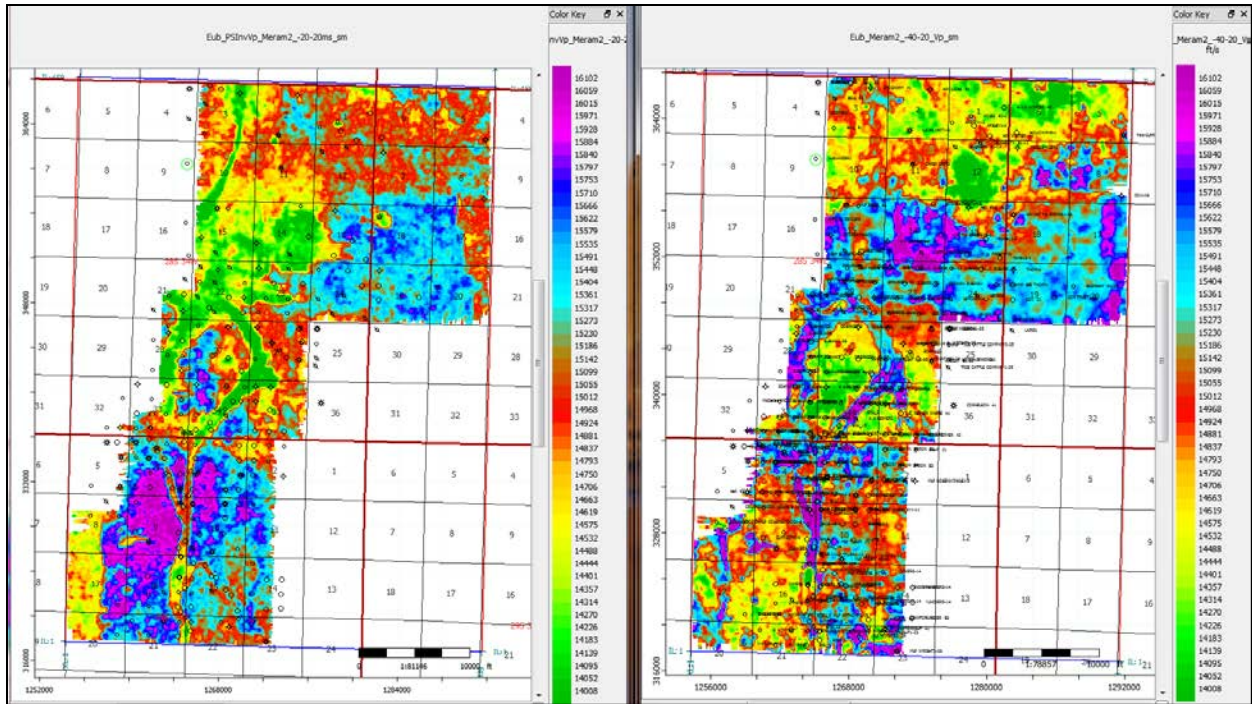


**Figure 39. Preliminary post- or pre-stack inversions of the velocity extraction 20-20 (20 ms above Meramec, with a window extending upward 20 ms) in Eubank Field.**

### **Seismic Interpretation of the Arbuckle at Cutter Field**

Clyde Redger, a student at KU, is conducting his thesis work titled, “*Seismic Reservoir Characterization of the Arbuckle Group and the Upper Morrow Sandstone from 3D-3C Seismic Data at the Cutter Field, southwest Kansas*”. This study will augment work by Hedke-Saenger and assess the capability of using multicomponent seismic methods to characterize Arbuckle and Upper Morrow sandstone reservoirs. Seismic attributes including acoustic impedance, shear impedance, and Vp/Vs ratios will be extracted from 3D P-wave and PS-wave volumes and will be used to generate reservoir property predictions. The accuracy of these predictions will be assessed with blind wells. This research is significant in that it will develop seismic methods for characterizing Arbuckle and Morrow reservoirs in the southwest Kansas region. Improved reservoir characterization in Arbuckle and Upper Morrow sandstone reservoirs could potentially benefit future enhanced oil recovery operations and CO2 sequestration projects.

- Subtask 17.6. Select location for Test Borehole #3**
- Subtask 17.7. Complete permitting requirements for Test Borehole #3**
- Subtask 17.8. Drill, retrieve core, log, and run DST – Test Borehole #3**
- Subtask 17.9. Openhole Wireline Logging – Test Borehole #3**
- Subtask 17.10. Wellbore Completion – Test Borehole #3**
- Subtask 17.11. Analyze wireline log - Test Borehole #3**

**Subtask 17.12. Test and sample fluids (water) from select intervals – Test Borehole #3**

**Subtask 17.13. Analyze Arbuckle core from Test Borehole #3**

**Subtask 17.14. Analyze Chester/Morrow core from Test Borehole #3**

**Subtask 17.15. PVT analysis of oil and water from Chester/Morrow oil reservoir**

**Subtask 17.16. Analyze water samples from Test Borehole #3**

**Update Kansas State University by Saugata Datta, Brent Campbell, Michael Vega**

### **Water Chemistry Analyses**

The analyses performed were for cation concentration determination in this quarter for both the swabbed and DST depths. Mass balance between cation and anion data was determined and was within the 5% acceptable range. Reanalysis of the water samples will be determined to ensure accuracy for both cations and anions. Samples will be analyzed again for cations at KGS this week for confirmation.

### **LLNL**

We will be working with Dr. Susan Carroll and Dr. Megan Smith from LLNL starting this summer. Our earliest projected start date, from Susan Carroll, is June 23rd. Our prediction that we will be able to analyze 1-2 cores this summer depending on the time it takes for each core plug. Core plugs have been sent to Dr. Jessie Maisano and Dr. Matthew Colbert of UT Austin's lab for our CT scans of the core plugs. We have sent 7 core plugs for pre-experimental flow through analysis and imaging. Michael Vega and Brent Campbell have been approved and received Academic Cooperation Participant status from LLNL.

Seven core plugs were chosen (five from Cutter, three from Wellington) to perform supercritical CO<sub>2</sub> flow through experiments at Lawrence Livermore National Laboratory. These designations were made based on mineralogical and petrophysical properties because these play a vital role in the overall water-rock geochemistry of CO<sub>2</sub> induced mineralization and precipitation reactions.

### **Mineralogy Updates**

Upon completion of the core plug analyses for Cutter KGS#1, further fine scale investigation was desired in order to supplement features observed in cores. Twenty-five new thin sections have thereby been processed where results will be shared in a few weeks' time:

The goal is to have a complete document with photomicrographs from each section and detailed descriptions by Mid-May, 2014.

## Cutter KGS #1 Brine Analyses

Field Data										
Name	Units	Swab 1	Swab 2	Swab 3	Swab 4	Swab 5	Swab 6	Swab 7	Swab 8	Swab 9
Date		6/25/2013	6/26/2013	7/1/2013	7/9/2013	7/10/2013	7/16/2013	7/22/2013	7/22/2013	7/23/2013
Depth	ft	7,543-7,532	7,442-7,430	7,234-7,218	7,056-7,046	6,904-6,880	6,686-6,676	6,558-6,543	6,204-6,194	6,010-6,000
Notes		45um filtered	unfiltered	unfiltered	10um filtered	10um filtered				
LDO	mg/L	-	-	2.04	2.15	2.2	5.05	5.78	2.9	1.87
Salinity	ppt	-	-	-	-	-	>70.74	64.56	>70.74	>70.74
Conductivity	mS/cm	-	683	-	-	-	29.3	90.2	52.1	6.49
ORP	mV	-293.1	-	240	-38.7	-128.4	-97	59.9	-64.1	-110.4
pH		7.19	6.71	6.79	6.52	6.71	6.9	8.07	6.6	6.77
Resistivity	MΩ-cm	6.61	-	3.1	2.42	2.01	3.44	1.11	2.08	1.14
Temp.	°C	34.4	38.6	-	30.4	34.7	21.3	25.8	36.7	37.6
TDS	mg/LQ	7.8	-	-	-	-	14.87	44.8	25.1	3.25

Cutter Major Ion Data						
Analyte Symbol	K	Mg	Ca	Na	Cl	SO4
Unit Symbol	mg/L	mg/L	mg/L	mg/L	mg/L	mg/L
Detection Limit	0.1	0.1	0.1	0.1	0.03	0.03
Analysis Method	ICP-OES	ICP-OES	ICP-OES	ICP-OES	IC	IC
SWAB 1	1460	1190	9010	52600	67800	294
SWAB 2	1360	1140	8400	49700	41700	241
SWAB 3	987	896	6090	35600	106000	882
SWAB 4-Bad Run	23.6	14.4	104	648		
SWAB 4-Good Run	1100	898	6510	34700	43000	443
SWAB 5	1410	1470	9100	47600	76000	417
SWAB 6	1250	1300	8810	40000	29200	268
SWAB 7	1060	247	2430	19800	143000	4730
SWAB 8	814	865	5410	28700	53100	375
SWAB 9	803	1020	5420	23700	115000	1620
SWAB 10	830	363	1650	15900	20900	1790
SWAB 11	930	1290	6950	29700	11500	202
DST 1	1280	1070	7820	46600	68400	295
DST 2	963	858	5640	34300	12200	228

- **Note:** Swab 4 was reran due to inaccurate data return. 2nd test gave data in-line with other ion chemistry.



**March '14 Cutter KGS#1 Thin Section  
Order**

<b>Order No.</b>	<b>Sample No.</b>	<b>Formation Name</b>	<b>Depth</b>
<b>1</b>	2-10	Morrow Sand	5261.1'
<b>2</b>	2-25	Morrow Sand	5276.5'
<b>3</b>	2-35	Morrow Sand	5286.25'
<b>4</b>	13-2	Kinderhookian	6501.3'
<b>5</b>	15-48	Simpson	6702.35'
<b>6</b>	16-27	Simpson	6741.45'
<b>7</b>	18-35	Simpson	6938.75'
<b>8</b>	19-9	Simpson	6972.8'
<b>9</b>	20-9	Gasconade	7098.85'
<b>10</b>	20-21	Gasconade	7110.35'
<b>11</b>	21-28	Gasconade	7177.25'
<b>12</b>	22-13	Gasconade	7190.7'
<b>13</b>	22-14	Gasconade	7191.4'
<b>14</b>	22-32	Gasconade	7209.9'
<b>15</b>	24-2	Gasconade	7235.25'
<b>16</b>	24-7-1	Gasconade	7340.55'
<b>17</b>	24-10	Gasconade	7343.2'
<b>18</b>	25-12	Gasconade	7405.3'
<b>19</b>	27-24	Gunter Sand	7553.65'
<b>20</b>	27-29	Gunter Sand	7558.7'
<b>21</b>	27-37	Gunter Sand	7566.2'
<b>22</b>	28-15	Gunter Sand	7582.1'

### *March '14 Wellington Thin Section Order*

<b>Order No.</b>	<b>Sample No.</b>	<b>Formation Name</b>	<b>Depth</b>
<b>23</b>	13-41	Upper Arbuckle	4225.7'
<b>24</b>	13-46	Upper Arbuckle	4230.3'
<b>25</b>	14-4	Upper Arbuckle	4247'

### **Cutter KGS#1 Depthwise Petrographic Summary**

#### Morrow Formation

The Pennsylvanian aged Morrow Formation is a ~200' thick tan to gray sandstone to mudstone that extends from 5250' to 5450' (roughly), with shaley mudstone to wackestone facies persisting within the latter 150'.

- Sands are poorly to moderately sorted (just a few times seen) with a prominence of fine to very fine grained sediments, however the variation in grain size approached very coarse grained in some samples (~5261.1', 5260.6'). Good intergranular porosity is exhibited throughout the upper half with the lower mudstone to wackestone portion being tight. Subrounded to subangular grains dominate the sandy portion of the formation. The Morrow shows quartz dominance in the upper sands and shaley argillaceous materials through the lower mostly micrite cemented mudstones, hinting at the possibility of carbonate cement in the sands.
- Wackestone to packstone facies in lower portion exhibit broken bioclasts, mostly in the form of crinoid stems and bivalves, at mostly <10% total surface area with ~30% at 5403'.
- Heavy oil show and odor is noticeable throughout the formation, as this represents the pay zone for Cutter field.

#### Chester Formation

The Mississippian Chester Formation is a ~180' thick gray/light gray to tan sandstone to siltstone to mudstone that extends from 5480'-5660', with gray to olive shaley mudstone to wackestone facies persisting in the first ~70', followed by ~10' of low porosity fine to very fine grained gray sandstone, then ~40' of gray/dark gray tight siltstone, ~30' of low to tight porosity of light gray to tan sandstone, with the final ~15' returning to tight gray mudstone to wackestone facies. Oil shows were present throughout the formation.

- The upper shaley mudstone to wackestone region (~5480'-5550) is tight with an abundance (~10-30%) of bioclasts (mostly crinoids) in the wackestone facies, although the overall zone is predominantly mudstone with wavy nonparallel shaley laminations (~50%).

- The upper sandstone (~5558'-5570') exhibits low porosity, is quartz dominated, and is fine to very fine grained. Wavy shaley lamination and small (mm wide) black shaley fragments are present throughout.
- The siltstone zone (~5571.6'-5610.4') shows to be very tight with mm scale pyrite grains present in almost half of the samples, sometimes as cherty replacement textures (low chert content overall i.e. <10% of samples). Dark wavy shaley laminae persist through a majority of samples and ~28% of samples exhibit bioturbation structures typically in the form of burrows. Quartz dominance and predominantly micrite cement make up the lithologic components in addition to scattered pyrite as described above.
- The lower sandy portion of the Chester (~5611.4-5643.9') is tan to light gray and fine grained. Slightly fractured regions exhibit low to moderate porosity (~50%) while the rest remains tight. This zone is again quartz dominated with mostly micrite cement, with one spotted pyrite occurrence and a possible glauconite nodule.
- The lower mudstone to wackestone zone (~5645.45'-5662.45') is similar to the upper facies of similar lithology, except the former is more mineralogically diverse. Pyrite was found in up to multi-cm scale nodules and as fracture infillings and distinct blue elongated chert nodules were observed towards the base.
- Only one sample (5664.8') was provided for the upper St. Louis lime, and it showed a tight white chalky fine grained limestone packstone supported by broken bioclasts that were too small to discern.

### **Osagean Stage**

The lower Mississippian aged Osage lime (~6361'-6370') is a white to light gray fine grained dolomite wackestone with an abundance of cm to multi-cm scale blue chert nodules. The zone exhibits an overall tight porosity with a slight vuggy region (~6363.7') bringing low to possibly moderate porosity. Vugs range from mm to cm scale. Larger vug (1/2 cm wide) showed infillings of secondary crystalline dolomite. Predominantly micrite cement supports broken mm scale bioclasts in the form of crinoids. 6368' shows shaley argillaceous banding along with mm scale pyrite grains.

### **Upper Kinderhookian Stage**

Upper Kinderhookian Stage rocks (~6373'-6650') show four distinct zones: gray/light gray fine grained dolomite wackestone to packstone (6370'-6470'), gray very fine grained sandstone to siltstone (~6473'-6484'), autoclastic cherty-dolomite brecciated zone (~6487'-6500'), and light gray/gray very fine grained dolomite mudstone (~6500'-6650').

- The uppermost wackestone to packstone facies is tight with an abundance of broken bioclasts (mostly crinoids (up to ~40%)) held intact by micritic cement. Cherty bedding is common in addition to shaley lamination and mineralogically it is relatively homogeneous with only dolomite, chert and argillaceous materials being observed.
- The very fine grained sandstone to siltstone zone is dominated by wavy argillaceous lamination, silty matrices and tight porosity, with observed minerals being dolomite, quartz, clays, and possibly chalcopyrite at ~6485'.
- The brecciated zone is composed of multi-cm scale angular chert clasts within a shaley mudstone (~30-40% shale) matrix and exhibits a significant amount of white powdery

clay material (~30%). Low to moderate intergranular and fracture porosity was observed. Brecciated region provides increased heterogeneity.

- The final mudstone zone throughout the lower half is characterized by light gray very fine grained dolomitic mudstones with tight porosity and a few notable accessory minerals (i.e. pyrite, chalcopyrite, clays) as well as the expected array of chert nodules (up to cm scale) and argillaceous fracture infillings. Micrite cement was dominant however a few sparry regions were noted, and a silty texture was observed throughout the zone.

### **Simpson Group**

The Simpson group is lithologically represented by gray to light gray dolomite mudstone to packstone facies and extends from ~6668' to 6986'. The upper half is packstone (fine to medium grained) dominated with the lower half being mostly mudstone (fine to very fine grained). The packstone zones typically exhibit low to moderate vuggy/intergranular porosity with vugs ranging from pinpoint to cm scale and often infilled with secondary crystalline dolomite. Mudstone zones are more commonly tight, however low vuggy and fracture porosity becomes prevalent towards the base.

- The uppermost ~20' of packstone (6668'-6696') contains mm scale skeletal fragments/bioclots, mostly in the form of crinoids, as well as pelloids, within micrite cement. Large cm scale chert nodules are not uncommon and in fact approach ~30-40% with depth (down to 6700'). Wavy argillaceous lamination and visible crystalline dolomite within matrix is also prevalent in this ~30' interval.
- A tight mudstone zone exists between 6702' and 6718', with visible mm scale pyrite grains at ~6705' and dark shaley banding throughout.
- A highly porous zone exists at ~6740' with brecciated dolomite mudstone lithology and vuggy pores visibly distributed within the entirety of the sample. Angular clasts contribute good intergranular porosity.
- Between 6900' and 6980' the lithology is predominantly mudstone with scattered packstone zones. A slight increase in fracture pathways and vuggy pores promotes relative heterogeneity and pore diversity, however overall porosity is still moderate to low. A slightly brecciated zone (autoclastic) at ~6940' provides enhanced zonal heterogeneity. White clayey infillings are common in this 90' zone, especially in fracture regimes. The cement type is mostly micrite with scattered regions of sparite, in particular around 6930'. Mineralogically this lower region of the Simpson group hosts dolomite (both in matrix and in secondary vitreous infillings), silica (in the form of chert nodules), and various clay minerals. A relative absence of observable sulfides in this lower depth was noted.
- The final 20' above the base is relatively homogeneous and increasingly tight in comparison to the pore types that precede it.

### **Gasconade Dolomite**

The Ordovician Gasconade dolomite is a fine to very fine grained gray/light gray dolomite mudstone to packstone that extends from ~7100'-7430'. A noticeable increase in vugs and fracture pathways in the middle of the formation (7191'-7339') promotes good vuggy and fracture porosity and therefore heterogeneity. A similar change is noted nearing the base (~7425'). Lithologically the Gasconade is dolomitic with large cm to multi cm scale chert

nodules, scattered sulfide minerals (mostly pyrite, some chalcopyrite ~7350') and clay minerals as fracture infillings that are likely Fe-rich (?). Some zones exhibited green claystone facies indicating the possibility of glauconite (7210', 7235'). Vugs are often infilled with vitreous crystalline dolomite rhombs, and such textures can often be seen in matrices. The cement type is mostly micrite with scattered regions of sparite (~7340', 7400'). Wavy laminae are present, but not common, throughout the formation. An autoclastic brecciated zone exists at ~7191' with angular cherty clasts providing increased intergranular porosity and overall heterogeneity.

### **Gunter Sand**

The Gunter sand is a fine to very fine grained light gray sandstone that extends from ~7530' to 7590'. Overall pore distribution is tight with a few zones showing low pinpoint and fracture porosity. Wavy nonparallel clayey/shaley lamination (gray to blue-green in color) persists through a majority of samples, with the green layers possibly indicative of glauconite and the gray layers demonstrating interbedded dolomite mudstone.

- A large cm scale chalcopyrite nodule was noted at ~7566' with a smaller mm scale nodule at ~7582'. Mm scale sub to euhedral glauconite crystals were spotted within the matrix of ~7558'.
- The upper region of this zone is moderately to well sorted with well-rounded grains with poorly sorted subrounded grains showing dominance nearing the base.
- Mineralogically the Gunter is composed of mostly quartz with scattered carbonate regions and a diverse array of accessory minerals (i.e. chalcopyrite, pyrite, glauconite and other clays, etc).

## **Task 18: Update Geomodels and Conduct Simulation Studies - Evaluate CO<sub>2</sub> Sequestration Potential in Arbuckle Group Saline Aquifer and by CO<sub>2</sub>-EOR in Select Chester/Morrow Field in the Western Annex**

**Subtask 18.1. Update geomodels of the Chester/Morrow sands and Arbuckle Group saline aquifer in selected field**

**Subtask 18.2. Optimize geomodel for simulation - Flow-unit identification, fracture characterization, and upscaling**

**Subtask 18.3. Simulate potential of CO<sub>2</sub> sequestration in Arbuckle Group saline aquifer**

**Subtask 18.4. Simulate of CO<sub>2</sub> sequestration potential by CO<sub>2</sub>-EOR in the selected Chester/Morrow field**

### **Simulation Studies of Chester/Morrow Oil Fields**

Shuck Field model simulations will be finished in the next quarter, slowed by the lack of well-scale data and what is there is paper (or pdf) rather than tabular digital. Cutter geomodel and the simulation will also be completed in the next quarter.

## **Task 19: Integrate Results with Larger 17+ County Regional Project in South-central Kansas**

### **Deliverables for the Final Report**

1. Reservoir geomodel of Wellington Mississippian Chat reservoir and its CO<sub>2</sub>-sequestration and CO<sub>2</sub>-EOR potential.
2. Reservoir geomodel of Arbuckle Group saline aquifer underlying Wellington field and its CO<sub>2</sub>-sequestration potential
3. Regional geomodel of OPAS covering 17+ counties in south central Kansas and its CO<sub>2</sub>-sequestration potential
4. Risk assessment studies related to CO<sub>2</sub> sequestration including characterization of leakage pathways, vertical communication within the Arbuckle Group, and well abandonment histories in the 17+ county study area and the Western Annex.
5. Geomodel and simulations of CO<sub>2</sub> sequestration potential of the Arbuckle Group saline aquifer and of CO<sub>2</sub>-EOR in a select Chester/Morrow incised valley sandstone oil reservoir in the Western Annex – a new addition of ~5,000 mi<sup>2</sup> to the regional study.
6. Results and interpretation of the seismic surveys, and interpretation of all laboratory analysis performed in the 17+ county study area and the Western Annex.

### **PRESENTATIONS AND PUBLICATIONS**

Watney, W.L., 2014, Carbon Storage and Utilization in Kansas – Are We Ready?: KU Department of Geology Colloquium, January 23.

Watney, W.L., 2014, Fluid Migration and Accumulation within the Mississippian: Why 2% oil cut here, 15% oil cut one mile away: AAPG Mississippian Forum, Oklahoma City (also brought Wellington KGS #1-32 core to workshop).

### **KEY FINDINGS**

1. Geomodels of Mississippian and Arbuckle being updated including a significant improvement in the resolution of the structural content in the seismic data.
2. The Mississippian reservoir geometry is closely tied to structural activity that was active at the time of deposition. The strata offlap to the west and toplap to the east. Overlying “chat” residual chert is thicker on the highest crestal, eastern portion of Wellington Field.
3. Conductive fractures dominate fluid flow into wellbore (PLT) in low K reservoirs. The Mississippian has both high and low permeability facies, thus fracture modeling is very important. CO<sub>2</sub> injection will likely be affected by the fractures presenting themselves as either conduits or barriers to the CO<sub>2</sub>.

4. Mississippian has similar tight basinal expressed as the “lower Cowley facies” that are part of the TST. These facies thicken unto the Wellington structure while the reservoir facies undergo toplap and truncation from west to east across the field.
5. Seismic attributes aid *comprehensive* characterization, particularly to delimit high angle fractures and faults that do not intersect the wellbores and have smaller offsets that are usually attributed to flexure.
6. Production decline can be overcome or injection of fluids like CO<sub>2</sub> can be tailored when fractures and faults are considered in the geomodeling and simulation activities.
7. Simulation of injecting 40,000 tonnes of CO<sub>2</sub> into the Arbuckle at Wellington results in maximum pressure at approximately hydrostatic and size of plume within 2000 ft in diameter.
8. Interactive mapper includes known and inferred faults; tools to filter oil fields by cumulative production, depth, production bubble map to show time change and relative difference between leases useful in scoping heterogeneity in the process of targeting opportunities for CO<sub>2</sub>-EOR.
9. A methodology to estimate horizontal and vertical permeability in wells with typical modern well log suites has been developed using core, log, and well test data from Wellington and Cutter fields. A neural network using gamma ray, total porosity, and connected porosity [ $p_{hir} = (R_{wa}/Res_{Deep})^{0.5}$ ] is used to extend permeability estimates to the key type wells in the region.
10. Regional flow units based on the permeability have been established for the type wells. The flow units conform to the conventional stratigraphic correlations. Local fracture and faulting or local cross flow dissolution will provide local variations. However, the controls of permeability are still tied closely to lithofacies and their pore type constrained by the strata architecture, namely a hierarchy of peritidal cycles. Larger scale cycles are widely correlatable.
11. Java Web Apps are undergoing revisions that will facilitate use, updating, and portability for use on other computer platforms. Moreover, the tools are being grouped to allow user to access software in a logical workflow. The archive data still remains the LAS 3.0 file that captures the resulting analyses.

## PLANS

1. Complete geomodeling and simulations of commercial scale CO<sub>2</sub> injection at the 10 regional sites and the regional CO<sub>2</sub> assessment.
2. Complete the updates for the Wellington geomodels simulations.
3. Complete the modeling of the SW Kansas fields.
4. Gather results for write final report.

## REFERENCES

- 1986 D. R. Collins and J. H. Doveton, Color Images of Kansas Subsurface Geology from Well Logs, *Computer & Geosciences*, Vol. 12, No. 4B, pp.519-526
- Collins, D. R., and Doveton, J. H., 1988, Application of color information theory to the display of lithologic images from wireline logs: *Trans. SPWLA, 29th Ann. Logging Symposium*, Paper II, 15 p. Reprinted in *Geobyte*, 1989, v. 4, no. 1, p. 16-24.
- Collins, D. R., and Doveton, J. H., 1988, Color image transformations of wireline logs as a medium for sedimentary profile analysis: *Bull. Canadian Petr. Geology*, v. 36, no. 2, p. 186-190.
- 1989 Doveton, The Dakota Aquifer Program Annual Report, FY89 Kansas Geological Survey, Open-File Rept. 90-27 Annual Report, FY89-Appendix B ([http://www.kgs.ku.edu/Dakota/vol3/fy89/app\\_b.htm](http://www.kgs.ku.edu/Dakota/vol3/fy89/app_b.htm))
- 1989 David R. Collins, Visualization of Subsurface Geology from Wireline Logs, Digital Mapping Techniques '98-Workshop Proceedings U. S. Geological Survey Open-File Report 98-487
- Doveton, J.H., 1994, Geological Log Analysis Using Computer Methods: AAPG Computer Applications in Geology, No. 2, AAPG,Tulsa, 169 pp.
- Macfarlane,P.A., Doveton,J.H., Feldman, H., Butler, J.J., Jr., Combes, J.M., and Collins, D.R.,1994, Aquifer/aquitard units of the Dakota Aquifer System in Kansas: Methods of delineation and sedimentary architecture effects on ground-water flow and flow properties: *Jour. Sedimentary Research*, v. B64, No. 4, p. 464-480.
- Canadian Well Logging Society, 1999, LAS 3.0 Log ASCII Standard Document File Structures [http://www.cwls.org/las\\_info.php](http://www.cwls.org/las_info.php)
- 2005 Matt Hall, Composite Colour Display of Spectral Gamma-Ray Logs, *Canadian Well Logging Society*, Dec 2005, v.24
- Victorine, J., Watney, W.L., and Bhattacharya, S., 2005, Use of XML and Java for Collaborative Petroleum Reservoir Modeling on the Internet, *Computers and Geosciences*, v. 31, no. 9, p. 1151-1164.
- Crangle, Jr., R.D., 2007, Log ASCII Standard (LAS) files for geophysical wireline well logs and their application to geologic cross sections through the central Appalachian basin: Open File Report 2007-1142, U.S.G.S., 14 p.
- Watney, W.L., Franseen, E.K., Byrnes, A.P., and Nissen, S.E., 2008, Contrasting styles and common controls on Middle Mississippian and Upper Pennsylvanian carbonate Platforms

in the Northern Midcontinent, U.S.A.: in Lukasik, J., and Simo, A., editors, Controls on Carbonate Platform and Reef Development, SEPM Special Publication 89, Society of Sedimentary Geology, Tulsa, p. 125-145.

Bhattacharya, S., Byrnes, A.P., Watney, W.L., and Doveton, J.H., 2008, Flow unit modeling and fine-scale predicted permeability validation in Atokan sandstones: Norcan East field, Kansas: AAPG Bulletin, v. 92, no. 6, p. 709-732.

Watney, W.L. et al., 2003, September 24, 2003, GEMINI Project Review Workshop (final release summary) <http://www.kgs.ku.edu/Gemini/Presentations/09242003/1-Overview.pdf>.

Lynn Watney, John H. Doveton, Timothy R. Carr, Geoffrey C. Bohling, John Victorine, JP Pakalapati, Saibal Bhattacharya, Alan P. Byrnes, Glen Gagnon, Ken Stalder, Melissa Morre, Martin K. Dubois, Willard J. Guy and Kurt Look, 2004, Collaborative Geo-Engineering Reservoir Characterization and Modeling on the Web: Kansas Geological Survey Open-File Report 2004-36, <http://www.kgs.ku.edu/PRS/publication/2004/AAPG/GEMINI/>.

John H. Doveton, W. Lynn Watney, and Geoffrey C. Bohling, 2004, Theory and Practice of a Web-based Intelligent Agent in the Location of Pay Zones on Digital Well Log Files: Kansas Geological Survey, Open-File Report 2004-28, <http://www.kgs.ku.edu/PRS/publication/2004/AAPG/Brine/>

Watney, W.L., Bhattacharya, S., Byrnes, A., Doveton, J., Victorine, J., and Brownrigg, R., 2004, PTTC Workshop - Practical Petroleum Reservoir Characterization and Modeling Using Free Web-Based Software Tools and Data, Lawrence, KS, November 16, <http://www.kgs.ku.edu/Gemini/gemini-reports.html>.

## **SPENDING PLAN**

Please see next page.

Baseline Reporting Quarter (From Q1A to Q1B)	Fiscal 2017				Fiscal 2018				Fiscal 2019				Fiscal 2020				Fiscal 2021				Fiscal 2022				Fiscal 2023				Fiscal 2024			
	12/30/16	1/18/17	3/15/17	4/11/17	3/21/18	4/11/18	3/21/18	4/11/18	3/21/19	4/11/19	3/21/19	4/11/19	3/21/20	4/11/20	3/21/20	4/11/20	3/21/21	4/11/21	3/21/21	4/11/21	3/21/22	4/11/22	3/21/22	4/11/22	3/21/23	4/11/23	3/21/23	4/11/23	3/21/24	4/11/24	3/21/24	4/11/24
Federal Share	\$1,007,622.75	\$1,007,622.75	\$1,007,622.75	\$1,007,622.75	\$0.00	\$0.00	\$0.00	\$0.00	\$1,189,543.00	\$1,189,543.00	\$1,189,543.00	\$1,189,543.00	\$1,189,543.00	\$1,189,543.00	\$1,189,543.00	\$1,189,543.00	\$1,189,543.00	\$1,189,543.00	\$1,189,543.00	\$1,189,543.00	\$1,189,543.00	\$1,189,543.00	\$1,189,543.00	\$1,189,543.00	\$1,189,543.00	\$1,189,543.00	\$1,189,543.00	\$1,189,543.00	\$1,189,543.00	\$1,189,543.00	\$1,189,543.00	\$1,189,543.00
Non-Federal Share	\$277,260.75	\$277,260.75	\$277,260.75	\$277,260.75	\$0.00	\$0.00	\$0.00	\$0.00	\$303,182.75	\$303,182.75	\$303,182.75	\$303,182.75	\$303,182.75	\$303,182.75	\$303,182.75	\$303,182.75	\$303,182.75	\$303,182.75	\$303,182.75	\$303,182.75	\$303,182.75	\$303,182.75	\$303,182.75	\$303,182.75	\$303,182.75	\$303,182.75	\$303,182.75	\$303,182.75	\$303,182.75	\$303,182.75	\$303,182.75	\$303,182.75
Total Planned (Federal and Non-Federal)	\$1,284,883.50	\$1,284,883.50	\$1,284,883.50	\$1,284,883.50	\$0.00	\$0.00	\$0.00	\$0.00	\$1,492,725.75	\$1,492,725.75	\$1,492,725.75	\$1,492,725.75	\$1,492,725.75	\$1,492,725.75	\$1,492,725.75	\$1,492,725.75	\$1,492,725.75	\$1,492,725.75	\$1,492,725.75	\$1,492,725.75	\$1,492,725.75	\$1,492,725.75	\$1,492,725.75	\$1,492,725.75	\$1,492,725.75	\$1,492,725.75	\$1,492,725.75	\$1,492,725.75	\$1,492,725.75	\$1,492,725.75	\$1,492,725.75	\$1,492,725.75
Cumulative Baseline Cost	\$1,284,883.50	\$2,569,767.00	\$3,854,650.50	\$5,139,534.00	\$5,139,534.00	\$5,139,534.00	\$5,139,534.00	\$5,139,534.00	\$6,329,077.75	\$7,518,620.75	\$8,708,163.75	\$9,897,706.75	\$11,087,249.75	\$12,276,792.75	\$13,466,335.75	\$14,655,878.75	\$15,845,421.75	\$17,034,964.75	\$18,224,507.75	\$19,414,050.75	\$20,603,593.75	\$21,793,136.75	\$22,982,679.75	\$24,172,222.75	\$25,361,765.75	\$26,551,308.75	\$27,740,851.75	\$28,930,394.75	\$30,119,937.75	\$31,309,480.75	\$32,499,023.75	\$33,688,566.75
<b>Actual Invoiced Costs</b>																																
Federal Share	\$4,619.93	\$84,603.97	\$484,428.37	\$111,465.52	\$238,675.97	\$1,902,936.55	\$625,853.17	\$275,754.50	\$523,196.12	\$453,026.11	\$238,793.52	\$1,282,545.00	\$1,314,155.54	\$395,519.33	\$299,654.96	\$465,714.15	\$190,945.64	\$234,648.28	\$32,999.36	\$15,863.56	\$15,863.56	\$15,863.56	\$15,863.56	\$15,863.56	\$15,863.56	\$15,863.56	\$15,863.56	\$15,863.56	\$15,863.56	\$15,863.56	\$15,863.56	\$15,863.56
Non-Federal Share	\$0.00	\$43,960.64	\$40,684.78	\$13,156.88	\$55,510.30	\$35,887.34	\$414,511.02	\$50,247.24	\$16,887.06	\$61,883.20	\$150,848.51	\$27,183.41	\$12,637.49	\$65,889.76	\$23,262.67	\$34,263.56	\$915,863.56	\$915,863.56	\$915,863.56	\$915,863.56	\$915,863.56	\$915,863.56	\$915,863.56	\$915,863.56	\$915,863.56	\$915,863.56	\$915,863.56	\$915,863.56	\$915,863.56	\$915,863.56	\$915,863.56	\$915,863.56
Total Invoiced Costs-Quarterly (Federal and Non-Federal)	\$4,619.93	\$128,564.61	\$525,113.15	\$124,622.40	\$294,186.27	\$1,938,823.89	\$1,040,364.19	\$226,001.74	\$69,083.18	\$514,909.31	\$389,642.03	\$1,510,728.41	\$1,426,793.94	\$461,409.09	\$322,917.63	\$499,977.71	\$1,006,809.20	\$1,006,809.20	\$1,006,809.20	\$1,006,809.20	\$1,006,809.20	\$1,006,809.20	\$1,006,809.20	\$1,006,809.20	\$1,006,809.20	\$1,006,809.20	\$1,006,809.20	\$1,006,809.20	\$1,006,809.20	\$1,006,809.20	\$1,006,809.20	
Cumulative Invoiced Costs	\$4,619.93	\$93,178.58	\$377,601.95	\$489,067.37	\$783,243.34	\$1,786,180.19	\$2,827,033.36	\$3,053,035.10	\$3,122,122.26	\$3,637,031.57	\$3,816,873.60	\$5,327,602.01	\$6,744,395.95	\$7,155,805.04	\$7,478,647.67	\$7,978,565.38	\$9,000,374.58	\$10,007,183.78	\$11,014,047.34	\$12,020,910.90	\$13,027,774.46	\$14,034,638.02	\$15,041,501.58	\$16,048,365.14	\$17,055,228.70	\$18,062,092.26	\$19,068,955.82	\$20,075,819.38	\$21,082,682.94	\$22,089,546.50	\$23,096,410.06	
<b>Variance</b>																																
Federal Share	\$1,003,002.82	\$920,018.78	\$513,194.38	\$896,217.23	\$238,675.97	\$1,902,936.55	\$625,853.17	\$275,754.50	\$523,196.12	\$453,026.11	\$238,793.52	\$1,282,545.00	\$1,314,155.54	\$395,519.33	\$299,654.96	\$465,714.15	\$190,945.64	\$234,648.28	\$32,999.36	\$15,863.56	\$15,863.56	\$15,863.56	\$15,863.56	\$15,863.56	\$15,863.56	\$15,863.56	\$15,863.56	\$15,863.56	\$15,863.56	\$15,863.56	\$15,863.56	
Non-Federal Share	\$277,260.75	\$277,260.75	\$277,260.75	\$277,260.75	\$0.00	\$0.00	\$0.00	\$0.00	\$303,182.75	\$303,182.75	\$303,182.75	\$303,182.75	\$303,182.75	\$303,182.75	\$303,182.75	\$303,182.75	\$303,182.75	\$303,182.75	\$303,182.75	\$303,182.75	\$303,182.75	\$303,182.75	\$303,182.75	\$303,182.75	\$303,182.75	\$303,182.75	\$303,182.75	\$303,182.75	\$303,182.75	\$303,182.75	\$303,182.75	\$303,182.75
Total Variance-Quarterly (Federal and Non-Federal)	\$1,280,263.57	\$1,200,279.53	\$790,455.13	\$1,173,478.00	\$238,675.97	\$1,902,936.55	\$625,853.17	\$275,754.50	\$826,378.87	\$756,208.86	\$541,976.27	\$1,585,727.75	\$1,617,338.29	\$698,702.08	\$602,937.71	\$768,896.90	\$494,128.39	\$537,831.03	\$63,181.11	\$47,046.31	\$47,046.31	\$47,046.31	\$47,046.31	\$47,046.31	\$47,046.31	\$47,046.31	\$47,046.31	\$47,046.31	\$47,046.31	\$47,046.31	\$47,046.31	
Cumulative Variance	\$1,280,263.57	\$2,480,533.10	\$3,270,988.23	\$4,444,466.23	\$4,683,142.20	\$6,586,078.75	\$7,211,931.37	\$7,487,685.87	\$7,656,882.03	\$8,171,791.34	\$8,351,633.86	\$9,862,361.37	\$11,479,700.66	\$12,097,402.74	\$12,397,057.70	\$12,865,954.60	\$13,360,082.99	\$13,854,211.38	\$14,348,339.77	\$14,842,468.16	\$15,336,596.55	\$15,830,724.94	\$16,324,853.33	\$16,818,981.72	\$17,313,110.11	\$17,807,238.50	\$18,301,366.89	\$18,795,495.28	\$19,289,623.67	\$19,783,752.06	\$20,277,880.45	

## APPENDIX A.

### *Diagenesis and distribution of diagenetic facies in the Mississippian of south-central Kansas*

Luis G. Montalvo<sup>1</sup>, Luis Gonzalez<sup>1</sup>, Lynn Watney<sup>2</sup>

1) Department of Geology, University of Kansas, Lawrence, KS

2) Kansas Geological Survey, University of Kansas, Lawrence, KS

#### **Key Findings**

- Paragenesis from four Mississippian cores suggests that chertification and dolomitization occurred early in the diagenesis.
- The majority of the porosity was developed during the onset of meteoric diagenesis with minor porosity developed during burial.
- Image analysis show that porosity is higher in dolomitized facies, and followed by sponge-spicule rich packstones and grainstones with high content of moldic and vuggy porosity.
- Calcite cementation plays an important role in porosity destruction after generation of porosity in meteoric settings.

#### **Significance**

The Mississippian system in south-central Kansas, a hydrocarbon prolific system of rocks, has very complex rock textures and petrophysical characteristics that resulted from passage through different diagenetic environments (Montgomery et al., 1998, Watney et al, 2001, Mazullo et al., 2009). Understanding how these textures were formed is important because producing hydrocarbon units are tied to a specific set of diagenetic textures (e.g. intercrystalline porosity in dolomites, sponge-spicule moldic porosity, chert microporosity). Therefore, any reservoir quality evaluation needs a deliberate knowledge of diagenesis in the formation to understand the generation and occlusion of porosity, and maximize the production capacity of the reservoir. The objective of this research is to determine the origin and nature of the different diagenetic facies in the Mississippian system and understand their stratigraphic distribution in south-central Kansas. Four Mississippian cores in three different localities are used to cover a broad spectrum of diagenetic alterations in the Formation (Fig. 1). The contribution of this research will enhance interpretations of stratigraphy, reservoir characteristics and paleotopographic reconstructions implied from interpreted diagenetic environments in the Mississippian system.

#### **Geologic Setting**

The Mississippian System is found on cores in south central Kansas at more than 4,000 ft below the surface. It was deposited in shallow tropical seas of a gently southward dipping carbonate platform that covered most of Kansas. In the southern region of Kansas the shelf edge of this platform is found and it borders the Anadarko basin near the Kansas-Oklahoma state line. The stratigraphy is predominantly restricted to Kinderhookian, Osagean and Lower Meramecian stages and include from base to top: (1) dark siltstone and shale of the Kinderhookian shale, (2) dark, argillaceous, skeletal lime wackestone and packstone interbedded with calcareous shales comprising the Osagean limestone, (3) brown, argillaceous and dolomitic limestones containing

intervals of dark-colored, bedded chert, composing the Cowley facies, and (4) light-colored, spiculitic chert of the “chat” (Figure 1)(Montgomery et al., 1998).

The Mississippian is characterized by a regional unconformity found throughout most of the subsurface of Kansas separating Mississippian and Pennsylvanian strata (Merriam, 1963). This unconformity resulted from a regional uplift (Central Kansas uplift) and eustatic drop in sea level near the end of the Mississippian (Gutschick and Sandberg, 1983). The surface of this unconformity is preserved as a paleokarst deposit. In many oil fields, a chert breccia, informally called “the Mississippian chat”, is the main reservoir rock that formed during karstification related to pre-Pennsylvanian unconformity. Recent interpretations by Mazullo et al. (2009) show that other minor unconformities can be found within the Mississippian strata. These minor unconformities resulted from fluctuations in sea level that intermittently exposed and submerged the shelf edge. Fluctuations in sea-level are important because they can change the diagenetic environment conditions through time.

### **Methods**

The petrography of four cores (Fig. 1) is interpreted to determine the properties and the origin of the different diagenetic facies and fit them into a paragenetic framework. Transmitted light microscopy, cathodoluminescence and scanning electron microscopy are used for thin section descriptions. In order to understand the relationship between diagenetic events and porosity, porosity calculations from point counting on photomicrographs is used. Diagenetic interpretations will be supported with geochemical analysis (stable isotopes; trace elemental concentrations of Ca, Mg, Sr, Fe and Mn from electron microprobe) to determine the environment at which minerals are precipitated and the source of the texture modifying fluids. X-ray diffraction analyses are performed to determine the mineral composition of complex facies. Petrophysical data is by far more abundant than core data and thus it will be used to determine the relationship between stratigraphy and paragenesis in each locality by building 3d static models using SIS Petrel software.

### **Preliminary Results**

#### *Rhodes Field (Cores: Harbaugh UB15 and George Michael 1-8)*

The Mississippian section covered in two cores from the Rhodes field belongs to the Cowley facies. Chert breccia (“chat”), green shale interbedded with lenses of spiculite wackestone or packstone, discontinuous porcelaneous chert beds, and echinoderm rich packstone or grainstone are the major lithologies recognized in cores on the basis of texture, grain types and diagenetic alterations. Of all the lithologies the chert breccia (“chat”) and spiculite wackestone or packstone contain the highest porosities, <8% and <13% respectively. The presence of microporosity in many chert fragments suggests that this numbers can be higher.

Paragenesis in the Cowley facies suggests at least nine events of porosity destructive cementation including: chertification, chalcedony cementation, clay cementation, calcite cementation, and baroque dolomite cementation. The relative time of their occurrence based on petrographic cross-cutting relationships is shown in a paragenesis diagram in figure 2. Porosity enhancing processes are less common and are particularly tied to dissolution of carbonate and silica during the onset of meteoric environment (karstification). A considerable amount of microporosity, vuggy porosity and siliceous sponge-spicule moldic porosity is found throughout the Formation. The monaxon sponge-spicules are made of amorphous Opal-A, a very metastable form of silica. In areas where the sponge-spicules are not preserved by early chertification (or by

other forms of silica) they dissolve out easily. This dissolution is interpreted to occur during meteoric alteration when the fluids were no longer supersaturated with respect to silica.

In particular facies, calcite cementation has occluded most of the sponge-spicule molds and fractures reducing porosity by <5%. Cross-cutting relationships and analysis of cathodoluminescence images suggest that calcite was precipitated during a meteoric environment and continued during the early burial conditions. Calcite fractures appeared compactionally deformed in core samples. A late void-filling calcite cement is also found after precipitation of baroque dolomite. Stable isotope data from these cements is being collected to support the diagenetic interpretations.

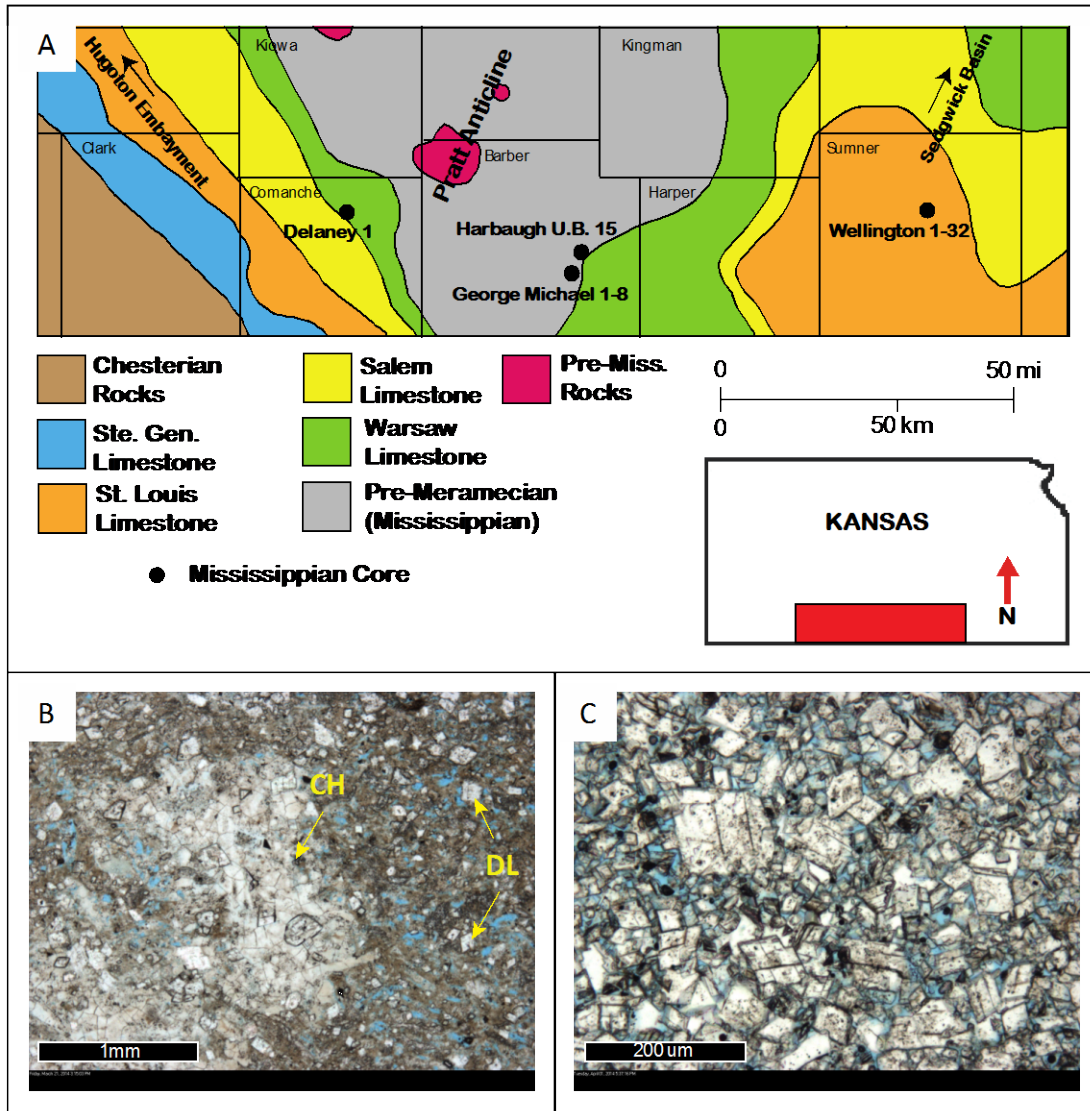


Figure 1. A) Mississippian-Pennsylvanian Unconformity subcrop map for the study area. The location of four Mississippian cores used in this study is illustrated. (Modified from Franseen, 2006). B) Photomicrograph of a sponge-spicule rich cherty and dolomitic limestone. Nodular chert (CH) still preserves some of the sponge-spicule textures. Sponge-spicules outside chert nodules were dissolved leaving a mosaic of moldic porosity (blue epoxy). Photomicrograph was taken in plane-polarized light (George Michel 1-8, 4611 ft). C) Photomicrograph of a dolomite

with a high content of intercrystalline porosity. Dolomite is characterized by finely to medium crystalline rhombs (20-180  $\mu\text{m}$ ) forming a planar-euhedral mosaic. Photomicrograph was taken in plane-polarized light (Wellington 1-32, 3892.25 ft).

Dolomite is locally found in both cores. It replaces the matrix of poorly silicified spiculites and inside chert nodules (Fig. 1). The exact timing and length of dolomitization with respect to chertification is still inconclusive but the occurrence of dolomite inclusions inside chert nodules and the absence of silica-replaced dolomites suggest that dolomitization occurred prior chertification. The variable range in dolomite crystal size and zonations seen in cathodoluminescence suggest that dolomitization occurred in various stages. Dolomite does not have a direct impact in the reservoir performance (Mazullo et al. 2009). This in part is explained by the relatively minor amounts of dolomite and the occurrence of dolomitization before secondary porosity was generated. Note from figure 1B that the dolomite is not found on the sponge-spicule molds, which suggest that dolomitization occurred before silica dissolution took place.

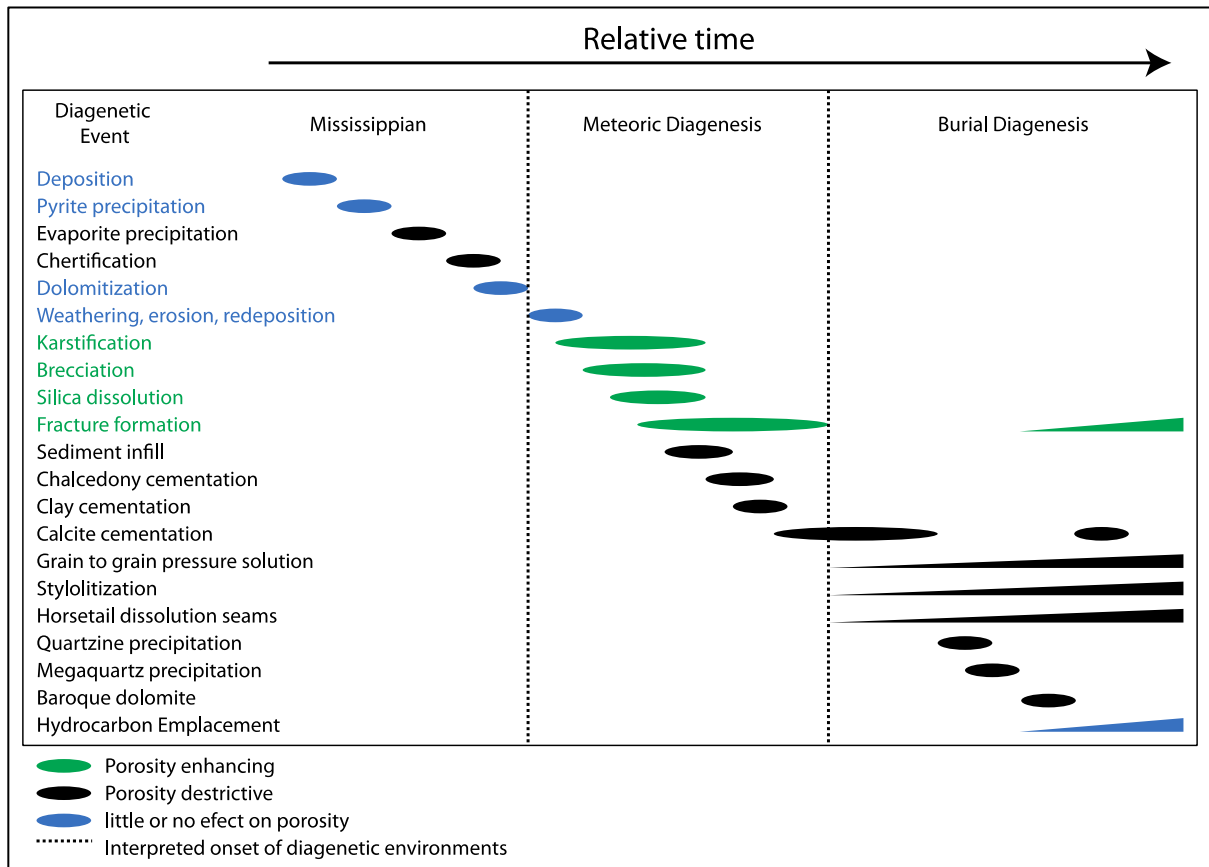


Figure 2. Paragenesis for the Cowley Formation from the wells Harbaugh UB 15 and George Michael 1-8 in Rhodes field, Barber county, south-central Kansas.

#### Wellington Field (Core: Wellington 1-32)

Mississippian time-equivalent strata are described from the Wellington 1-32 core. Lithologies recognized in core include: chert breccia and conglomerate (“chat”), chert nodule-rich dolomite, argillaceous dolosiltite, dolomitized bioclastic packstones and echinoderm-rich wackestones and packstones. The main reservoir in the field is 20 ft thick brown colored, finely

crystalline dolomite with scattered sponge-spicule-rich chert nodules, with up to 30% intercrystalline pores. The breccias and conglomerates are not good reservoir rocks in the Wellington field.

Stratigraphically, the Mississippian strata in the Wellington field are in a more distal and deeper locality than the Rhodes field with respect to the Mississippian carbonate shelf. Differences in the paragenesis are readily seen in the pervasive replacement with dolomite and the occurrence of calcite cements much later in the paragenesis (King, 2013). Dolomitization was early and pervasive, replacing almost the entire Mississippian section whereas in the Rhodes field dolomite is found locally. In addition the presence of silica-replaced evaporite nodules is far more abundant in the Wellington field.

#### *Chertification and Dolomitization*

Our results show that chertification and dolomitization occurred at relatively close times in all cases. The change-over from dolomitization and silicification may occur several times in the diagenetic history of a sediment (Hess, 1990). Knauth's (1979) model for shallow-water early chert in limestone is coincided by analogy with the Dorag mixing-zone model for dolomitization (Badiozamani, 1973). A mixing zone of marine connate waters and meteoric waters represents a convenient geochemical environment for silica (opal-CT and quartz) or dolomite precipitation (Knauth 1979 and Badiozamani 1973). Although these models have been challenged before, it gives us an alternative to think about the environments in which both minerals can precipitate at relatively close times during the Mississippian. Selective replacement, mixing-water ratios and other kinetic parameters will play an important role in precipitating either dolomite or chert.

## APPENDIX B.

### ***Geological and Microbiological Influences on Reservoir and Seal Material During Exposure to Supercritical CO<sub>2</sub>, Arbuckle Group, Kansas***

*Christa Jackson<sup>1</sup>, David Fowle<sup>1</sup>, Brian Strazisar<sup>3</sup>, W. Lynn Watney<sup>1,2,3</sup>, Aimee Scheffer<sup>4</sup>, and Jennifer Roberts<sup>1</sup>*

*1) KICC, Department of Geology, University of Kansas, Lawrence, KS*

*2) Kansas Geological Survey, Lawrence, KS*

*3) National Energy Technology Lab, Pittsburgh, PA*

*4) ConocoPhillips, Houston, TX*

#### **Key Findings**

- Dolomite dissolution occurs during exposure of reservoir (Arbuckle dolomite) and seal (dolomitic Lower Mississippian informal Pierson formation) materials to 100% pCO<sub>2(SC)</sub>, as a result of a 0.5-1.0 unit drop in pH
- Pyrite dissolution occurs during exposure of Pierson formation (seal) to 100% pCO<sub>2(SC)</sub>
- Secondary precipitation of iron oxides occurs during exposure of Pierson formation (seal) to 100% pCO<sub>2(SC)</sub>, which could improve seal integrity by decreasing porosity and permeability

#### **Significance**

The Arbuckle Group (reservoir) and Lower Mississippian (informal) Pierson formation (seal) in southern Kansas are being investigated for storage of captured CO<sub>2</sub> emissions, a process referred to as Carbon dioxide Capture and Storage (CCS) (IPCC, 2005).

CO<sub>2</sub> exposure effects during and after subsurface injection vary depending on temperature, pressure, injection rate, formation geology, fluid geochemistry, and native microbial ecology. These effects must be explored to provide necessary data for optimization of injection and well-monitoring plans.

Injection of super critical CO<sub>2</sub> is targeted at the base of the Arbuckle Group (~1500 m depth). Here we investigate experimentally the geochemical and microbiological effects of supercritical CO<sub>2</sub> exposure on the Arbuckle Group cherty dolomite (reservoir) and Pierson formation dolomitic silty shale (seal). Changes in geochemistry and microbiology during CO<sub>2</sub> injection can affect porosity and permeability, which in turn, can affect seal integrity and the injectivity and storage capacity of the reservoir.

#### **Research Summary**

##### *Background*

The Cambro-Ordovician Arbuckle Group, a deep saline reservoir, in southern Kansas is being evaluated for CO<sub>2</sub> storage. The Arbuckle Group is generally composed of cherty dolomite, with some interbedded carbonate shales. CO<sub>2</sub> injection will occur at the base of the Arbuckle reservoir (~1500 m below land surface). The Arbuckle is ~305 m thick and average injection zone conditions are 50 °C and 172 bar, at which CO<sub>2</sub> will be in a supercritical state (Span and Wagner, 1996). Supercritical CO<sub>2</sub> (CO<sub>2(SC)</sub>) behaves like a buoyant fluid, and will naturally

migrate towards shallower formations. Mechanisms of CO<sub>2(SC)</sub> sequestration include structural/stratigraphic trapping, residual trapping, mineral trapping, and solubility trapping (Han et al., 2010).

Arbuckle Group pore waters increase in salinity with depth, from 32-128 ppt, and range in pH from 6.32-7.08. Pore water geochemistry shows an increase in methane at the base of the Arbuckle, which indicates the presence of methanogenic microorganisms (Scheffer, 2012). Methanogens can sequester CO<sub>2</sub> by metabolically reducing it to CH<sub>4</sub> (e.g. Balch et al., 1979; Konhauser, 2007). Methanogens are also more resistant to the damaging effects of high pCO<sub>2</sub>. The presence of these microorganisms in the injection zone may enhance CO<sub>2</sub> sequestration.

The Pierson formation is considered an alternate seal for the Arbuckle and overlying Simpson groups (Scheffer, 2012). At injection, the Pierson formation is approximately 1200 m deep, and 36 m thick. Due to the variable thickness of the primary seal (Chattanooga shale), this alternate seal is an important part of the CO<sub>2</sub> storage system. The Pierson formation is an organic rich, low permeability, dolomitic silty shale.

#### Experimental Design and Methodology

Powdered Arbuckle dolomite (core plugs from 1302 m and 1408 m) and Lower Mississippian dolomitic shale (core plugs from 1215 m and 1219 m) were reacted with artificial brine and 100% pCO<sub>2</sub> under reservoir temperature and pressure (50°C, 172 bar) for at least 30 days. A rock/brine ratio of 10 g/250 ml was used for all experiments. These experiments were conducted in duplicate using Teflon-lined static steel autoclaves at the National Energy Technology Lab in Pittsburgh, PA. The artificial brine was based on the chemistry of Arbuckle pore waters (based on analyses of drill stem tests from KGS well #1-32; e.g. Scheffer, 2012), and was deoxygenated by bubbling with N<sub>2</sub> (see figure 1). Experimental controls were conducted in parallel to the CO<sub>2</sub> experiments, and were exposed to 100% pN<sub>2</sub>. 2 mg/l of peptidoglycan, purified from the cell walls of *Bacillus subtilis*, was added to a set of experiments as a proxy for microbial biomass.

	Cation and Anion Concentrations (mg/L)										
	Ca <sup>2+</sup>	Mg <sup>2+</sup>	K <sup>+</sup>	Na <sup>+</sup>	Fe <sup>2+</sup>	Si	B	Cl <sup>-</sup>	SO <sub>4</sub> <sup>2-</sup>	Br <sup>-</sup>	HCO <sub>3</sub> <sup>-</sup>
DST 4	2546.82	565.20	259.14	19310.62	0.39	47.92	9.80	36000.00	910.00	180.00	375.30
Artificial Brine	2603.55	552.17	275.56	19824.91	BDL	BDL	11.49	35186.73	833.97	175.51	244.06

\*BDL = below detection level

Figure 1: Brine Chemistry. An artificial brine based on the chemistry of an Arbuckle drill stem test (DST 4 at 1279 m depth, from KGS Well # 1-32) was used in all experiments. The artificial brine was gassed with N<sub>2</sub> to remove dissolved O<sub>2</sub> prior to starting the experiments.

Brine samples were syringe-filtered (0.22-0.45 µm) and acidified with HNO<sub>3</sub> to preserve them at the end of each experiment. Brines were analyzed for major cations using ICP-OES, and major anions using IC. Bulk changes in mineralogy were determined via x-ray diffraction. Dissolution features, and evidence of secondary mineral precipitation were observed via SEM.

## Results

Results from experimental vessels (biotic/sterile with CO<sub>2</sub>) were compared to controls to assess changes in mineralogy and brine chemistry after CO<sub>2</sub> exposure. Changes in mineralogy and brine chemistry could impact seal integrity and reservoir storage capacity and injectivity.

### Brine Chemistry

Exposure to 100%  $p\text{CO}_{2(\text{SC})}$  caused a 0.5 to >1 unit decrease in brine pH. An increase in Mg, Ca, and  $\text{HCO}_3$  concentrations occurred in Arbuckle and Lower Mississippian experiments, which indicates dolomite ( $\text{CaMg}(\text{CO}_3)_2$ ) dissolution. The dissolution of Lower Mississippian sulfur-bearing minerals, like pyrite, upon exposure to  $\text{CO}_2$  is indicated by an increase in total S concentrations.

### Mineralogy

No changes in bulk mineralogy were indicated for the Arbuckle dolomite experiments. Dissolution features were observed in dolomite crystals via SEM, which corroborates the brine chemistry results (see figure 2).

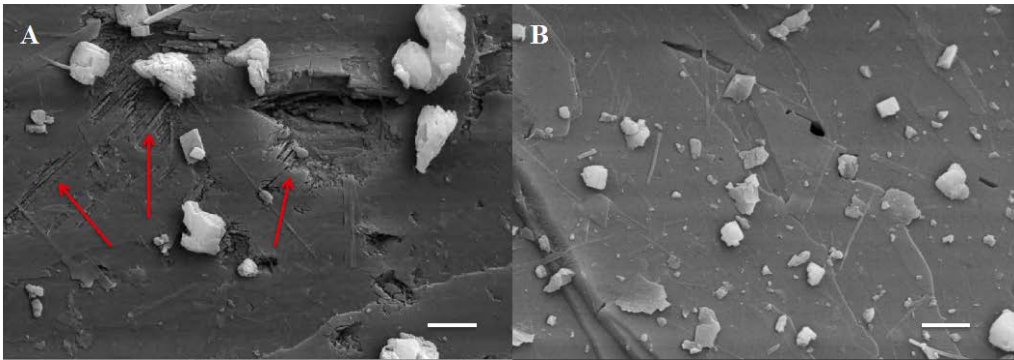


Figure 2: Dolomite Dissolution. Dissolution features, denoted by red arrows, can be seen on the surface of  $\text{CO}_{2(\text{SC})}$ -reacted dolomite grains from the Arbuckle Group (A). These features are absent from the surface of unreacted Arbuckle dolomite (B). Images were taken using the secondary electron detector of a LEO field emission scanning electron microscope. Scale bars are 1  $\mu\text{m}$  in length.

Framboidal pyrite was observed in the unreacted Pierson formation, and secondary precipitation of iron oxides was observed in the  $\text{CO}_{2(\text{SC})}$ -reacted Pierson formation experiments (see figure 3). These observations are consistent with the brine chemistry data, which shows an increase in total S concentrations for the  $\text{CO}_{2(\text{SC})}$ -reacted experiments. While the dissolution of pyrite would release Fe and S into solution, we do not see an increase in Fe concentrations because it is conserved in the solid phase as an Fe-oxide.

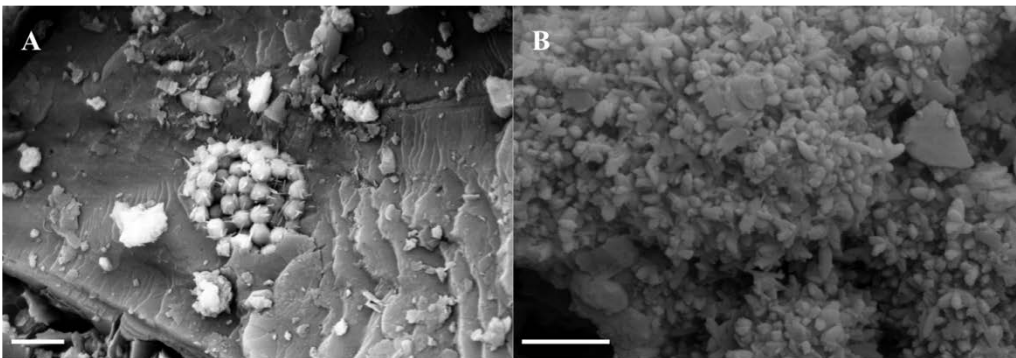


Figure 3: Framboidal Pyrite and Secondary Precipitation of Iron Oxides. Framboidal pyrite crystals are present in unreacted Lower Mississippian material, and may be dissolved upon exposure to  $\text{CO}_{2(\text{SC})}$  (A, center). Pyrite dissolution would release Fe and S into the brine, where it

*could react with other ions to form secondary minerals, or could remain in solution. Secondary precipitation of Fe-oxides can be seen in CO<sub>2(SC)</sub>-reacted Lower Mississippian material (B). Images were taken using the secondary electron detector of a LEO field emission scanning electron microscope. Scale bars are 1µm in length.*

## **Implications**

The dissolution of dolomite due to pH decrease during CO<sub>2</sub> injection could enhance porosity and permeability in the Arbuckle reservoir. This may facilitate injectivity and enhance storage capacity. The dissolution of dolomite and pyrite within the Pierson formation, however, could negatively impact seal integrity, as enhanced permeability may allow the CO<sub>2</sub> to migrate into shallower formations. Dissolution of pyrite could also result in the mobilization of arsenic, as arsenic can be associated with iron and sulfur-bearing minerals. Toxic metal mobilization is of great environmental concern in CO<sub>2</sub> injection settings, because CO<sub>2</sub> migration into a shallow freshwater reservoir could result in toxic metal contamination of drinking water. The secondary precipitation of Fe-oxyhydroxides, however, may sequester toxic metals and clog pore space (Richmond et al., 2004). Trace metal analysis of the experiment brines is currently underway, which will assess the presence, and determine the fate of toxic metals such as As, Pb, Cr, and Cu.

## **References**

- Balch, W.E., Fox, G.E., Magrum, L.J., Woese, C.R., and Wolfe, R.S., 1979, Methanogens: a reevaluation of a unique biological group: *Microbiological Reviews*, v. 43, p. 260-296.
- Han, W.S., McPherson, B.J., Lichtner, P.C., and Wang, F.P., 2010, Evaluation of trapping mechanisms in geologic CO<sub>2</sub> sequestration: Case study of SACROC northern platform, a 35-year CO<sub>2</sub> injection site: *American Journal of Science*, v. 310, p. 282-324.
- IPCC, 2005, In: Metz, B., Davidson, O., Coninck, H., Loos, M., Meyer, L. (Eds.), *Special Report on Carbon Dioxide Capture and Storage*: IPCC, Cambridge.
- Konhauser, Kurt, 2007, *Introduction to Geomicrobiology*. Blackwell Publishing, 425 p.
- Richmond, W.R., Loan, M., Morton, J., and Parkinson G.M., 2004, Arsenic removal from solution via ferrihydrite crystallization control: *Environmental Science and Technology*, v. 38, p. 2368-2372.
- Scheffer, Aimee, 2012, *Geochemical and microbiological characterization of the Arbuckle saline aquifer, a potential CO<sub>2</sub> storage reservoir; implications for hydraulic separation and caprock integrity*: University of Kansas unpublished thesis.
- Span, R., and Wagner, W., 1996, A new equation of state for carbon dioxide covering the fluid region from the triple-point temperature to 1100 K at pressures up to 800 MPa: *Journal of Physical Chemistry*, v. 25, p. 1509-1596.

## APPENDIX C.

### ***Determination of Capillary Pressure Curves in the Mississippian Lime Play, Kansas, Based on the New Method Which Relates Pc Curves to RQI (Reservoir Quality Index)***

*Mina Fazelalavi<sup>1</sup>, Lynn Watney<sup>1</sup>, John Doveton<sup>1</sup>, Jason Rush<sup>1</sup>, Mohsen Fazelalavi<sup>2</sup>, Maryam Fazelalavi<sup>3</sup>, Minh C. Nguyen<sup>4</sup>*

*1) KICC, Kansas Geological Survey, Lawrence, KS*

*2) Independent Consultant, Iran*

*3) Senergy, Stavanger, Norway*

*4) KICC, Dept. of Petroleum Engineering, University of Kansas, Lawrence, KS*

#### **Key Findings**

- According to an investigation of SCAL data from several fields, there are strong correlations between endpoints of capillary pressure curves and RQI (Reservoir Quality Index).
- Both the entry pressure of the non-wetting phase and the irreducible saturation of the wetting phase of rocks with similar pore size distributions (unimodal, bimodal, or trimodal) can be defined as functions of RQI.
- Pc curves are normalized to find a general equation. A single equation relating normalized non-wetting saturation to equivalent radius (EQR) is determined for all rock types with similar pore size distributions.
- The Mississippian reservoir consists of two main zones, Tripolitic chert (Chat) and Carbonate. The Chat zone overlies the Carbonate section in the Mississippian of the Wellington field.
- Pore size distributions are mainly bimodal in the Chat (tripolite) and unimodal in the carbonate. Therefore; two different sets of Pc curves were derived.

#### **Significance**

Capillary pressure curves are essential for accurate reservoir characterization and reservoir simulation to optimize oil recovery. On the other hand, accurate representation of capillary pressure curves is also crucial on modeling capillary trapping of CO<sub>2</sub> during the post-injection period and saturation distribution.

Based on the oil migration path in the reservoir, drainage or imbibition capillary pressure can be used for the description of initial water saturation. When oil migrates from the side of the reservoir to the top of the structure and then downwards to the spill point, the initial water saturation is described by drainage capillary pressure curves. In some reservoirs, based on log data, it seems that oil migration has been from below the oil-water contact (OWC) to the top of the reservoir and all over the entire reservoir area. In these cases, there is residual oil saturation below the OWC, as indicated by log saturations. When oil has migrated from below the OWC to the top of the reservoir, imbibition Pc curves are more appropriate for the description of the initial water saturation.

Pc curves are often related to permeability of the rock or the Flow Zone Indicator (FZI) in studies reported in the literature. However, in rocks deposited in a variety of geological sedimentary environments, different Pc curves could exist for a single permeability or a specific FZI. In this method, based on our studies on SCAL data of several carbonate reservoirs, entry pressure, irreducible water saturation and therefore Pc curve of a rock are better related to its Reservoir Quality Index (RQI).

In this project, both drainage and imbibition capillary pressure curves were derived in the Mississippian reservoir. The Mississippian reservoir is comprised of two main zones: Tripolitic chert (Chat) and Carbonate. The two layers have different properties i.e different permeability, porosity and mainly different pore size distribution (bi-modal and unimodal). Due to this heterogeneity, the model was divided into two main zones or layers, Chat and Carbonate, and six capillary pressure curves were derived in each zone for different RQI ranges.

## **Methodology**

Both drainage and imbibition Pc curves were calculated for each zone in the reservoir i.e. Chat and Carbonate. In this abstract, only drainage capillary pressure curves are discussed which were used in the model. Since permeability in all wells (Fazelalavi et al., 2013) as a function of depth was estimated prior for this project, the RQI at each depth could be determined. Therefore, Pc curves are defined for each RQI range in the Mississippian. The Grid of the dynamic or static model of the reservoir is divided into several Saturation Regions, each with a specific RQI range. For each region, a specific Pc curve is prepared.

Generalized Pc curves for the Mississippian formation of the Spivey-Grabs field (Watney et al., 2002; Bhattacharya et al., 2003) in addition to those based mainly on NMR data from well 1-32 and well 1-28 in the Wellington field were used to generate Pc curves for both Chat and Carbonate sequences of the Mississippian reservoir. The shape of the generalized Pc curves of Spivey-Grabs field were normalized and used in the process. Generated Pc curves from NMR log of well 1-32 were used to find correlations between endpoints and RQI for determination of Pc curves.

### *a. Entry Pressure*

Based on SCAL data of other fields, a good correlation can be found between capillary entry pressure and RQI. The entry pressure in Well 1-32 was determined from NMR data using oil and water interfacial tension. In the Mississippian formation two correlations were obtained; one for the Chat conglomerate and another for the carbonate section of this formation.

### *b. Irreducible Water Saturation*

Irreducible water saturation is needed to calculate normalized Non-Wetting phase saturation (Snwn). Based on Irreducible water saturation of SCAL data, mainly from carbonate reservoirs, irreducible water saturation at certain capillary pressure can be correlated, very well, to the RQI of the rock. There is a good correlation between irreducible water saturation of reservoir rocks and RQI. NMR data of Well 1-32 was used to determine irreducible water saturation at a Pc of

20 Bars (290 psi). Interfacial tension between Oil and water was given to the Tech-Log Module to find  $S_{wir}$  versus depth for this well.

*c. Shape of the Normalized Pc curve*

Pc curves, which were obtained from NMR logs, were normalized by plotting  $S_{nwn}$  (Normalized Non-Wetting Phase Saturation) versus EQR (Equivalent Radius). EQR is obtained from division of entry pressure over Pc. Therefore Equivalent Radius is a function of entry pressure and capillary pressure; where, entry pressure is a function of RQI. Therefore, the shape of normalized Pc curves can be expressed in terms of Pc and RQI.

$$S_{nwn} = \left(1 - a \frac{P_e}{P_c}\right) \left(1 - \frac{P_e^b}{P_c}\right) \tag{Eq. 1}$$

*d. Calculation of Drainage Capillary Pressure Curves*

The following equation was used to calculate drainage water saturation in the Mississippian Chat and Carbonate:

$$S_{wi} = 1 - S_{nwn}(1 - S_{wir}) \tag{Eq. 2}$$

Initial water saturation ( $S_{wi}$ ) is a function of  $S_{nwn}$ . It was shown in Eq. 1 that  $S_{nwn}$  is a function of  $P_e$  and  $P_c$  where  $P_e$  is a function of RQI.  $S_{nwn}$  in Equation 2 can be replaced by respective functions and an equation can be obtained which expresses  $S_{wi}$  in terms of RQI and PC.

**Results**

Drainage capillary pressure curves were calculated for Mississippian Chat and Carbonate using Eq 2, Fig. 1 and 2:

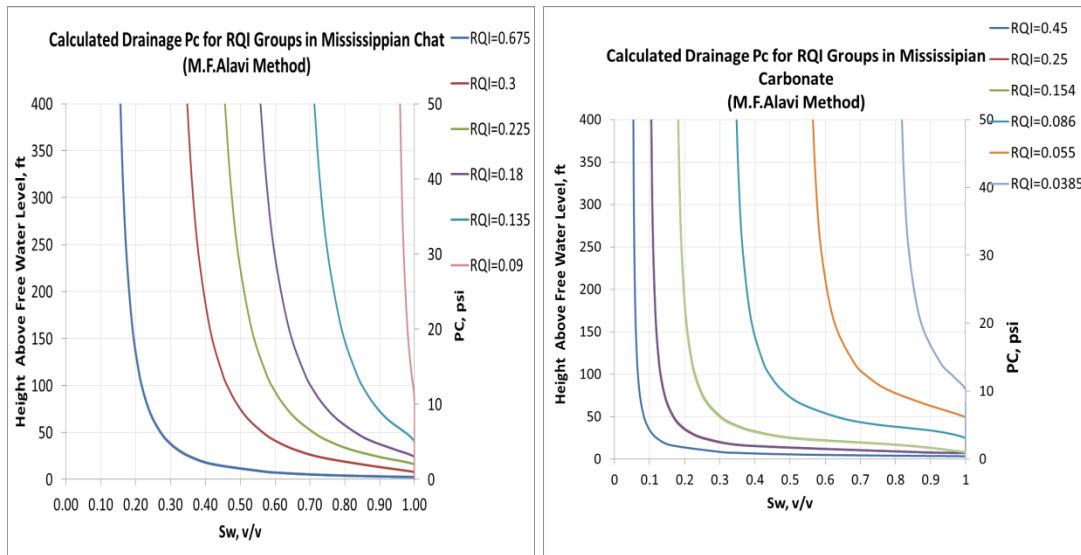


**Figure 1: Drainage Pc curves for Chat**

Drainage Capillary pressure curves for each saturation region for each RQI range were given to Petrel and Water saturation were modeled for both Mississippian Chat and Carbonate, Fig. 3 and 4:

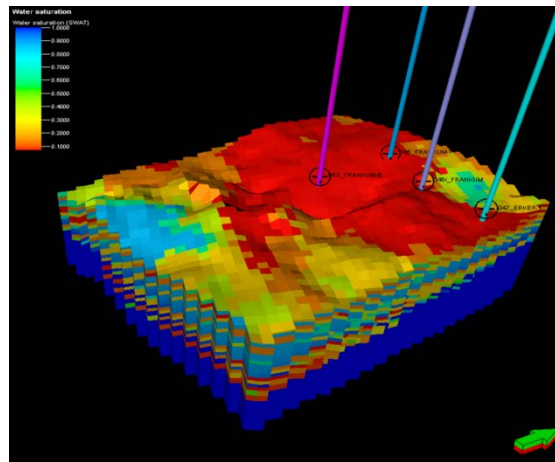
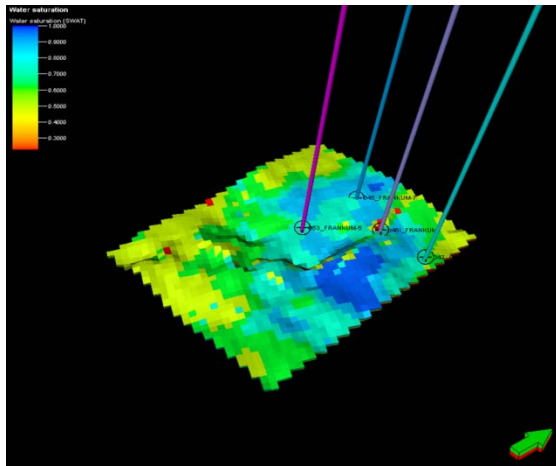


Figure 3: Water Saturation Distribution for Chat

Figure 4: Water Saturation Distribution for Carbonate

## APPENDIX D.



**IPTC-17429-MS**

**Determination of Reservoir Permeability Based on Irreducible Water Saturation and Porosity from Log Data and Flow Zone Indicator (FZI) from Core Data**

M. Fazel Alavi, Independent Consultant; M. Fazel Alavi, IPTC, Senergy; and M. Fazel Alavi, IPTC, Kansas Geological Survey

Copyright 2014, International Petroleum Technology Conference

This paper was prepared for presentation at the International Petroleum Technology Conference held in Doha, Qatar, 20–22 January 2014.

This paper was selected for presentation by an IPTC Programme Committee following review of information contained in an abstract submitted by the author(s). Contents of the paper, as presented, have not been reviewed by the International Petroleum Technology Conference and are subject to correction by the author(s). The material, as presented, does not necessarily reflect any position of the International Petroleum Technology Conference, its officers, or members. Papers presented at IPTC are subject to publication review by Sponsor Society Committees of IPTC. Electronic reproduction, distribution, or storage of any part of this paper for commercial purposes without the written consent of the International Petroleum Technology Conference is prohibited. Permission to reproduce in print is restricted to an abstract of not more than 300 words; illustrations may not be copied. The abstract must contain conspicuous acknowledgment of where and by whom the paper was presented. Write Librarian, IPTC, P.O. Box 833836, Richardson, TX 75083-3836, U.S.A., fax +1-972-952-9435

---

### **Abstract**

The Flow Zone Indicator (FZI) core analysis method is an accurate approach for defining different Hydraulic Units (HUs) in a well with core data, and finding accurate  $k$ - $\phi$  relations for

each HU according to  $k = C_n \phi^n$ . Determining HUs in un-cored wells from logs or geological information is the main challenge for the FZI method. Several methods have been proposed for finding HUs in un-cored wells. In many approaches, HUs are correlated with log attributes in cored wells, and this relationship is applied to un-cored wells. However, since a persistent relationship between log attributes and FZI does not exist in all litho-facies, this does not always give reliable results.

Based on a study of core and log data from several carbonate reservoirs, a practical, straightforward technique designated as the FZI-SWPHI (Flow Zone Indicator – Irreducible Water Saturation and Porosity) method is proposed. A theoretically sound relationship between FZI and  $S_{wir} \phi_e$  exists for a sedimentary environment. To find this relationship, FZI values from cores of the well are statistically related to the irreducible water saturation and porosity values from log data. The resulting equation, similar to the Wyllie and Rose, Tixier, Timur, and Coates equations, relates permeability directly to effective porosity and irreducible water saturation.

Unlike these general equations, however, this new equation is specific to the reservoir under investigation because constants are defined for the reservoir. The derived equation can be directly applied to wells or reservoir model grid blocks, where water saturation and porosity are known. This method is more straightforward to use and generates more precise permeability estimates with higher vertical resolution. Several examples demonstrate the accuracy and practical applications of this technique.

## Introduction

The Flow Zone Indicator (FZI) method for classifying core data into Hydraulic Units (HUs) with specific FZI was introduced by Amaefule et al. (1993) and is one of the best techniques for reservoir description. This method provides accurate correlations between permeability and porosity when FZI of the reservoir rock is known. FZI is determined from core data in the cored wells and it is often applied to wells without cores through correlations with log attributes. However, existing correlation methods do not always generate accurate permeability values for wells without core data.

The FZI method is based on the Kozeny-Carman (1927; 1937) general relation given in Eq. 1, where permeability is in md:

$$k = 1014 \frac{\phi_e^3}{(1-\phi_e)^2} \left[ \frac{1}{F_s \tau^2 S_{gv}^2} \right] \quad (1)$$

Determining permeability with this equation have not been successful (Amaefule et al. 1993) because the shape factor ( $F_s$ ), tortuosity ( $\tau$ ) and surface area per grain volume ( $S_{gv}$ ) are not typically known, as they are not constant within a reservoir and cannot be measured easily. However, Amaefule et al. designated the square root of the term  $1/F_s \tau^2 S_{gv}^2$  in the Kozeny-Carman equation as the “Flow Zone Indicator” FZI ( $\mu m$ ) and showed that this indicator could be calculated from core permeability and porosity according to Eq. 2:

$$FZI = \frac{RQI}{\phi_z} \quad (2)$$

Where RQI is the Reservoir Quality Index and  $\phi_z$  is the pore volume to grain volume ratio, obtained using Eq. 3 and Eq. 4 respectively. Note that permeability in Eq. 3 is in md.

$$RQI = 0.0314 \sqrt{\frac{K}{\phi_e}} \quad (3)$$

$$\phi_z = \left( \frac{\phi_e}{1-\phi_e} \right) \quad (4)$$

Substituting the term  $1/F_s \tau^2 S_{gv}$  in the Kozeny-Carman formula with  $FZI^2$  (Eq. 5):

$$K = 1014 FZI^2 \frac{\phi_e^3}{(1-\phi_e)^2} \quad (5)$$

This equation can calculate permeability in wells accurately when FZI of the formation versus depth is known. FZI in cored wells can be obtained through Eq. 2, but FZI in wells without cores must be found by correlating or identifying the litho-facies in all of the wells and assigning a FZI for each facies (Shenawi et al. 2007). To facilitate the determination of FZI in un-cored wells, core data are usually grouped into several Hydraulic Units (HU) or Discrete Rock Types (DRTs) using Eq. 6 (Guo et al. 2005):

$$DRT = \text{Round} (2 \ln(FZI) + 10.6) \quad (6)$$

When RQI is plotted against  $\phi_z$  on a log-log scale, the data from each DRT forms a straight line with a unit slope, as shown in **Fig. 1**. The average FZI, or FZI constant of each DRT can be determined from the intercept of the unit-slope straight line at  $\phi_z=1$ . To find a correlation between permeability and porosity for each DRT, the log of permeability is plotted versus porosity, and a power trendline is fitted through the data points, as shown in **Fig. 2**. A power relation of the general form shown in Eq. 7 can be obtained from this trendline:

$$k = c_n \phi^{x_n} \quad (7)$$

Eq. 7 is a simplified form of Eq. 5 where the constant  $c_n$  is almost proportional to the average FZI of the DRT to the second power and  $\phi^{x_n}$  replaces the term  $(\phi_e^3 / (1-\phi_e)^2)$ . The exponent  $x_n$  normally varies between 3.1 to 3.9 depending on the porosity range of DRT data and statistical error in the data. Eq. 7 can be used to calculate permeability accurately at any depth of a well if the DRT at that depth is known. One of the main challenges for engineers, however, is the determination of DRT in wells without core data.

An oil reservoir is normally developed with tens or hundreds of wells. Only a few of these wells are cored, while log data is typically available in all wells for determination of porosity and water saturation. Several methods have been proposed to find FZI or DRT in wells without core data. Often, the DRT or FZI values from the core data of a cored well are related to well log attributes of other wells with regression models, neural networks and empirical correlations are obtained (Kharrat et al. 2009, Guo et al. 2005; Balan et al. 1995a, 1995b). Therefore, DRT or FZI can be predicted in other wells based on correlations between DRT and log attributes.

Experience has shown that the main deficiency of the FZI method is the lack of a proper method for finding FZI in the wells without cores. The above methods do not always result in reliable permeability estimates from log attributes, and cannot typically calculate actual changes in permeability with depth. There are fundamental reasons for the inaccuracy of correlations between log attributes and FZI from core data. The lack of a proper relationship between FZI and log data has been elaborated by other authors. (Svirsky et al. 2004)

In this paper, a new technique is proposed to calculate permeability, designated as the FZI-SWPHI (Flow Zone Indicator – Irreducible Water Saturation Porosity) method. It is based on a relationship between FZI and  $(1 / S_{wir} \phi_e)$ . FZI in Eq. 5 is replaced by this relationship, which results in an equation relating permeability directly to effective porosity and irreducible water saturation. Since the effective porosity and irreducible water saturation are known in wells with log data, the determination of permeability is much more straightforward and provides for a more precise reservoir description. Additionally, the vertical resolution of calculated permeability provides another advantage.

### **Statement of the Problem**

FZI is inversely proportional to the surface area per grain volume, tortuosity and square root of the shape factor. Normally FZI or DRT is correlated with neutron porosity, bulk density, sonic transient time, standard GR, computed GR, and resistivity logs. However, there is no theoretical relationship between the responses of most of these logs with the identified parameters. Additionally, FZI from a core sample represents the flow characteristics of the formation for a very small volume of reservoir rock (about 1 cubic inch), while log data at the same depth represents an average value of the physical properties of a larger volume of the rock. This volume can range from hundreds of cubic inches to several cubic meters, depending on the resolution and depth of investigation for the specific logging tool. Log attributes may or may not correspond to a core sample at the same depth depending on the vertical and lateral heterogeneity in the reservoir. FZI calculated from core data may fluctuate significantly at a certain depth, while porosity logs and resistivity logs often do not exhibit dramatic changes in properties with depth. Inaccurate depth matching of core and log data may also complicate correlations.

**Neutron Porosity.** Neutron logs measure the hydrogen concentration of the formation versus depth. The output of a neutron logging tool is calibrated to give the true porosity if the formation is limestone and filled with water. Therefore, neutron log responses depend on the porosity of the formation, the mineral composition and the type of the fluid in the formation.

No relationship exists between neutron response and FZI because a high neutron log response may correspond to both high and low FZI values. When grain sizes are large, well-sorted and clean, the formation has high porosity and FZI is large, and the neutron response is high.

However, a high neutron log response can also be recorded in a very fine grain formation with shale where FZI is very small.

Another example of this contradictory relationship between neutron log response and FZI is the very low response of the neutron log in the gas cap of a porous and highly permeable formation where FZI is very high. The response of this log in the oil bearing interval with the same FZI will be very high.

The vertical resolution of the neutron tool is several inches and its depth of investigation is also several inches. Therefore, the response of this tool gives an average attribute of a volume of the rock close to hundreds of cubic inches. Core plugs give the FZI of a rock volume of about 1-2 cubic inches. Porosity and permeability of a reservoir rock can change significantly within inches, however, and the FZI of the core plug sample could be completely different from the average of the surrounding material at the same depth. In these instances, the correlation of log attributes at that depth with FZI would likely be inaccurate.

**Bulk Density.** The density tool gives the bulk density of the formation. The bulk density is related to the porosity, the type or density of fluid in the pore space and density of minerals in the formation. Contradicting relationships may exist between FZI and the density tool response. In a very porous clean sand interval with very high permeability where FZI is very high, a low bulk density would be recorded by the density tool, while this tool would also give a low bulk density for intervals with a very low FZI where grains are very fine but porosity is high, minerals are light or the pore space is filled with gas instead of oil.

The density log attribute is an average value for a volume of rock which is much greater than the volume of core plug samples used for FZI determination. Therefore, these two parameters cannot be correlated effectively when vertical and horizontal heterogeneity exists in the formation.

**Sonic Log.** The sonic logging tool measures compression wave transit time in rock. Its response is related to the minerals in the formation, the porosity and the type of fluid in the pore space. A strong relationship does not exist between the sonic tool response and FZI. Very contradictory relationships may exist in a well between FZI from a core and the sonic tool response. One interval in a well may be clean, porous, and coarse-grained with high permeability and have a high FZI where its sonic log response is moderate. The same response could be obtained from another interval where the formation is tight, porous but fine-grained or clayed with very low permeability and low FZI. This tool also gives the average acoustic properties of the formation over a long interval. In vertically heterogeneous formations, the correlation of sonic log response with FZI may be inaccurate. Clay in the reservoir also increases sonic tool responses similar to an increase in porosity. An increase in porosity gives a higher FZI while an increase in clay content in the formation increases surface area and reduces FZI.

**Standard Gamma Ray (SGR).** The SGR tool measures the radioactivity of the formation from uranium, thorium and radioactive potassium. Thorium, potassium and uranium all exist in clay minerals, while uranium may be found in clean formations as well. Often, the standard GR tool response is related to shale content of the formation, and shale increases surface area per grain volume. Therefore, this log attribute can be related to FZI if uranium does not exist in clean intervals. There are different types of clay with different SGR responses and they may exist in the formation in several forms such as bedding, laminar, dispersed, and structural. Each of these

types and forms increases the surface area per grain volume and changes the permeability differently, which cannot be seen in the SGR response data.

In contrast with core data, SGR has a deep depth of investigation and poor vertical resolution. This means that the SGR data can be related to a larger volume of rock significantly greater than the core plug sample volume. This may adversely affect the correlation between FZI and SGR.

**Computed Gamma Ray (CGR).** CGR is a measure of thorium and potassium radioactivity. These elements are generally associated with different clay minerals. A high CGR response generally means high clay content and increased surface area per grain volume. Hence, FZI can be related to CGR to some extent. Different clay types have different CGR responses, different surface area per grain volume and they can appear in the reservoir rocks in different forms. Therefore, the correlation of FZI with CGR may not always be accurate. The resolution and depth of investigation of this tool is similar to SGR, with a coarser resolution and volume of investigation as compared to core plug samples. The lack of resolution may affect accuracy of correlations.

**Deep Resistivity Tool.** Deep resistivity is mainly influenced by formation water saturation, formation water salinity, tortuosity, shape factor and porosity. Since the water saturation in the formation is related to surface area per grain volume and FZI is also a function of surface area, deep resistivity can be related to FZI. However, several factors can result in inaccurate correlations between FZI and deep resistivity tool response: conductive minerals in some intervals, clay minerals, changes in water salinity in wells or intervals, changes in porosity and changes in water saturation due to proximity of the interval or well to oil-water contact. Another cause of inaccuracy is the depth of investigation of this tool; this depth is very large and for heterogeneous rocks, these data may not correlate well with FZI from core samples.

**Other Resistivity Tools.** Medium, shallow and proximity resistivity tools do not provide good correlations with FZI from core data for the same reasons as the deep resistivity tool. There are also other factors which could make correlation of response of these tools with FZI inaccurate, including variable depth of mud filtrate invasion, variable mud filtrate resistivity in different wells, hole rugosity and other borehole effects.

### **Fundamental Theory**

The FZI method relates permeability of the rock to FZI and effective porosity according to Eq. 5. Wyllie and Rose (1950), Tixier (1949), Timur (1968), Coates and Dumanoir (1974) and Coates (Schlumberger Log Interpretation/Principles, 1987) relate rock permeability to effective porosity and irreducible water saturation according to Eq. 8a to 8e.

Wyllie and Rose:

$$k = \frac{c \phi^x}{(S_{wir})^y} \quad (8a)$$

Tixier:

$$k^{\frac{1}{2}} = 250 \frac{\phi^3}{S_{wir}} \quad (8b)$$

Timur:

$$k^{\frac{1}{2}} = 100 \frac{\phi^{2.25}}{S_{wir}} \quad (8c)$$

Coates-Dumanoir:

$$k^{\frac{1}{2}} = \frac{300}{w^4} \frac{\phi^w}{S_{wir}^w} \quad (8d)$$

Coates:

$$k^{\frac{1}{2}} = 70 \frac{\phi_e^2(1-S_{wir})}{S_{wir}} \quad (8e)$$

There is general consensus among these sources that permeability can be expressed as a function of only porosity and irreducible water saturation, suggesting a relationship between FZI and irreducible water saturation. In all of the above equations, permeability is inversely proportional to the irreducible water saturation raised to a power. However, the exponent for the irreducible water saturation used in each equation is different. There is also no agreement about the value of the pre-factor in the equations or the exponent for the porosity term. Therefore, while permeability is directly proportional to porosity raised to a power and inversely proportional to the irreducible water saturation raised to a power, each equation gives a different permeability for a single reservoir. Moreover, if the pre-factor of the equation is known for a zone in a reservoir, the same pre-factor will not give accurate results in other zones where the sedimentary environment is different. Therefore, the general relationship between permeability, porosity and irreducible water saturation would appear to be correct, but each sedimentary and diagenetic environment should be described using an equation with different pre-factors.

The objective of this paper is to present a permeability equation based on effective porosity and irreducible water saturation. For each geological setting, the power term of the irreducible water saturation, the power term for porosity and the pre-factor for the equation are obtained from core FZI and log results.

According to the FZI method each DRT has a constant FZI. Other investigators have proposed that the product of porosity and irreducible water saturation ( $S_{wir}\phi_e$ ) is constant for a given rock type (Buckles 1965). Therefore, FZI can be related to  $S_{wir}\phi_e$ . Since better rock types have larger FZI and smaller  $S_{wir}\phi_e$  values, FZI should be proportional to the reciprocal of  $S_{wir}\phi_e$ .

Core data and log data from several carbonate reservoirs are analyzed to find a relationship between FZI and the reciprocal of irreducible water saturation multiplied by porosity. FZI was obtained from the porosity and permeability of core samples. Additionally, log data from the same intervals provides effective porosity and irreducible water saturation. FZI from core is

correlated statistically to  $(1 / S_{wir} \phi_e)$ . It is observed that an empirical correlation as given by Eq. 9 exists between FZI and  $(1 / S_{wir} \phi_e)$ . **Fig. 3** shows a good example of the observed relationship in Well X3, where the calculated  $R^2$  is 0.99.

$$FZI = \frac{a}{S_{wir} \phi_e} + b \tag{9}$$

From a combination of Eq. 5 and Eq. 9, an equation for determination of permeability (Eq. 10) can be obtained based on effective porosity and irreducible water saturation:

$$k = 1014 \left[ \frac{a}{S_{wir} \phi_e} + b \right]^2 \frac{\phi_e^3}{(1-\phi_e)^2} \dots\dots\dots(10)$$

Eq. 10 can also be derived by another method. Special core analysis data of carbonate reservoirs indicate that the mean hydraulic unit radius can be related to  $S_{wir}$ . This relation seems to be theoretically correct because mean hydraulic radius is related to surface area per unit grain volume according to Eq. 11:

$$r_{mh} = \frac{\phi_e}{S_{gv}(1-\phi_e)} \tag{11}$$

$S_{wir}$  is also related to surface area per grain volume of the rock. Small grains which have a large surface area per grain volume typically have higher irreducible water saturation than larger grain sizes, and vice versa. Therefore, there should be a relationship between  $1/S_{wir}$  and  $r_{mh}$ .

Mercury injection capillary pressure data provides  $r_{mh}$  as well as  $S_{wir}$  at different capillary pressures. Data sets from several carbonate reservoirs were analyzed, and it can be demonstrated that a general correlation exists between  $1/S_{wir}$  and the mean hydraulic unit radius when the shape of the pore throat distribution curves are similar (**Fig. 4**).

$$\frac{1}{S_{wir}} = c r_{mh} + d\phi_e \tag{12}$$

Note that all of samples in the analyzed group had a unimodal pore throat distribution.

The mean hydraulic radius is related to FZI and surface area per grain volume, as per Eq. 13:

$$r_{mh} = \frac{\phi_e}{S_{gv}(1-\phi_e)} = FZI \phi_z \sqrt{F_s} \tau \quad (13)$$

When the mean hydraulic radius from Eq. 13 is expressed in terms of RQI, Eq. 14 is obtained:

$$r_{mh} = RQI \sqrt{F_s} \tau \quad (14)$$

Combining Eq. 14 and Eq. 12 results in Eq. 15:

$$\frac{1}{S_{wir}} = c RQI \sqrt{F_s} \tau + d \phi_e \quad (15)$$

When both sides of Eq. 15 are divided by  $\phi_e$  and replacing RQI by FZI, Eq. 16 is obtained, which relates the reciprocal of  $S_{wir}\phi_e$  to FZI:

$$\frac{1}{S_{wir}\phi_e} = c FZI \frac{\sqrt{F_s} \tau}{(1-\phi_e)} + d \quad (16)$$

By rearranging Eq. 16, FZI is expressed in terms of  $S_{wir}$  and  $\phi_e$  according to Eq. 17:

$$FZI = \frac{1}{c} \left[ \frac{1-\phi_e}{\sqrt{F_s} \tau} \right] \frac{1}{S_{wir}\phi_e} - d \left[ \frac{1-\phi_e}{\sqrt{F_s} \tau} \right] \quad (17)$$

This equation is similar to Eq. 9 which was derived before. From Eq. 9 and Eq. 17, the following relations are concluded in Eq. 18 and Eq. 19, where  $a$  and  $b$  are the coefficients in Eq. 9:

$$a = \frac{1}{c} \left[ \frac{1-\phi_e}{\sqrt{F_s} \tau} \right] \quad (18)$$

$$b = d \left[ \frac{1-\phi_e}{\sqrt{F_s} \tau} \right] \quad (19)$$

The relationships from Eq. 18 and Eq. 19 indicate that the coefficients  $a$  and  $b$  change when the shape factor or tortuosity changes. Therefore, the permeability equation is a function of the shape factor of grains as well as the tortuosity of the pore space which are related to geology of the rock.

Generally, wells are logged for determination of porosity and water saturation. Therefore, Eq. 10 can easily be applied to these wells to accurately predict permeability. This equation should be applied to well intervals above the oil/water transition zone. Water saturation in the transition zone can be converted to irreducible water saturation by a method which will be discussed in another paper.

### **Geological Significance**

Examinations of data from several reservoirs have shown that where the sedimentary and diagenesis environment and pore size distributions are similar in a reservoir or well interval, a single equation in the form of Eq. 10 can be used for that reservoir or interval. However, pore size distribution shape may not be similar in all zones and sedimentary environment may change. The shape of the pore size distribution may be bimodal, tri-modal or skewed in some intervals. In these cases, two or three equations for permeability can be obtained from the analysis of core and log data.

As noted previously, coefficients  $a$  and  $b$  in Eq. 10 are functions of the shape factor and tortuosity, which are in turn influenced by sedimentary and diagenesis environments. Although a single equation often predicts good permeability values for a reservoir, in cases where there is significant variation in the deposition and diagenesis environment in the reservoir, zones with similar geology should be treated separately and specific equations should be derived for different zones. This can provide a more accurate permeability prediction.

### **Procedure of FZI-SWPHI Method**

To find a specific permeability function of the form of Eq. 10 for a reservoir or a geological zone, the following methodology is proposed:

- Select a key well that has both good routine core and log data and log analysis results.
- Ensure that the well interval for analysis is above the transition zone of the reservoir to ensure that reservoir water saturation is close to irreducible water saturation.
- Match the depth of core data with depth of logs.
- Review the core permeability and core samples description, and remove samples with fractures and fissures from the analysis. As the FZI method evaluates matrix permeability, only matrix permeability data should be used.
- Calculate FZI of the core samples.
- Calculate  $(1 / S_{wir} \phi_e)$  from the log derived effective porosity and irreducible water saturation values for the cored interval.
- Determine the 10th, 20th ... 90th percentiles of the  $(1 / S_{wir} \phi_e)$  population.
- Determine the 10th, 20th ... 90th percentiles of the FZI population.

- Plot the calculated percentiles of FZI population versus the calculated percentiles of the  $(1 / S_{wir} \phi_e)$  population and fit a linear trendline to find the constants  $a$  and  $b$

If there is good correlation and the  $R^2$  coefficient of determination for the trend line is close to unity, a single permeability equation can be used to describe the entire interval or reservoir. Otherwise, zones with similar geological setting should be detected and separately analyzed as follows:

- Calculate the average  $(1 / S_{wir} \phi_e)$  from log in the cored interval.
- Find the ratio ( $R$ ) of the average FZI to the average of  $(1 / S_{wir} \phi_e)$ .
- Plot FZI from the core and  $(1 / S_{wir} \phi_e)$  multiplied by the ratio  $R$  versus depth on the same plot.
- Determine geological zones with similar sedimentary and diagenesis environments from this plot. Other geological information such as rock description and log data like GR could also be used.
- Select the intervals where FZI data points are parallel with  $R / S_{wir} \phi_e$  curve and the separation between the two is equal. Each of these intervals will have a separate correlation.
- Find the new correlation between FZI and  $(1 / S_{wir} \phi_e)$  for each interval defined above.
- Calculate the permeability for all intervals in the key well from Eq. 10 using the derived correlations.
- Taper calculated permeability at the interface of the two consecutive zones.
- Compare the core permeability with the predicted permeability in the key well. If a satisfactory match is not obtained, the geological intervals are likely not properly delineated.
- Find equivalent geological intervals in other wells by correlating the well logs of the key well with other wells.
- Calculate the permeability of other wells using equations derived from the key well.

### Case Studies (Validation of FZI-SWPHI Technique)

**Example 1: Middle Cretaceous Carbonate Reservoir, Well X3.** Well X3 is drilled in a carbonate oil reservoir of Middle Cretaceous age in the Middle East. It contains several billion barrels of oil and is developed by several wells. Reservoir thickness is about 100 meters and 155 meters of core were available for two of the wells (Well X3 and Well X7). The reservoir interval in both of these wells is located above the transition zone; the log derived water saturation is very close to irreducible water saturation in both wells.

The reservoir thickness in Well X3 is 100.1 m and 97.2 m of routine core data were available. Routine core data of Well X3 were reviewed, and samples that were described as fracture were removed from the analysis. The core porosity was compared with the log porosity and generally log porosity was in the middle of core porosity.

The FZI of core samples of well X3 were correlated with  $(1 / S_{wir} \phi_e)$  from the logs in the cored interval, **Fig. 5** and Eq. 20.

$$FZI = 0.0154 \frac{1}{S_{wir} \phi_e} + 0.0124 \quad (20)$$

The correlation between FZI and  $(1 / S_{wir} \phi_e)$  is not perfect in this case ( $R^2 = 0.86$ ). Better correlations will be obtained by dividing the interval into several zones which will be done later. Eq. 21 was derived for calculating permeability for the entire reservoir interval:

$$k = 1014 \left[ \frac{0.0154}{S_{wir} \phi_e} + 0.0124 \right]^2 \frac{\phi_e^3}{(1 - \phi_e)^2} \quad (21)$$

Permeability predictions from Eq. 21 are compared with core plug permeability in **Fig. 6** (column 4). Although there is a reasonable match between predicted and measured permeability, some discrepancies exist; therefore, the whole interval was divided into several zones.

To accomplish this, FZI from core and  $(R / S_{wir} \phi_e)$  versus depth were plotted in Fig. 6 (column 5). The departure of  $(R / S_{wir} \phi_e)$  curve from the FZI curve is indicative of separate geological zones. Based on the difference between the  $(R / S_{wir} \phi_e)$  and core FZI curves, and the Archie (1950) description of core samples, the thickness of Well X3 was divided into seven geological zones, as given in **Table 1**. It is observed that the shifts of the  $(R / S_{wir} \phi_e)$  curve relative to the FZI curve coincide with changes in the Archie description.

The core FZI in all seven zones were correlated to the reciprocal of porosity and the irreducible water saturation. The results are given in **Table 2**. As can be seen, better  $R^2$  values are obtained (0.90 to 0.99) after reservoir zonation.

The permeability of each zone was calculated based on Eq. 10 as shown in Fig. 6 (column 6), using specific correlations coefficients for each zone. There is a good match between the predicted permeability and the core permeability. Any discrepancies can be attributed to small core plug sizes (approximately one cubic inch), which may not represent the average permeability of the entire formation at a given depth.

**Example 2: Middle Cretaceous Carbonate Reservoir, Well X7.** Well X7 and Well X3 are in the same reservoir described in Example 1. While there is routine core data for almost all of the reservoir thickness in Well X3, only part of the reservoir is cored in Well X7 (3125m-3180m). To check the validity of the model derived from the data in Well X3 and its applicability to other wells, the permeability of Well X7 was calculated by equations which were derived in Example 1 and the results were compared with the actual measured permeability of the core.

The equivalent geological zones which correspond to seven zones in Well X3 were found by log correlation to other wells of the field including Well X7. Only zones three to five have core data in Well X7 as shown in **Table 3** and log correlation layout in **Fig. 7**. Equations derived for zones 3 to 5 in Well X3 were directly applied to respective zones in Well X7. The predicted permeability in Well X7 is compared with core permeability in **Fig. 8** (column 4), which shows a good match between predicted and actual values.

**Example 3: Mississippian Formation, Wellington Field, Well 1-32.** The Wellington Field is located in southern Kansas, Sumner County (T 31S-R1W). The Mississippian formation of the

Wellington Field is under study for CO<sub>2</sub> EOR, and Well 1-32 was drilled in late 2010 for data acquisition. Conventional, geochemical and NMR logs were recorded in the Mississippian formation for evaluation of the reservoir. The formation was also cored for porosity and permeability measurement.

The Mississippian formation from 3656 to 3760 ft was divided into 5 zones based on the separation between FZI and  $(R / S_{wir} \phi_e)$  versus the depth curves as shown in **Fig. 9** (column 4). **Table 4** shows the lithology of the formation and a description of shape of the T2 distribution curves of these zones. Shape of T2 distribution changes with lithology of the formation.

FZI percentile was correlated with  $(I / S_{wir} \phi_e)$  percentile in each zone, and the coefficients  $a$  and  $b$  for the permeability equation were derived for all zones given in **Table 5**. The  $R^2$  values of zones 4 and 5 are low because of limited core samples in these zones, with four and five core samples, respectively.

The permeability of the Mississippian formation was calculated by Eq. 10 based on the NMR porosity and the irreducible water saturation using coefficients  $a$  and  $b$  in Table 5. The calculated permeability and core permeability are plotted against depth in Fig. 9 (column 5). As can be seen, there is a good match between the calculated permeability and the core permeability.

**Comparison with Neural Network Method.** The Artificial Neural Network (ANN) method has been widely used to correlate FZI with log data. Experience has shown that this method of predicting permeability lacks accuracy. When there are high and low permeability zones in the well, this method often predicts low permeabilities for very permeable zones and higher permeabilities are estimated for zones that are tight.

Permeabilities in the cored intervals of Well X3 and Well X7 were predicted with ANN using core FZI and log attributes. ANN-predicted permeabilities for these two wells are compared with the core permeability in **Fig. 10** (column 5) and Fig 8 (column 5). The permeabilities of some of the layers are significantly overestimated or underestimated by the ANN method. These results would have significant negative impacts on the output of a simulation model of the reservoir.

To compare the ANN method with the FZI-SWPHI technique, the averages of core permeabilities in the seven geological zones of Well X3 along with corresponding averages of predicted permeabilities calculated by both methods (ANN and FZI-SWPHI) are presented in **Table 6**. The ANN method overestimated the average permeability of one zone by 49.5% while the average permeability of another is underestimated by 65.5 %.

The cored interval in Well X7 is also divided into six 10m intervals and the averages of core and ANN-predicted permeabilities are calculated in these intervals, as shown in **Table 7**. The averages from the ANN method indicate errors of up to 72 % when compared with core averages.

**Comparison with Regression Technique.** Regressions are often used to find a relationship between FZI and log data, and predict permeability from log attributes. This method does not estimate permeability accurately as demonstrated by the results from Wells X3 and X7. The permeability of these wells by regression is compared with core values in Fig. 10 (column 5) and Fig. 8 (column 5) respectively. These figures show that permeabilities are overestimated when the interval has low permeability and underestimated for high-permeability intervals.

The averages of permeability values calculated by regression for the seven zones of Well X3 are given in **Table 8**. The overestimation of average permeability is as high as 53% (zone 2), with

underestimates of up to 62.6% (zone 1). For Well X7, averages of interval permeabilities are given in **Table 9**; errors range in this calculation from +49 % to -30%.

**Comparison with Coates and SDR Models.** NMR permeabilities after Coates and SDR (Schlumberger Doll Research Center) are calculated in Well 1-32 of Wellington Field using the following equations:

$$k_{Coates} = A * (10 * \phi)^4 * \left(\frac{FFI}{BWT}\right)^2 \dots\dots\dots(21)$$

$$k_{SDR} = A * (\phi)^4 * (T_2)^2 \dots\dots\dots(22)$$

The prefactor of Coates and SDR equations are adjusted from the default value of 1 and 4 to 0.1 to obtain the best match with the core data in the porous interval of the Mississippian formation. Permeability values from NMR using these methods are compared with the core permeability and the FZI-SWPHI method in Fig. 9 (column 6). Although there is good agreement between the predicted permeability and the core permeability in the interval from 3670 to 3690 ft (Zone 3) in Fig. 9 (column 6), significant differences are observed between the core data and the predicted permeability by SDR and Coates methods in other intervals.

**Conclusions**

1. The permeability of a reservoir rock is a function of the porosity and the irreducible water saturation.
2. The FZI from core data can be related to water saturation and porosity from log to find a permeability equation for the reservoir rock.
3. The authors have developed a new, practical and theoretically correct technique called the FZI-SWPHI method relating FZI from core data, and water saturation and porosity from log data to provides a specific permeability equation (Eq.10) for a reservoir or reservoir interval.
4. Coefficients *a* and *b* in Eq. 10 are functions of the shape factor of the grains and the tortuosity of the pore space.
5. The irreducible water saturation and porosity from both conventional logs and NMR logs can be used to derive the coefficient *a* and *b* of the permeability equation.
6. Generally when the sedimentary and diagenetic environment of a reservoir does not vary significantly, a single equation can give accurate permeability for the reservoir.
7. When intervals with different sedimentary environments or diagenesis exist in a reservoir, a separate equation for each interval provides more accurate permeability.

8. Previously, the FZI from core data was correlated to log attributes by regression or ANN to find FZI and permeability in the un-cored wells. These techniques do not have a theoretical basis and can often provide inaccurate permeability predictions for wells.
9. It has been shown that FZI-SWPHI method provides more accurate permeability relative to all the other techniques.
10. The application of the FZI-SWPHI technique to wells without core is more straightforward than the use of regression and ANN methods.
11. Generally, permeability from the NMR log is determined by the Coates and SDR models. The new technique can also be applied to the NMR data for determination of permeability.
12. The FZI-SWPHI method derives more accurate permeabilities from the NMR data than the Coates and SDR models.

## Nomenclature

- $\tau$  = tortuosity  
 $\phi_e$  = effective porosity (fraction bulk volume)  
 $\phi_z$  = pore volume to grain volume ratio  
 $a$  = constant  
 $b$  = constant  
*BWT* = total bound water, v/v  
*CGR* = computed gamma ray, API units  
 $c_n$  = constant  
*DRT* = discrete rock type  
*FFI* = free fluid index, v/v  
 $F_s$  = shape factor  
*FWL* = free water level  
*FZI* = Flow Zone Indicator ( $\mu\text{m}$ )  
*FZI-SWPHI* = Flow Zone Indicator- Irreducible Water Saturation and Porosity  
*GR* = gamma ray, API units  
*HU* = Hydraulic Units  
 $k$  = permeability ( $\mu\text{m}^2$ )  
*NMR* = Nuclear magnetic resonance  
 $R$  = ratio  
 $r_{mh}$  = mean hydraulic radius ( $\mu\text{m}$ )  
*RQI* = Reservoir Quality Index ( $\mu\text{m}$ )  
*SGR* = standard gamma ray, API units  
 $S_{gv}$  = surface area per unit grain volume ( $\mu\text{m}^{-1}$ )  
 $S_{wir}$  = irreducible water saturation (fractional pore volume)  
 $T2$  = NMR transverse relaxation time (ms)  
 $x_n$  = constant

## Acknowledgements

The authors would like to thank the Kansas Geological Survey for permission to use sample data from the Wellington field. The authors would also like to thank Schlumberger for their permission to use the Techlog software at KGS. The authors appreciate reviews of earlier drafts of the document by Dr. Daveton at KGS and Andrew Bjorn.

## References

1. Amaefule, J.O., Altunbay, M., Tiab, D. et al. 1993. Enhanced Reservoir Description: Using Core and Log Data to Identify Hydraulic (Flow) Units and Predict Permeability in Uncored Interval/Wells. paper SPE 26436 presented at the SPE Annual Technical Conference and Exhibition in Houston, Texas, 3-6 October.
2. Archie G.E. 1950. Introduction to petrophysics of reservoir rocks. *Bulletin of the American Association of Petroleum Geologists*, Tulsa, **34** (5): 943-961.
3. Balan, B., Mohaghegh, S., and Ameri, S. 1995. State-Of-The-Art in Permeability Determination From Well Log Data: Part 1- A Comparative Study, Model Development. paper SPE 30978 presented at the SPE Eastern Regional Conference and Exhibition held in Morgantown, West Virginia, 17-21 September.
4. Balan, B., Mohaghegh, S., and Ameri, S. 1995. State-Of-The-Art in Permeability Determination From Well Log Data: Part 2- Verifiable, Accurate Permeability Predictions, the Touch-Stone of All Models. paper SPE 30979 presented at the SPE Eastern Regional Conference and Exhibition held in Morgantown, West Virginia, 17-21 September.
5. Buckles, R. S. 1965. Correlating and Averaging Connate Water Saturation Data. *J. Cdn. Pet. Tech.*, **9** (1): 42-52.
6. Carman, P.C. 1938. Fluid Flow Through Granular Beds. *J Soc Chem Ind.* **57**, 225.
7. Coats, G.R. and Dumanoir, J.L. 1974. A New Approach to Improved Log-Derived Permeability. *The Log Analyst*, **15** (1).
8. Guo G., Diaz M.A., Paz F. et al. 2005. Rock Typing as an effective Tool for Permeability and Water Saturation Modeling: A Case Study in a Clastic Reservoir in the Oriente Basin. paper SPE 97033 presented at the SPE Annual Technical Conference and Exhibition, Dallas, Texas, 9-12 October.
9. Kharrat R., Mahdavi R., Bagherpour M.H. et al. 2009. Rock Type and Permeability Prediction of a Heterogeneous Carbonate Reservoir Using Artificial Neural Networks Based on Flow Zone Index Approach. paper SPE 120166 presented at the SPE Middle East Oil and Gas Show and Conference, Bahrain, 15-18 March.
10. Kozeny, J. 1927. Sitzber. Akad. Wiss. Wien. Math. Naturw. Klasse. **136**, 271.
11. Schlumberger Well Services. 1986. Log Interpretation Principles/Applications. Houston, Texas.
12. Shenawi S.H., White J.P., Elrafie E.A. et al. 2007. Permeability and Water Saturation Distribution by Lithologic Facies and Hydraulic Units: A Reservoir Simulation Case Study. paper SPE 105273 presented at the 15th SPE Middle East Oil & Gas Show and Conference, Bahrain, 11-14 March.
13. Svirsky, D., Ryazanov, A., Pankov, M. et al. 2004. Hydraulic Flow Units Resolve Reservoir Description Challenges in a Siberian Oil Field. Paper SPE 87056 presented at the SPE Asia Pacific Conference on Integrated Modeling for Asset Management held in Kuala Lumpur, Malaysia, 29-30 March.

14. Timur, A. 1968. An Investigation of Permeability, Porosity, and Residual Water Saturation Relationship for Sandstone Reservoirs. *The Log Analyst*, **9** (4): 8
15. Tixier, M.P. 1949. Evaluation of Permeability from Electric-Log Resistivity Gradients. *Oil & Gas J.* pp.113
16. Wyllie, M.R.J. and Rose, W.D. 1950. Some Theoretical Considerations Related to the Quantitative Evaluation of the Physical Characteristics of Reservoir Rock from Electric Log Data. *J.Pet. Tech.* **189**, pp. 105.

**Table 1. Zonation in Well X3.**

<b>Zone</b>	<b>Interval</b>	<b>Dominant Archie Rock Description</b>	<b><math>R/S_{wir}\phi_e</math> from Log Compared with Core FZI</b>
1	3099.3-3104.9	I,A, I,A/B, & I/II,A	Less than core FZI
2	3105.0-3114.9	II/I,A/B	More than core FZI
3	3115.1-3134.9	II,A/C,VUG & II/I,A/C,VUG	Equal to core FZI
4	3135.0-3149.4	II,A/C,VUG	More than core FZI
5	3149.5-3180.4	II,A/C,VUG, II,B & II/I,A/B	Equal to core FZI
6	3180.6-3190.5	II/I,A/B & II/I,A/C VUG	Less than core FZI
7	3190.6-3197.5	I/II,A/B & A/C	Less than core FZI

**Table 2. Correlation coefficients between FZI and  $1/S_{wir}\phi$  in Well X3.**

<b>Zone</b>	<b>Depth, m</b>	<b><i>a</i></b>	<b><i>b</i></b>	<b><math>R^2</math></b>
1	3099.3-3104.9	0.025	-0.196	0.930
2	3105.0-3114.9	0.014	-0.292	0.909
3	3115.1-3134.9	0.028	-0.574	0.978
4	3135.0-3149.4	0.037	-1.02	0.901
5	3149.5-3180.4	0.027	-0.378	0.967
6	3180.6-3190.5	0.133	-2.14	0.996
7	3190.6-3197.5	0.361	-5.7	0.984

**Table 3. Correlations between zones in Wells X3 and X7.**

<b>Zone</b>	<b>Depth in Well X, m3</b>	<b>Depth in Well X7, m</b>
1	3099.3-3104.9	Not logged
2	3105.0-3114.9	3114.9-3125.0
3	3115.1-3134.9	3125.1-3145.2
4	3135.0-3149.4	3145.4-3159.4
5	3149.5-3180.4	3159.6-3192.5

6	3180.6-3190.5	3192.6-3197.2
7	3190.6-3197.5	Not drilled

**Table 4. Zonation in Well 1-32.**

Zone	Depth	Lithology description	NMR T2 distribution
1	3656-3663.5	Sandstone with more than 20% clay	Multi modal
2	3663.5-3667.5	Sandstone with less than 10% clay	Mainly bimodal
3	3667.5-3696	Sandy dolomite with low clay content	Mainly single modal, high mean T2
4	3696-3714.5	Sandy dolomite with higher clay content	Mainly single modal, decreasing mean T2
5	3714.5-3759.5	Dolomitic and calcitic sandstone	Low mean T2, multimodal, low porosity

**Table 5. Correlation coefficients between FZI and  $1/S_{wir}\phi$  in Well 1-32.**

Zones	Depth, ft	<i>a</i>	<i>b</i>	<i>R</i> <sup>2</sup>
1	3656.0-3663.5	0.065	-0.625	0.96
2	3661.5-3667.5	0.201	-0.966	0.95
3	3670.5-3690.5	0.011	0.311	0.94
4	3696.0-3714.5	0.012	0.101	0.75
5	3714.5-3759.5	0.088	-1.474	0.69

**Table 6. Comparison of average permeability by FZI-SWPFI and ANN with core permeability in Well X3.**

Zone	Core	FZI-SWPFI		ANN	
	<i>k</i> , md	<i>k</i> , md	Error, %	<i>k</i> , md	Error, %
1	6.4	4.8	-24.8	2.2	-65.5
2	3.0	3.5	17.8	4.4	49.5
3	11.3	10.4	-8.2	8.9	-21.1
4	7.3	6.9	-5.3	8.9	22.6
5	10.6	9.6	-8.9	6.9	-34.9
6	4.2	3.8	-11.3	3.5	-18.2

7	2.4	1.8	-23.9	1.6	-31.8
---	-----	-----	-------	-----	-------

**Table 7. Comparison of average permeability by FZI-SWPHI and ANN with core permeability in in Well X7.**

Zone	Core	FZI-SWPHI	ANN		
	<i>k</i> , md	<i>k</i> , md	Error, %	<i>k</i> , md	Error, %
1	10.4	11.0	5.3	12.0	14.5
2	8.6	7.4	-14.3	11.4	32.6
3	6.6	6.0	-8.8	11.4	72.9
4	9.5	9.3	-2.0	11.5	20.3
5	13.6	14.8	8.9	10.5	-22.6
6	11.5	12.2	5.9	9.7	-16.0

**Table 8. Comparison of average permeability by FZI-SWPHI and regression with core permeability in Well X3.**

Zone	Core	FZI-SWPHI	Regression		
	<i>k</i> , md	<i>k</i> , md	Error, %	<i>k</i> , md	Error, %
1	6.4	4.8	-24.8	2.4	-62.6
2	3.0	3.5	17.8	4.5	53.1
3	11.3	10.4	-8.2	10.2	-9.6
4	7.3	6.9	-5.3	9.5	29.6
5	10.6	9.6	-8.9	6.7	-36.2
6	4.2	3.8	-11.3	3.0	-29.1
7	2.4	1.8	-23.9	1.4	-40.7

**Table 9. Comparison of average permeability by FZI-SWPHI and regression with core permeability in Well X7.**

Zone	Core K	FZI-SWPHI		Regression	
	$k, \text{ md}$	$k, \text{ md}$	Error, %	$k, \text{ md}$	Error, %
1	10.4	11.0	5.3	14.4	37.7
2	8.6	7.4	-14.3	11.1	29.3
3	6.6	6.0	-8.8	9.8	49.3
4	9.5	9.3	-2.0	11.4	19.6
5	13.6	14.8	8.9	11.8	-13.2
6	11.5	12.2	5.9	8.1	-30.2

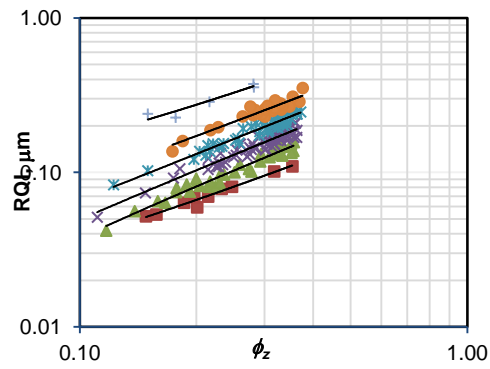


**Figure 5. RQI versus  $\phi_z$  in Well X3.**

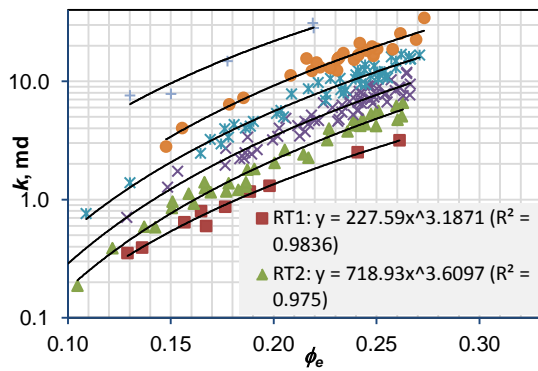


**Figure 2. Permeability versus  $\phi_e$  in Well X3**

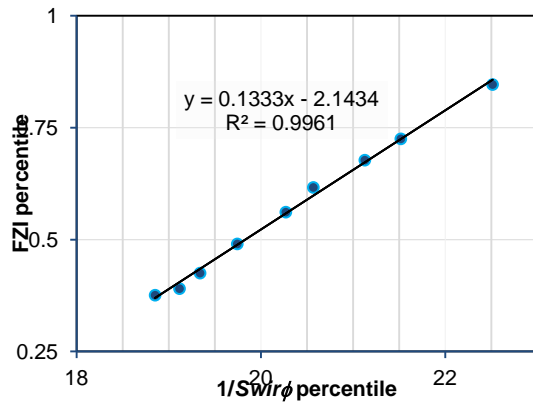


**Figure 3. FZI versus  $1/Swir\phi$  in zone 6 of Well X3.**

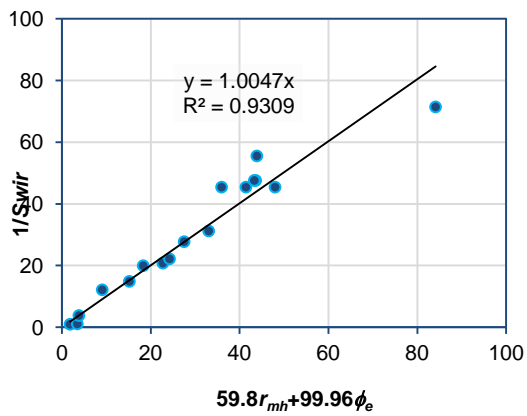


**Figure 4. Relation between mean hydraulic radius (rmh) and Swir.**

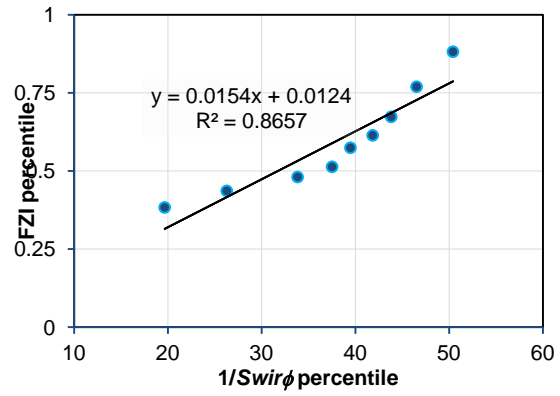


**Figure 5. FZI versus  $1/S_{wir}\phi$  in the entire zone of Well X3.**

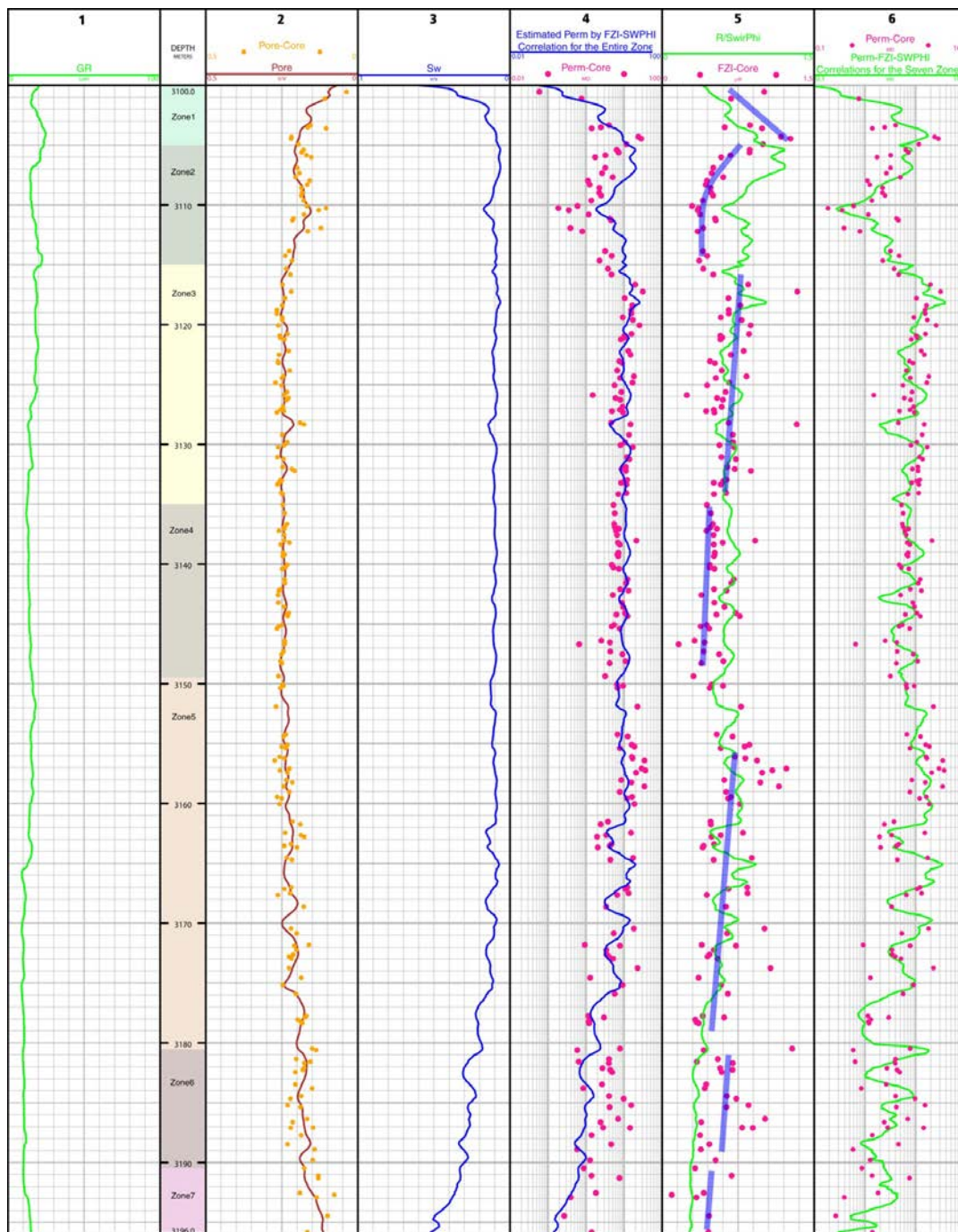


**Figure 6. Well X3, estimated permeability by a single correlation (FZI-SWPHI method) and correlations for seven zones.**

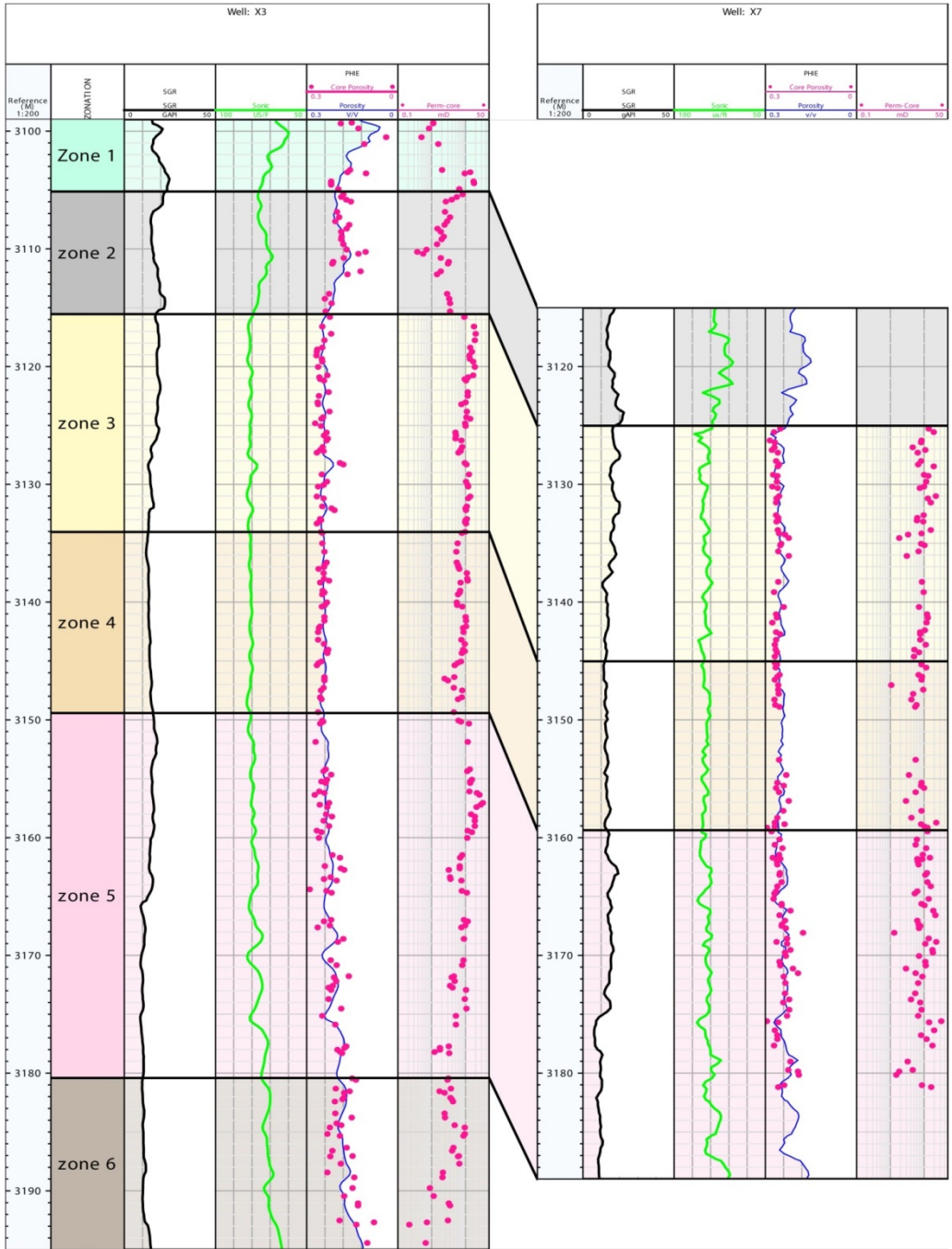


**Figure 7. Zonation in Well X7 based on geological zones in Well X3.**

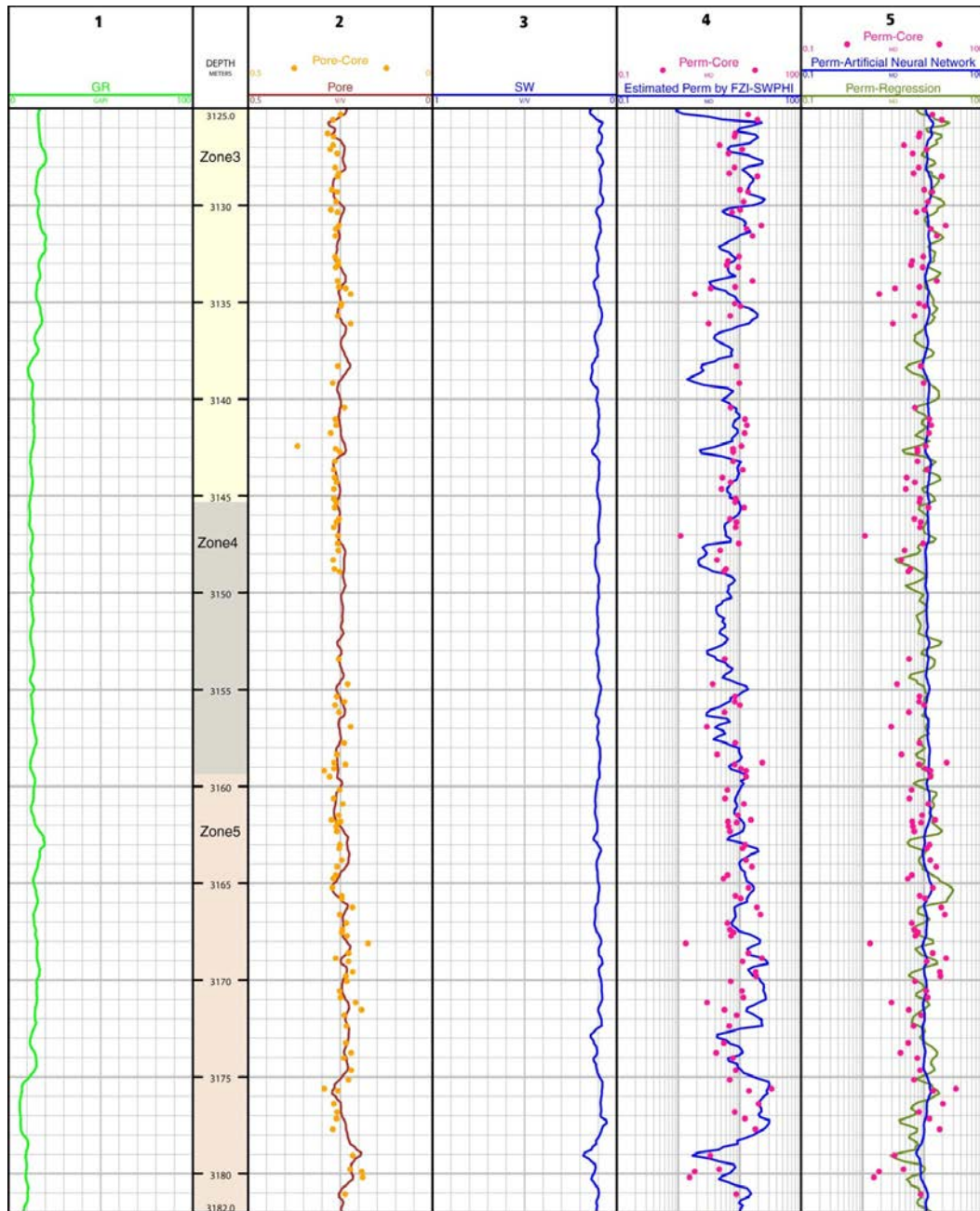


Figure 8. Well X7, estimated permeability by FZI-SWPHI, ANN and regression methods.

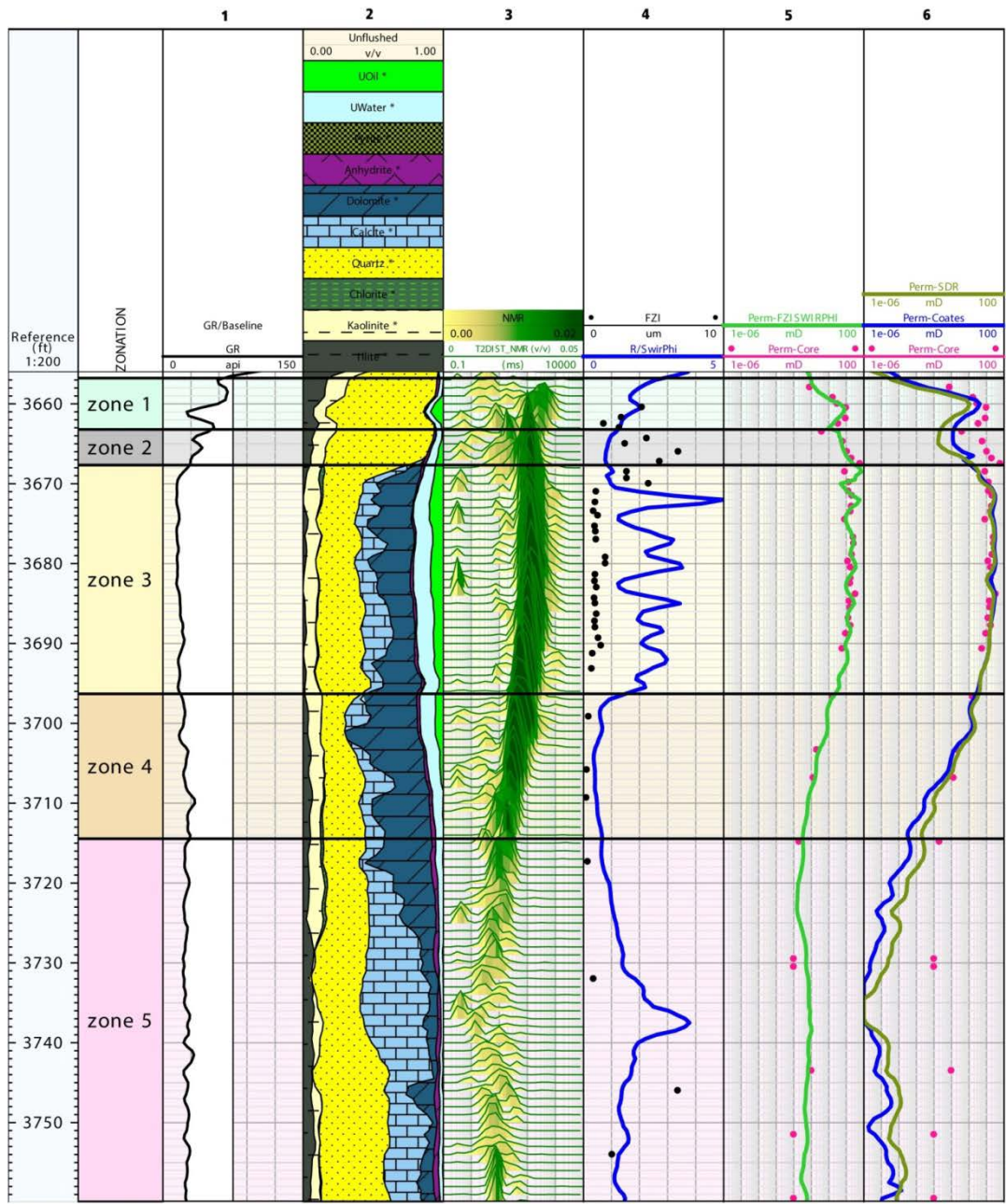
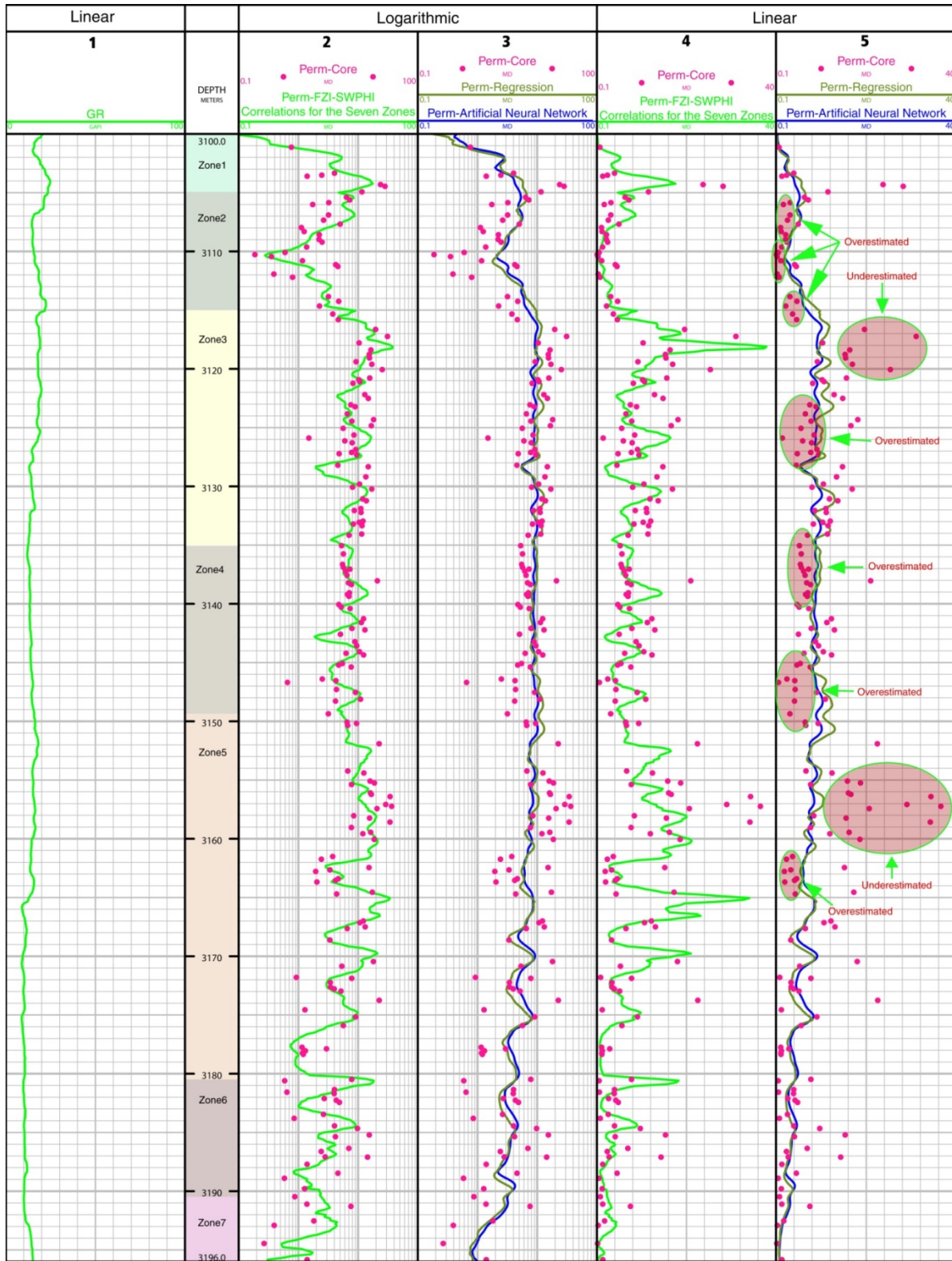


Figure 9. Well 1-32 zonation and permeability by FZI-SWPHI, Coates and SDR methods.



**Figure 10. Well X3, comparison of permeability by FZI-SWPHI method with ANN and regression methods.**

## APPENDIX E

### **January 21, 2014 Prospectus Governor's Conference Implementing CO<sub>2</sub> Utilization and Storage (CCUS) in Kansas**

To discuss the potential and challenges of large-scale carbon dioxide utilization and storage (CCUS) in Kansas, the Kansas Geological Survey proposes a one-day conference engaging industry, decision makers, and public.

CCUS offers significant potential for economic development for Kansas. A 2010 report for the Midwest Governor's Association indicated more than 750 million barrels of oil is potentially recoverable with enhanced recovery methods using carbon dioxide<sup>1</sup>. Oil prices and improved technology have rekindled interest by Kansas petroleum industry in the cost-effective application of CCUS to revive older fields. However, CO<sub>2</sub> will necessarily come from man-made sources such as ammonia, ethanol, refinery, and power plants requiring capital investments to capture the CO<sub>2</sub> and readiness of the oil fields to receive the CO<sub>2</sub>. Stakeholders must understand the oil resource, infrastructure requirements, financial and human resource needs, and the environmental and regulatory environment to develop a unified vision of large-scale CCUS in Kansas. The Governor's Conference would be dedicated to strengthening understanding and establishing comprehensive goals.

**Date:** (TBD)

**Location:** Hyatt Regency in Wichita, KS

**Target participants:** 150 total from Governor's Office, KCC, KDHE, Kansas Dept. of Commerce, Kansas Dept. of Agriculture, KIOGA, Kansas Geol. Society, industry including petroleum and CO<sub>2</sub> sources (ethanol, ammonia, power plant, refinery; gas suppliers), legislators, informed public, environmental advocacy groups, academia, KGS, TORP, PTTC, Interstate Oil and Gas Compact Commission, Groundwater Protection Council, Kansas Water Office, DOE, RPSEA, AAPG, Permian CCUS Center, Midwest Governor's Association

**Goals:**

1. Convey benefits and potential challenges of large-scale deployment of CCUS in Kansas.
2. Introduce infrastructure and workforce needs for large-scale CCUS in Kansas.
3. Understand importance of man-made CO<sub>2</sub> for large-scale CCUS in Kansas.

**Objectives:**

---

<sup>1</sup> CCI for MGA, 2012, CO<sub>2</sub>-EOR Potential in the MGA Region, 16 p. --  
<http://www.midwesterngovernors.org/Publications/EOR2011.pdf>

- Establish potential of CCUS as a major boost to rural economic development in Kansas.
- Address safety and environmental considerations based on implementation in other locations.
- Describe CO<sub>2</sub> behavior and its management when stored underground.
- Summarize beneficial use of CO<sub>2</sub> in an oil reservoir, reference to large-scale examples.
- Introduce management of CO<sub>2</sub> in oil fields for long-term storage.
- Review readiness of oil fields and petroleum industry to conduct large-scale CCUS in Kansas.
- Assess of size and locations of oil resource in Kansas for CCUS.
- Analyze current and potential delivery of CO<sub>2</sub> for use in CCUS.
- Describe investment requirements and economics of CO<sub>2</sub>-EOR.
- Discuss steps toward large scale implementation of CO<sub>2</sub>-EOR.

**Format:** One day with 1) plenary session with keynote speakers, 2) breakout, 3) plenary session #2 with a panel providing summaries of breakout meetings, 4) summary with keynote speakers.

**Product:** White paper with meeting summary, recommendations, and action items.

## **PROPOSED AGENDA FOR GOVERNORS CONFERENCE**

### **“Implementing CO<sub>2</sub> Utilization and Storage (CCUS) in Kansas”**

- 7:30-8:30 Registration, coffee, continental breakfast, posters, exhibits
- 8:30-9:00 Overview, concepts, and goals of the meeting (Governor/KGS)
- 9:00-10:30 Presentations from stakeholders in CO<sub>2</sub> supply and distribution, readiness and needs of Kansas petroleum industry for CO<sub>2</sub> utilization, regulations for CO<sub>2</sub> capture and utilization, economic impact assessment, viewpoint of state policy makers, KGS summary
- 10:30-11:00 Break (discussion, exhibits posters)
- 11:00-12:00 Continue presentations
- 12:00-1:30 Networking lunch with keynote presentation (Potentially – “challenges and opportunities for aggregation of CO<sub>2</sub> supply and distribution to Kansas oil fields”)
- 1:30-3:00 Breakout sessions:
1. Steps toward implementing large-scale CCUS in Kansas
    - i. CO<sub>2</sub> supply – sources and transportation
    - ii. CO<sub>2</sub> utilization -- Readiness and needs
    - iii. Aggregation of CO<sub>2</sub> supply and CO<sub>2</sub> utilization in Kansas oil fields
  2. Economic incentives for CO<sub>2</sub> capture and CO<sub>2</sub> suppliers
  3. Regulation
    - i. Well and Field permitting
    - ii. Primacy of Class VI Injection permitting and implications of using added storage for CO<sub>2</sub> beneath the oil reservoir in deep saline aquifers

#### 4. Environmental Concerns

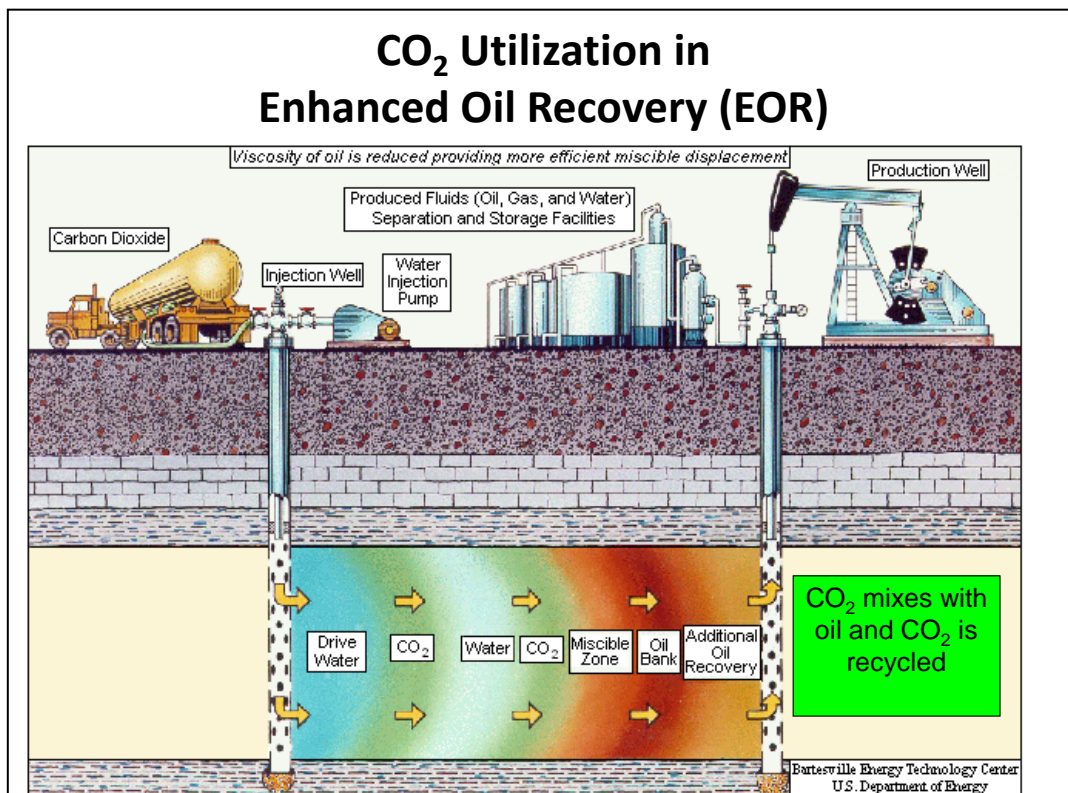
- i. Secure CO<sub>2</sub> storage
- ii. Induced seismicity

3:00-4:30 Plenary session to discuss breakout sessions via panel with session chairs and wrap-up with key points, action items, and future plans

4:30-5:30 Discussion with posters and exhibits

### Background

1. CO<sub>2</sub> supply, resource, projections
  - a. CO<sub>2</sub> behavior in an oil reservoir and capability for incremental oil recovery
  - b. Geologic (naturally occurring) CO<sub>2</sub>, e.g., supplying west Texas, Wyoming, Montana
  - c. Anthropogenic CO<sub>2</sub>, e.g., industrial sources – fertilizer, cement, ammonia, and ethanol plants; power plants in Kansas and Midwest
  - d. Readiness – factors influencing supply
    - i. Regulation
    - ii. Capture technology and economics
    - iii. Distribution – rail and pipeline distribution system
2. Utilization of CO<sub>2</sub> in Kansas
  - a. Establish demand for CO<sub>2</sub> in the oil field
  - b. Future use – develop plans for implementation and infrastructure
  - c. Technical timeframe
    - i. Oil field and operator readiness
    - ii. Field modeling and implementation plan to ensure success
    - iii. Scenarios for aggregating CO<sub>2</sub> supply and distribution to the field
    - iv. Economic incentives?



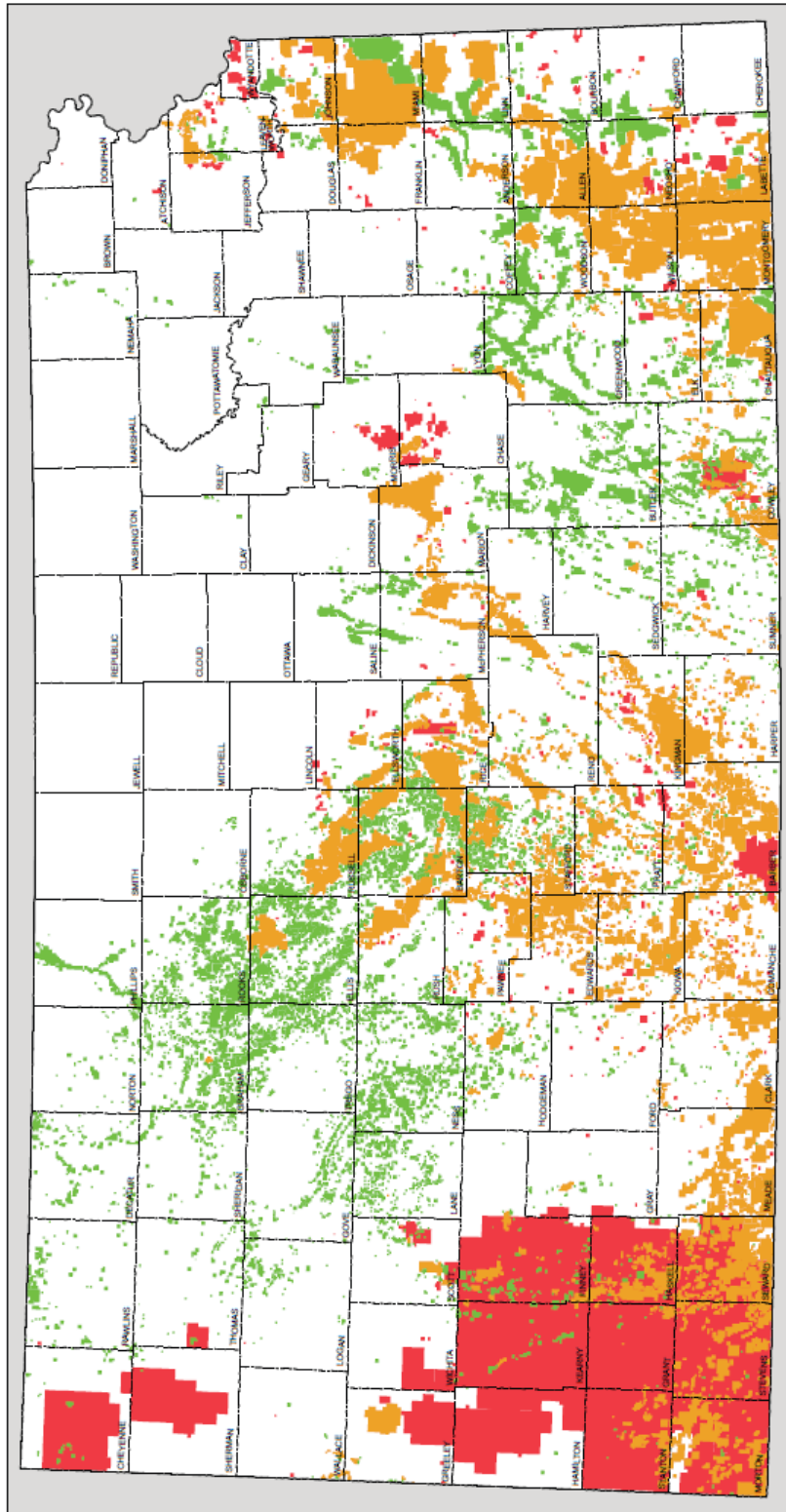
## STEPS TOWARD CO<sub>2</sub> UTILIZATION AND STORAGE IN KANSAS

1. **Core Concepts and Goals –**
  - a. Combine oil field and deeper saline aquifer storage to provide large capacity storage for long term,
  - b. Regulatory primacy over EPA to manage CO<sub>2</sub> in Kansas,
  - c. Public awareness and support for carbon management,
  - d. Business opportunities and advocacy
  - e. R&D support and integration with needs of Kansas – aquifer and public health, petroleum, transportation from CO<sub>2</sub> source to sink
2. **Increase capacity of storage with underlying saline aquifer storage**
  - a. Insure injection rate with backup disposal
  - b. Analogous to Wellington and southwestern fields modeled as part of SW KS CO<sub>2</sub>-EOR Initiative
3. **Identify fields for miscible and immiscible CO<sub>2</sub> oil recovery**
4. **Refine KGS interactive CO<sub>2</sub> oil and gas mapper for access to key information**
  - a. Highlight and extract cumulative oil; depth; temperature; oil gravity
    - i. Screen and highlight candidate fields/plays for CO<sub>2</sub> miscibility, total field and lease performance, recoverable reserves and CO<sub>2</sub> requirements (volume and rates)
  - b. Identify resources for CO<sub>2</sub>-EOR via **interactive map of Kansas oil fields** utilizing web apps to analyze the data “*on the fly*”
  - c. Develop scoping models of oil fields to forecast technical success and favorable economics currently
  - d. Reply results of **CO<sub>2</sub> test injection at Wellington Field (DE-FE0006824)** and four fields (Shuck, Eubanks, Cutter, and Pleasant Prairie South) in as part of **SW Kansas CO<sub>2</sub>-EOR Initiative (DE-FE0002056)**.
5. **Monitoring and compliance for carbon trading and effective and economic use to satisfy regulators**
  - a. Continue dialog with our legislators to encourage support of carbon management in Kansas
6. **Establish interest and participation of field operators and CO<sub>2</sub> suppliers**
  - a. Develop portfolio of prospective oil fields with operator interest
  - b. Establish infrastructure scenarios (location and transportation options for CO<sub>2</sub>)
7. **Engage stakeholders to develop, support and underwrite strategic initiative**
  - a. Planning grant to administrate and develop components of a Kansas CO<sub>2</sub> initiative/Kansas Model for CO<sub>2</sub> Utilization and Storage
    - i. Secure advisory group of operators, gas suppliers, officials with Department of Commerce and KU, lawmakers and regulators
    - ii. Define needs to address uncertainties and concerns, weigh challenges and concerns against benefits to affect public perception, sequestration defined, state of readiness, engaging community, leveraging what has been learned, priorities, and opportunities via **Governor’s Conference**
    - iii. Timetable and costs for planning and development
    - iv. Establish state of the technology in Kansas via research and workshop workshops and share resources and scoping models
8. **Encourage collaborative research in carbon management**

- 9. KU Research Initiative -- Sustaining the Planet, Powering the World**
- 10. Education and public acceptance with open dialog**

# OIL AND GAS FIELDS OF KANSAS

2009



## Named Fields

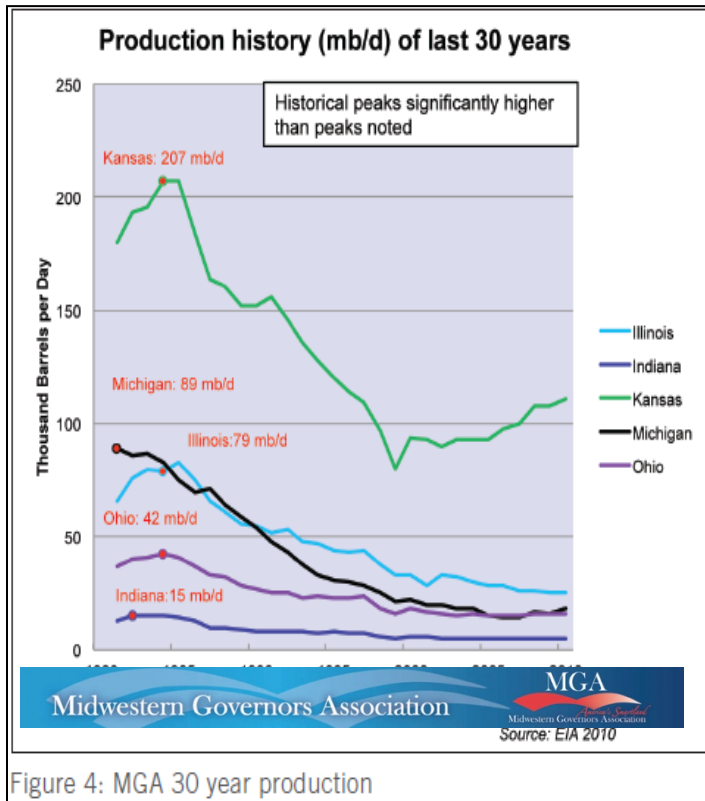


SCALE 1:2 600 000  
LAMBERT CONFORMAL CONIC PROJECTION  
WITH STANDARD PARALLELS AT 37° AND 45°N  
CENTRAL MERIDIAN 98°20' W  
NORTH AMERICAN DATUM OF 1983

This map was prepared by the staff of the Kansas Geological Survey and is based on Oil and Gas Fields in Kansas (1967) and subsequent revisions with the same name (1975, 1989, 1990, and 1993). Fields are represented according to their status as of June 1, 2009. Listings of fields by location, name, and cumulative production are found in the Survey's interactive oil and gas map viewer, located at <http://maps.kgs.ku.edu/oilgas/index.cfm>. For viewer instructions, click on the "Help" tab at the top of the page. Due to frequent data updates, field and production area boundaries may differ slightly from those shown on this map. All fields are shown without differentiation between active and inactive. Areas of annual gas production from coal are not included on this map.

As set forth in Kansas Administrative Rule 82-3-102, field boundaries are determined by the Kansas Corporation Commission after considering the recommendations of the Conservation Division, Kansas Corporation Commission, and the Nomenclature Committee, Kansas Geological Society.

The Kansas Geological Survey does not guarantee this map to be free from errors or inaccuracies and disclaims any responsibility or liability for interpretations made from the map or decisions based thereon.



**Kansas is well positioned to receive CO<sub>2</sub> from neighboring anthropogenic sources to the north and east.**

<http://www.midwesterngovernors.org/Publications/EOR2011.pdf>

**CO<sub>2</sub>-EOR Potential in the MGA Region**

February 26, 2012 | Washington D.C.

- Kansas holds more than **750 million barrels** of technical CO<sub>2</sub>-EOR potential.
- Kansas has by far the largest oil resources in the MGA region.
- Economic results based on Hall Gurney field suggest an after-tax project IRR of about 20%.
- Kansas ...would have access to the significant volumes of ethanol-based CO<sub>2</sub> in Nebraska, which produces approximately 6 million metric tons per annum.

Basin	EOR potential (Mil bbl)	Net CO <sub>2</sub> Demand (MMT)	Direct Jobs Created
Illinois/Indiana	500	160 – 250	1,550 – 3,100
Ohio	500	190 – 300	1,550 – 3,100
Michigan	250	80 – 130	800 – 1,800
Kansas	750	240 – 370	2,300 – 4,600
<b>TOTALS</b>	<b>2,000</b>	<b>670 – 1,050</b>	<b>6,200 – 12,400</b>

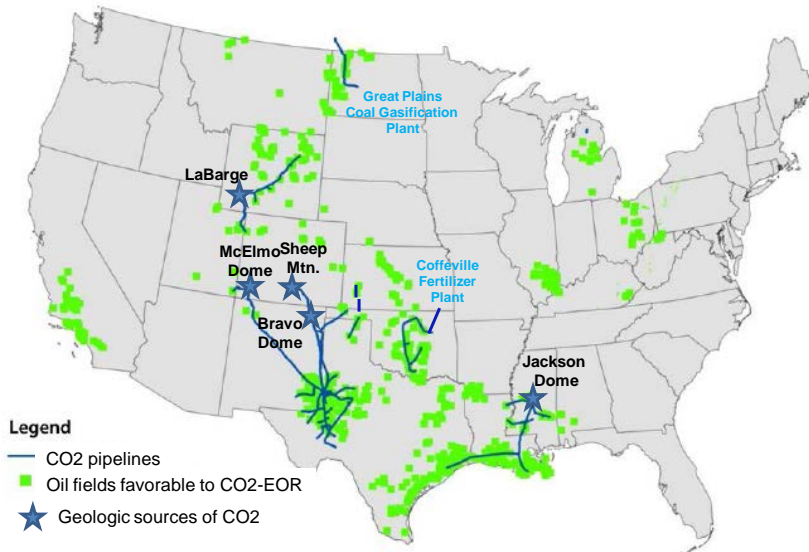
**Study sponsored by MGA indicates Kansas has considerable CO<sub>2</sub>-EOR potential. 750 million barrels would require an estimated 240-370 million metric tons of CO<sub>2</sub> (4.62-7.12 BCF CO<sub>2</sub>).**

19.25 MCF/tonne

Current market value of compressed pipeline CO<sub>2</sub> is 2% price of oil.

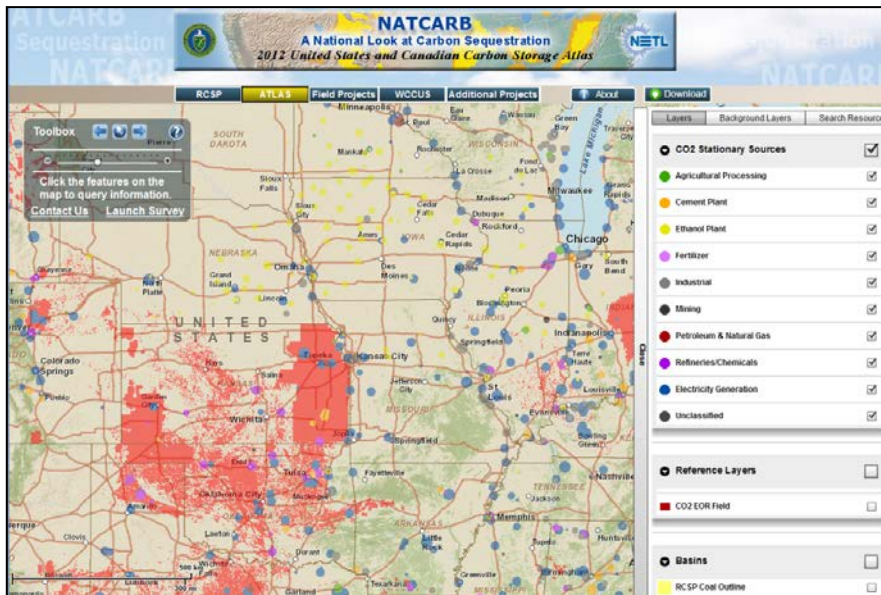
\$2.00 cost per MCF  
**\$38.50 cost per tonne**

## Current CO<sub>2</sub> Pipeline Infrastructure

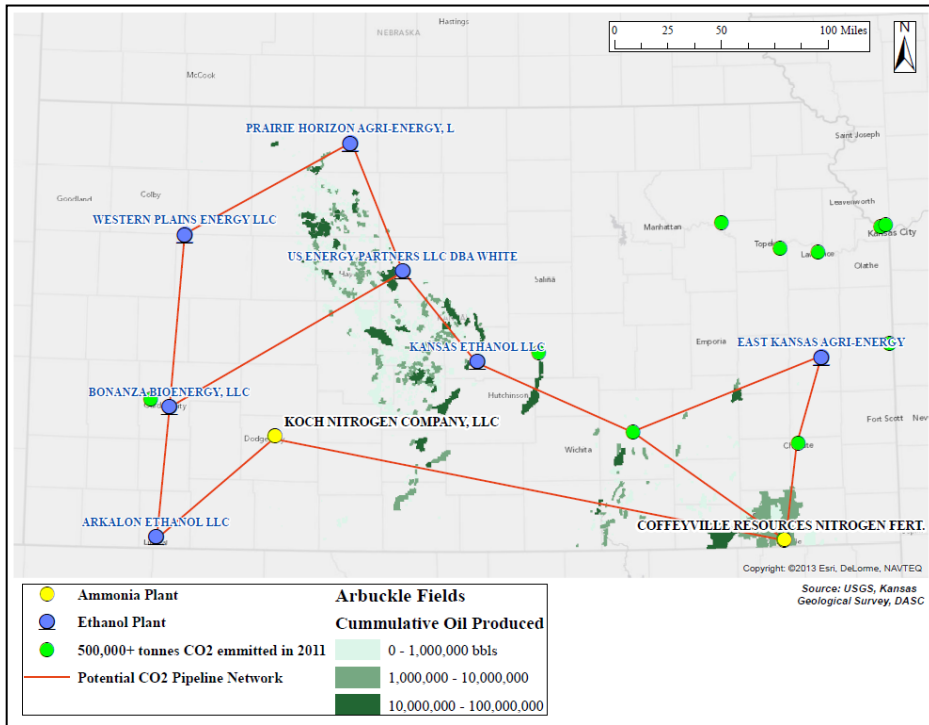


Oil-bearing formations favorable for CO<sub>2</sub>-EOR, onshore lower 48 states.  
 (Source: ARI disaggregated database, Ventex Velocity Suite Database)

oil and gas  
 e currently  
 from the  
 regional CO<sub>2</sub>  
 systems that  
 ng  
 opi,  
 ia, Texas,  
 xico,  
 na,  
 o, Wyoming,  
 a, and North

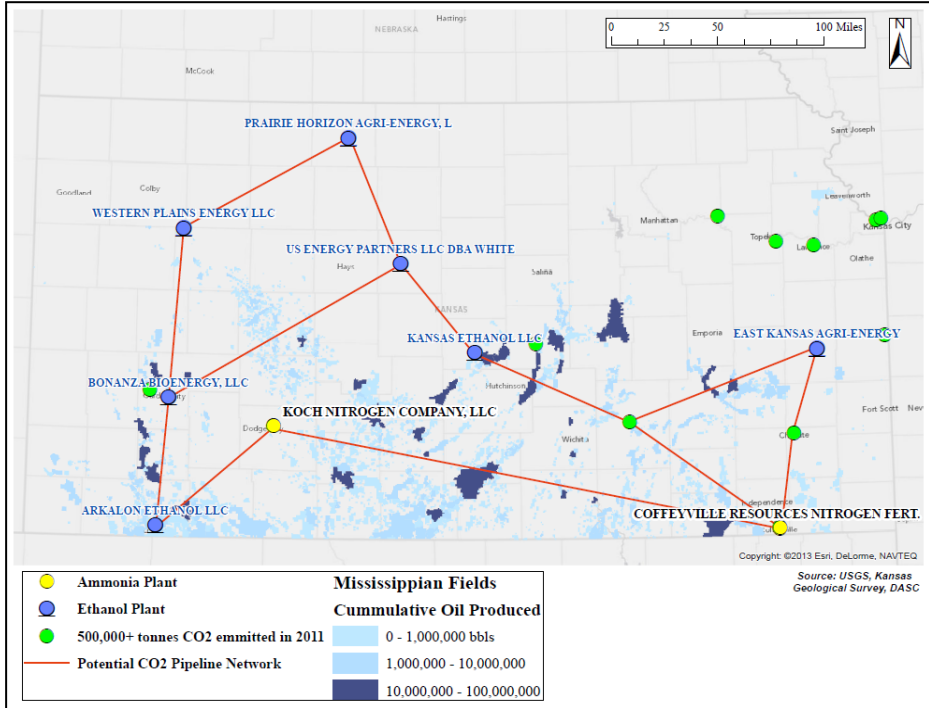


Kansas has it's own  
 local sources of CO<sub>2</sub>,  
 but ethanol plants  
 (yellow dots on map)  
 are numerous in  
 Nebraska, which has  
 limited oil and gas  
 resources. MGA  
 suggests CO<sub>2</sub> could  
 potentially be  
 transported to  
 Kansas.

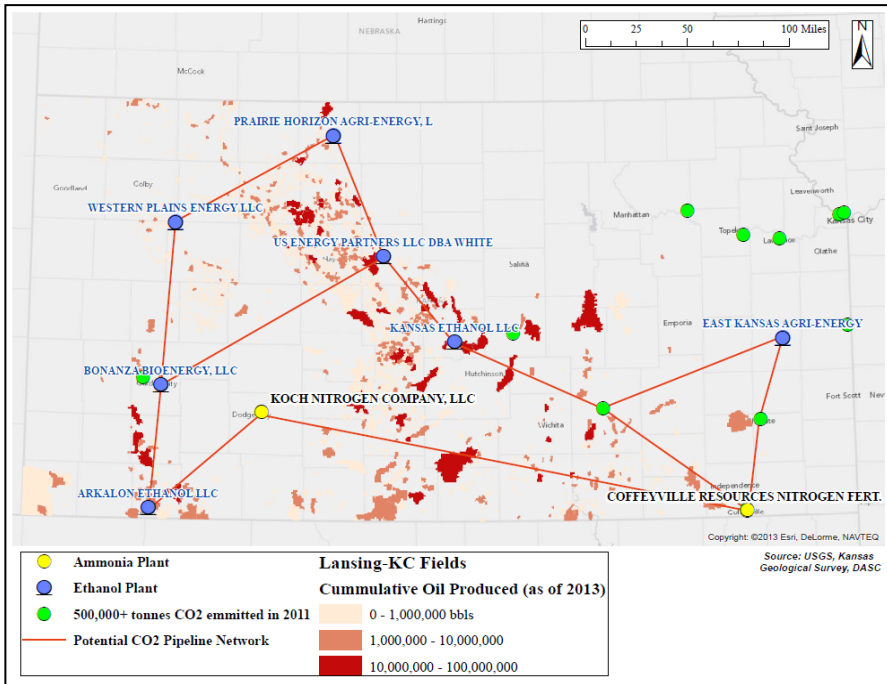


**Kansas oil fields producing from Arbuckle Group reservoirs. CO<sub>2</sub>-EOR would vary from partial to fully miscible recovery, affecting efficiency of oil recovered. Ethanol (blue dots) and ammonia plants (yellow dots), and large stationary CO<sub>2</sub> including power plants and refineries (green dots) are**

down with potential pipeline system providing CO<sub>2</sub> to oil fields.



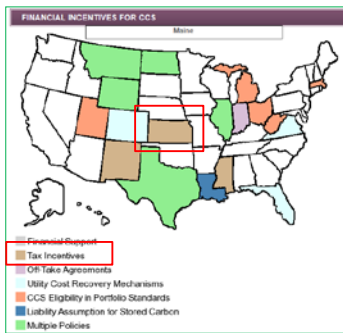
**Kansas oil fields producing from Mississippian reservoirs. Most of these reservoirs would likely have miscible CO<sub>2</sub>-EOR.**



**Kansas oil fields producing from Lansing-Kansas City reservoirs. Most of these reservoirs would likely have miscible CO<sub>2</sub>-EOR.**

**Kansas Incentive for carbon capture and storage**

**Kansas H.B. 2419 creates tax incentives for carbon capture and storage, namely income tax deductions for the amortization of CCS equipment costs and property tax exemptions.**



<http://www.c2es.org/us-states-regions/policy-maps/ccs-financial-incentives>

**HOUSE BILL No. 2419**

**AN ACT** enacting the carbon dioxide reduction act, providing for income tax reductions and property tax exemptions; providing for regulation of carbon dioxide injection wells; amending K.S.A. 2006 Supp. 79-32,117, 79-32,120 and 79-32,138 and repealing the existing sections; also repealing K.S.A. 2006 Supp. 79-32,117I.

*Be it enacted by the Legislature of the State of Kansas:*

**New Section 1.** Sections 1 through 7, and amendments thereto, may be cited as the carbon dioxide reduction act.

**New Sec. 2.** (a) As used in sections 2 through 5, and amendments thereto:

(1) "Carbon dioxide injection well" means any hole or penetration of the surface of the earth used to inject carbon dioxide for underground storage or for enhanced recovery of hydrocarbons and any associated machinery and equipment used for such injection of carbon dioxide. "Carbon dioxide injection well" does not include underground storage.

(2) "Commission" means the state corporation commission.

(3) "Underground storage" means any underground formation where carbon dioxide is injected for sequestration.

(b) For the purposes of protecting the health, safety and property of the people of the state, and preventing escape of carbon dioxide into the atmosphere and pollution of soil and surface and subsurface water detrimental to public health or to plant, animal and aquatic life, the commission, on or before July 1, 2008, shall adopt separate and specific rules and regulations establishing requirements, procedures and standards for the safe and secure injection of carbon dioxide and maintenance of underground storage of carbon dioxide. Such rules and regulations shall include, but not be limited to: (1) site selection criteria; (2) design and development criteria; (3) operation criteria; (4) casing requirements; (5) monitoring and measurement requirements; (6) safety requirements, including public notification; (7) closure and abandonment requirements, including the financial requirements of subsection (e); and (8) long-term monitoring.

**Tax deductions and property tax exemptions are in place.**

## CO2 EOR technology & Geologic Carbon Management Research in Kansas

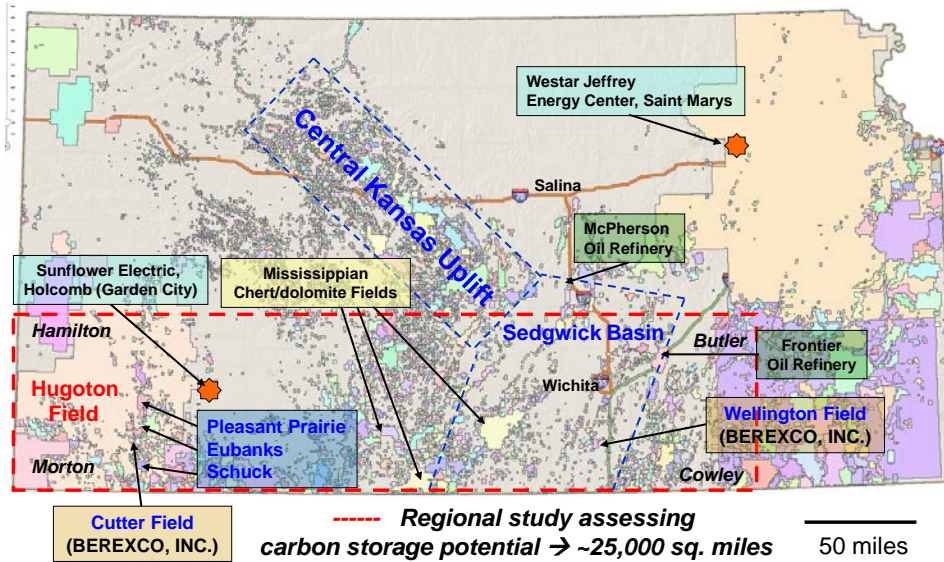


- Surface infrastructure, equipment, and wells used for EOR parallel those envisioned for carbon storage
- Comparable subsurface simulation and characterization tools (well logs, three-dimensional (3-D) seismic, petrophysical analysis, etc.)
- KGS Class VI geologic sequestration well
  - possibly first in the country
- Evaluating 10 sites for commercial scale application or carbon storage beneath existing oil fields
  - promising findings
- KU & partners have performed extensive research on:
  - monitoring
  - verification
  - accounting of the CO2 over the long term



Kansas has been conducting research in CO<sub>2</sub>-EOR since the late 1990s and work continues today to facilitate this technology as it is applied to Kansas oil reservoirs.

## Project Study Areas with Oil and Gas Fields and Major CO<sub>2</sub> Sources



Current research conducted by KU and KGS are focused on field studies and main reservoir types to make them ready for CO<sub>2</sub>-EOR.

## CO2 EOR Projections – Pleasant Prairie South Field

### Assumptions:

1. Convert WIW to CO2 IW
2. Oil wells as is
3. Inject 5 mmcf CO2, not exceeding bhp 2600 psi
4. Continuous CO2, no WAG
5. Injection = production
6. No optimization

### Projections:

#### OIL (mmbo)

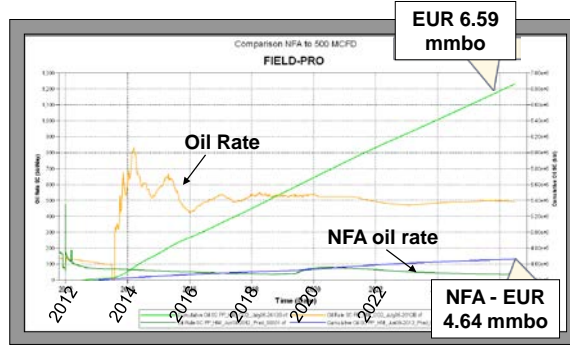
Cumulative 2011	4.48
NFA cum. 2026	4.64
CO2 case cum.	6.59

Increment. CO2	1.95
Cum. 2012-2026	2.11

#### CO2

	mm tons	
CO2 injected (mmcf)	23.7	1.38
CO2 produced (mmcf)	13.2	0.77
CO2 sequestered (mmcf)	10.5	0.61

Gross utilization (mcf/bo)	11.2
Net utilization (mcf/bo)	5.0



13 years injection

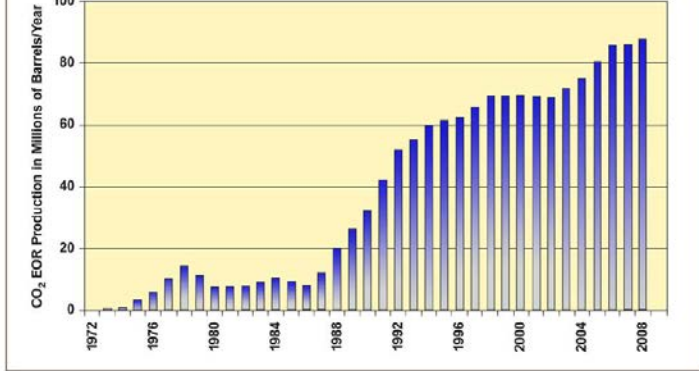
#### RF as f(OOIP)

Primary	15.8%
Secondary	15.8%
CO2	13.3%
<b>Total</b>	<b>45.0%</b>

assume 56%  
CO2 is recycled

Example of analysis of a Mississippian oil reservoir in southwest Kansas simulating recovery of oil using CO<sub>2</sub>.

## CO2- EOR Oil Production trends



Major U.S. CO<sub>2</sub> Operators (OGJ Biennial EOR Survey 2008)

Company	Miscible Projects	Locations	Incremental Production (MBO/D <sup>a</sup> )
Occidental	29	TX, NM	90.2
Hess	6	TX	25.3
Kinder Morgan	1	TX	24.2
Chevron	4	CO, TX, NM	21.3
Denbury Resources	13	MS, LA	17.8
Merit Energy	7	WY, OK	13.6
ExxonMobil	2	TX, UT	11.7
Anadarko	4	WY	9.0
Whiting Petroleum	3	TX, OK	6.9
ConocoPhillips	2	TX, NM	5.5
12 other independents	28	TX, OK, UT, KS, MI	14.9
<b>Total</b>	<b>99</b>		<b>240.4</b>

<sup>a</sup> thousand barrels of oil per day

### Illustrative Costs and Economics of a CO<sub>2</sub> EOR Project

Oil Price (\$/Barrel)	\$70
Gravity/Basis Differentials, Royalties and Production Taxes	(\$15)
<b>Net Wellhead Revenues (\$/Barrel)</b>	<b>\$55</b>
Capital Cost Amortization	(\$5 to \$10)
CO <sub>2</sub> Costs (@ \$2/Mcf for purchase; \$0.70/Mcf for recycle)	(\$15)
Well/Lease Operations and Maintenance	(\$10 to \$15)
<b>Economic Margin, Pre-Tax (\$/Barrel)</b>	<b>\$15 to \$25</b>

[http://www.netl.doe.gov/technologies/oil-gas/publications/EP/small\\_CO2\\_eor\\_primer.pdf](http://www.netl.doe.gov/technologies/oil-gas/publications/EP/small_CO2_eor_primer.pdf)

Carbon Capture & Sequestration Technologies @ MIT

Home | Bibliography | Research | C.S.I. | CCS Project Database | Tools | About Us

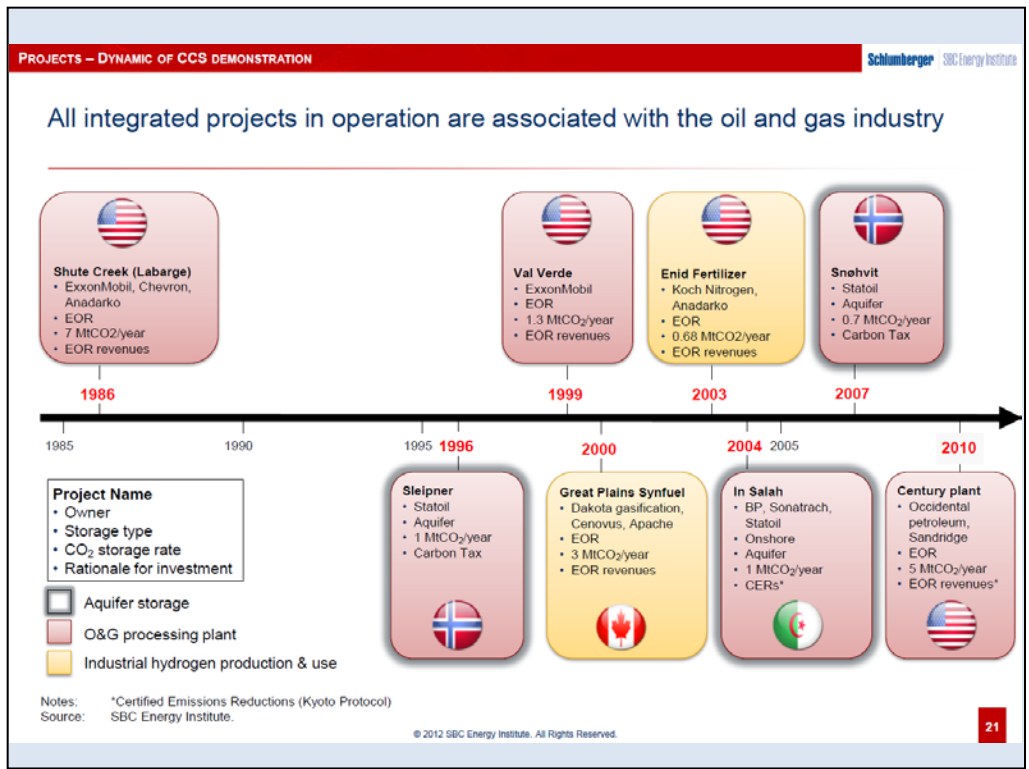
### Commercial EOR Projects using Anthropogenic Carbon Dioxide

Click on Project Name to go to Fact Sheet  
Click on country name to go to regional financial summary

USA						
Project	Leader	Location	CO2 Source	Size Mtyr	CO2 Sink	Status
Val Verde	Multiple operators	Texas	Gas Processing	1.3	EOR	Operational 1972
La Barge	Exxon Mobil	Wyoming	Gas Processing	6	EOR	Operational 1986
Enid Fertilization	Koch Nitrogen Company	Oklahoma	Fertilizer Production	0.68	EOR	Operational 2003
Century Plant	Occidental Petroleum	Texas	Gas Processing	5	EOR	Operational 2010
Coffeyville	CVR Energy	Kansas	Fertilizer Production	1	EOR	Operational 2013
Lost Cabin	ConocoPhillips	Wyoming	Gas Processing	1	EOR	Operational 2013
Rest of the World						
Project	Leader	Location	CO2 Source	Size Mtyr	CO2 Sink	Status
Lula	Petrobras	Brazil	Gas Processing	0.7	EOR	Operational 2013
Uthmaniyah	Saudi Aramco	Saudi Arabia	Gas Processing	0.8	EOR	Planning

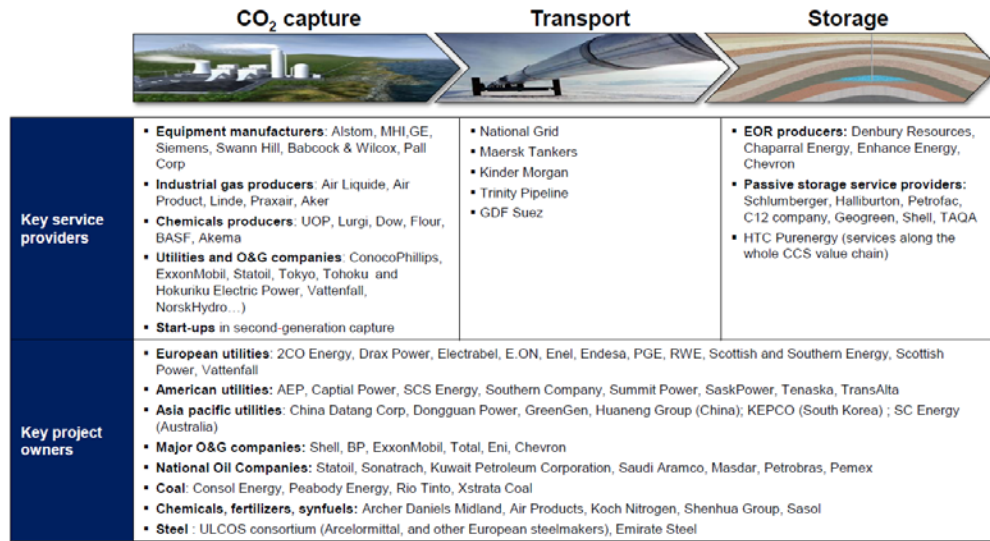
[http://sequestration.mit.edu/tools/projects/index\\_eor.html](http://sequestration.mit.edu/tools/projects/index_eor.html)

Gas Processing and fertilizer plants commercially capture CO<sub>2</sub> today including Koch Dodge City fertilizer plant. CO<sub>2</sub> is used primarily for beverages while their Enid plant is in part used for CO<sub>2</sub>-EOR.



Large industrial gas suppliers are interested in the CO<sub>2</sub>-EOR market in Kansas.

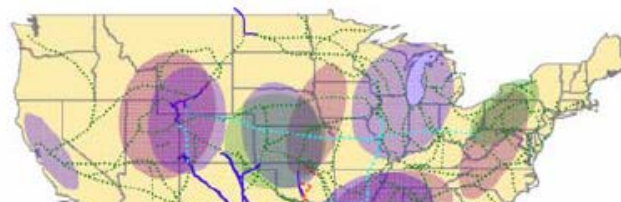
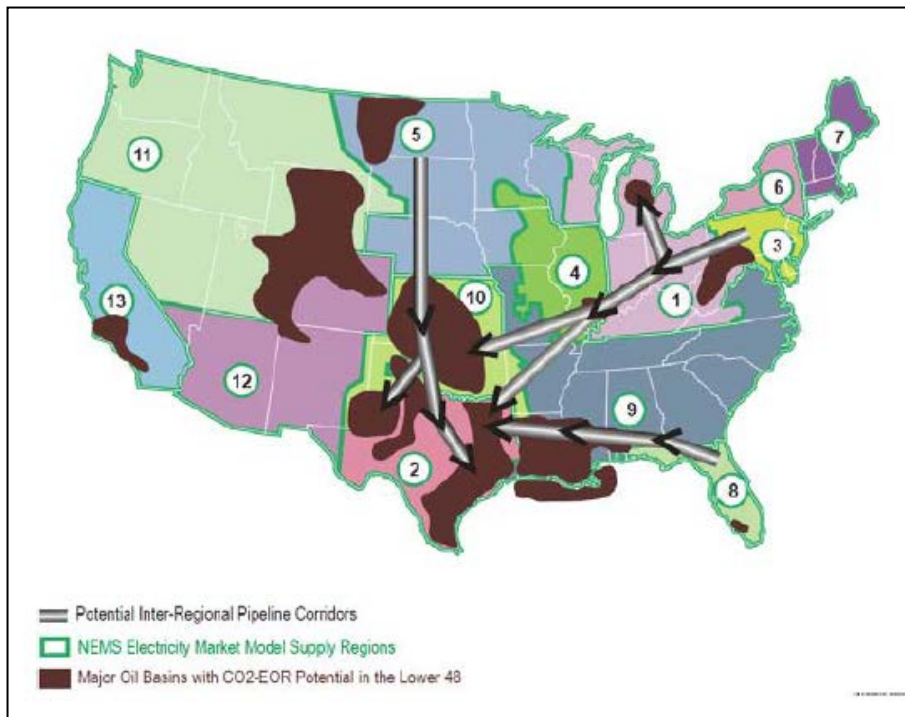
### Many companies are now involved in CCS demonstration



Source: SBC Energy Institute

© 2012 SBC Energy Institute. All Rights Reserved.

**Study published by Schlumberger indicating that CO<sub>2</sub> abatement potential for power plants using carbon storage in oil and gas reservoirs is reasonable.**



## APPENDIX F.

### **Improving efficiency and user-friendliness of the Java Applications**

#### **Proposal submitted to KU --**

*Integrated Real-Time Subsurface Analysis Web Applications*, W. Lynn Watney, P.I. , John Doveton, Co-I, John Victorine, Technician, Jennifer Raney, Technician, Budget Requested

#### **Abstract (1/2 page)**

Proof of concept (POC) funding is requested from KUIC to extend the utilization of the GEMINI (*Geo-Engineering through INternet Informatics*) computing platform to a unique and likely commercial application for personal computers, smartphones, and tablets that could be used by industry, government, education to access and query subsurface data in proximity to the user. Mobile GEMINI would access digital borehole data and provide analytical and imaging solutions based on location of user or locations of projects. The objectives of the POC activity includes reconfiguring multiple software modules for access through a single entry point, maximize features of the mobile devices to “mine” the digital borehole data in real-time, and use standard LAS (log ascii standard) 3.0 format to easily to save, update, share, and archive data and results.

To establish proof of concept, Mobile GEMINI will be tested using digital borehole data that is publically available on the Kansas Geological Survey website. This will set the stage for future integration with proprietary industry databases and other public information, with the latter having grown markedly in the past decade.

#### **Lay Description of Technology (1/2 page)**

The technology behind Mobile GEMINI closely resembles the Geographic Information Systems (GIS) that is frequently used on most mobile GPS devices and smartphones, e.g., Google Earth. Much like popular street mapping programs, mobile GEMINI would provide GIS-like investigation of the Earth’s subsurface using the primary and most abundant source of information available, borehole information records obtained in the search for water, oil, and gas or disposal and injection of material. Large and growing public data sites such as the Kansas Geological Survey have built large inventories of digital borehole data. The POC funding will tailor software to efficiently access, manage, and illustrate the subsurface information on the mobile devices giving the informed user the ability to view the subsurface using their location coordinates or these specified by the user. The information would be most useful to industry, regulators, educators, and others who wish to learn about the subsurface. The team has extensive experience in building Java web applications and interfacing with databases. A niche market for

this mobile software application is believed to be untapped and is an important next step for the development team.

John Victorine is the principal programmer who will build Mobile GEMINI. He will spend half his time in the coming year on this activity. Jennifer Raney will apply here expertise in GIS and database management and familiarity with the software and mobile computing technology to assist in the development, testing, and working with our industry partner with the goal to take the Mobile GEMINI to commercialization.

### **1) General Background**

Novel web-based petrophysical software developed by the Kansas Geological Survey (KGS) over the past 13 years is poised for commercialization across a broad marketplace. Existing programs will be enhanced to enterprise computing levels for use as a mobile application and extending its use far beyond its current implementation at the KGS. Rapid, consistent, quantitative analytical and visualization software are essential to understand the earth's subsurface and resolve challenges currently faced in managing natural resources, environmental characterization, and remediation practices, e.g., enhanced targeting of unconventional oil and gas resources via horizontal drilling, managing groundwater extraction, and storing CO<sub>2</sub> in the subsurface. We have coined the term, "Subsurface Information Systems (SIS)" to capture the parallel to GIS in our efforts to provide imaging of the subsurface that is comparable to the functionality and expectations of GIS (Doveton, 1994). Over the past decade, our petrophysical research has demonstrated the growing demand for use of the in-house petrophysical software and the developers now wish to elevate the software to commercial status. The POC funding would allow us to utilize our experience and observations to focus on creating a product with the most viable commercial application.. We believe that extending the application to mobile devices such as cell phones and tablets will fulfill the rapidly growing demand for intuitive, accessible, and informative means to independently investigate the subsurface.

The commercialization would proceed in parallel to research and development of new tools supported to date by federal agencies, industry partners, and the KGS. The existing petrophysical tools are freeware developed as part of the GEMINI (*Geo-Engineering through INternet Informatics*) project sponsored by the Department of Energy (*DE-FC26-00BC15310*) from 2000 to 2003. Of late, the programming effort has been reinforced with support from DE-FE0002056, "*Modeling CO<sub>2</sub> Sequestration... in South-Central Kansas*" from 2009 to present. The software, written in Java and using XML tables referenced by the software features 13 separate modules released as applets as described at <http://www.kgs.ku.edu/Gemini/Tools/Tools.html>. The Java applets provide user-friendly access, analysis, and visualization of single and multiple borehole measurements, and analyses obtained from rocks recovered from the boreholes. The software modules read and write output into standard, simply formatted ascii files (LAS 3.0, Heslop et al., 1999) that permit ease of use, data sharing, adding new information, and archiving. Several of the Java applets are accessed through ESRI mapping software to provide a familiar interface to

locate the boreholes and initiate the software. The applets are used many times a day by the public without issue, so the software has clearly been tested and is deemed very reliable and stable. October 2013 web hits on GEMINI tools totaled 990. Oracle database access in same period was 56,000.

## **2) Commercial Application of Research (Patent, Market size, comparisons with currently available products, similar applications or use)**

The technical capabilities of these unique subsurface analysis tools are diverse, and will therefore be applicable to multiple markets, both public and private. Generally, the tools are valuable to geologically-related industries interested in markets such as mining (e.g., oil & gas), geothermal, environmental, geotechnical, as well as for higher-level educational purposes. Due to the integrity and robustness of the database management system, the software sets an unprecedented standard for collecting and maintaining the geological and petrophysical data required to characterize and evaluate subsurface conditions. By integrating this information with highly intuitive, automated software, a broad spectrum of users will find value in the tools that were once constrained to only the highest level of industry.

Input parameters into the database will be maintained and updated using techniques exclusive the KGS combined with the former Log ASCII Standard (LAS) 2.0 format to achieve unparalleled dataset capabilities. The LAS 2.0 is rapidly becoming the industry standard to store and transmit digital geological information, but is only capable of storing a narrow spectrum of the types of subsurface data available today (Heslop, 1999; Qiang, 2005). The newly improved LAS 3.0 version incorporates an unforeseen amount of data into a single archive, which can analyzed to accomplish a wider set of goals. For example, the LAS 3.0 has already gained wide popularity in the Middle East, where the high functionality and detail of the data format enables its use in drilling horizontal wells (Naji, 2012). The KGS has a strong awareness of the burgeoning petroleum industry, and predicts that trend will continue to proliferate throughout the United States. By the end of last June, 247 active horizontal wells in Kansas were producing 260,000 barrels per month of oil (<http://www.kansascommerce.com/index.aspx?NID=520>). This recent surge of horizontal drilling pales in comparison to the more than 88,000 vertical oil and gas wells currently active or producing in Kansas, making it the 8<sup>th</sup> largest oil and natural gas producer in the United States. However, dispersed resources and high exploration costs have begun to make traditional drilling practices less viable for independent oil and gas operators in Kansas, which, according to the president of the Kansas Independent Oil & Gas Association, make up 92% of oil and 63% gas wells drilled in the state ([www.kioga.org](http://www.kioga.org))

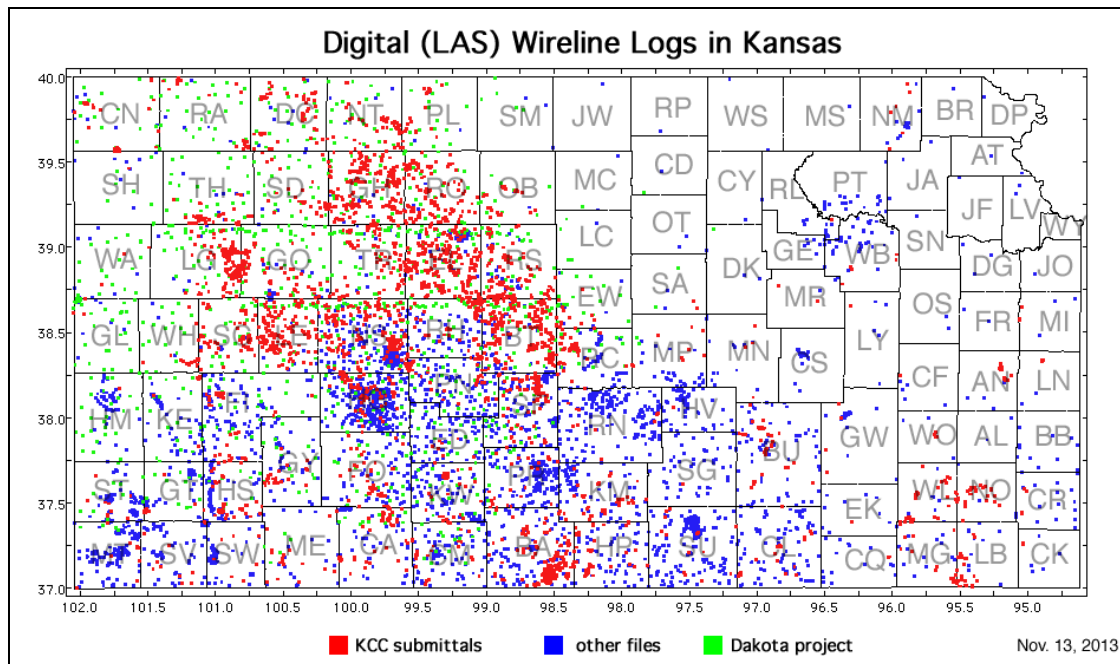
Advancements to the SIS developed by the KGS will provide smaller independents with proven, state-of-the-art technology necessary to carry out successful exploration activity, protect the environment, and continue to support local Kansas communities. While similar software tools are available, exorbitant licensing fees, expert-level training requirements, and immense computer processing capacity has made them practically unusable outside of the largest enterprises. For example, SubsurfaceViewer is a Java and XML based program from Germany

that can perform functions such as regional geospatial surveys, integrated well log analysis, and subsurface visualization that are analogous to the SIS tool being promoted by the KGS. However, commercial licenses to this software are expensive, and more importantly, are designed primarily for highly skilled professional geologists with strong backgrounds in computer modeling (<http://subsurfaceviewer.com/ssv/index.php?id=1#thema02>). Similar tools are offered by RockWare Inc. (<http://www.rockware.com/>), Paradigm Epos applications (<http://www.pdgm.com/Products/Epos>), and the industry-giant Schlumberger (<http://www.software.slb.com>). Performing even simple subsurface investigations with these tools is notoriously time and labor intensive and demands a high level of skill (Samberg, 2007). To move beyond this user base, the software must work intelligently with minimal complexity to extend its use to practicing geoscientists and technical teams, those who may have limited expertise in petrophysical analysis. The SIS tools will directly address these budgeting and operability issues to create something well suited to an untapped niche market, while simultaneously building a framework that optimizes interoperability to expand into larger industries in the future (Crangle, 2007).

### **Technology innovation**

**Industry demand and anticipated market** -- The mobile version of GEMINI would provide targeted integrated analysis obtaining similar outcomes as 3D modeling including high-resolution stratigraphic correlation, characterize hydrocarbon pay zones and pore systems by employing predictive modeling techniques, and using automated, quantitative color imaging to enhance visual tracking and characterization.

The growth and access to digital databases collected by state, federal, and international governments has opened vast amounts of subsurface borehole data inventories. Federal divisions such as Bureau of Ocean Energy Management (BOEM), Bureau of Land Management, and US Geological Survey have vast amounts of digital borehole. The POC grant will focus on the KGS borehole database. An intelligent mobile application such as Mobile GEMINI could allow user to “mine” the information (see map below).



The current generation of GEMINI software is solid working technology that works with the computing environment and data repository at the KGS. A U.S. Patent was proposed to KU for GEMINI in 2013 (File No. 05KU008L), but while there was interested, it not pursued. Funding has remained focused on tool refinement suited to meet obligations of our multi-million dollar external funding from DOE and serve users accessing the KGS website.

The total lines of GEMINI code, version 2.6, in October 2002 was 157,000 as part of 502 source files. Programming standards used to date include: 1) instituting policies and procedures of software development utilized in some sectors of the federal government, 2) Java Code Convention Document, 3) informal design and code review process, 4) Code Review Documentation, 5) periodic releases, and 6) Version Directories. The POC funding would bring the modules under a single application so that it can easily be certified under current self-regulating policies pertaining malware attacks.

Endorsements of GEMINI modules have been received internationally and modules have been used in our research (e.g., Doveton et al., 2004, Watney et al., 2004, Victorine et al., 2005, Bhattacharya et al. 2008, Watney et al. 2008, Doveton, 1994).



saved in standard ascii file structure (LAS 3.0), a simple output file that can be used in high-end 3-D modeling software or in Excel spreadsheets.

#### **4) Description of project plan, including anticipate barriers and technical difficulties**

The project plan is described above under Milestones that take the POC grant through the 1-year of support. John Victorine is the programmer/technician who has worked at the KGS on GEMINI and the 2<sup>nd</sup> generation software for the past 13 years. He is efficient, a dedicated hard worker, focused on excellence in programming. He is a physicist by education and a programmer in his distinguished career in federal and state institutions. John routinely accurately scopes out his work. During the original GEMINI 3-year build, he also commissioned portions of the programming to a three-person team. He managed the various skill sets and schedules, and successfully integrating their work to meet our lofty contract objectives. John is always aware of feature creep and stays focused on overall objectives. His goal is success, which is clearly where we have gone in our extended collaboration. Jenn Raney brings new perspectives with her background in GIS, database management, and skillset and interest in mobile computing.

John will continue to be the key player in the commercial release of this software and support would similarly be sought – including maintenance, coordinating with the licensing company on upgrades and improvements based on user feedback. The bottom line is that he really wants to do this and see commercialization. We as a team are similarly committed to continue to explore petrophysical applications that will continue to improve the software.

#### **COMMERCIAL SUPPORT (1 PAGE)**

According to recent updates, Kansas is the 8<sup>th</sup> largest oil and gas producer in the country, and the petroleum industry provides 67,000 jobs in the state. However, unlike other states, the oil and gas industry is largely dominated by independent operators that manage just a cluster of wells in localized areas. This framework called for the development of a unified state Geological Survey to provide widespread access to subsurface data, and also explains the close interaction between the KGS with independent operators throughout Kansas.

Alternatively, recent advancements in drilling technology have raised public awareness and environmental concerns. Often, environmental consulting agencies must evaluate subsurface conditions to verify the protection of drinking water sources, formulate decisions for corrective action when contaminants are involved, and investigate any potential hazards such as seismic events. With these issues receiving more attention in the press, questions are on the rise as to what is known about the subsurface, and how the information can be shared. The tools provided by the KGS can be equally useful to these individuals from an environmental protection vantage point, just as they are to the opposing industry.

These are reasons why the KGS is strongly relied upon as resource for environmental research, resource exploration, and drilling ventures, and how it continues to support the needs of both

independents and commercial industry members. The KGS GEMINI tools currently receive consistent use from visitors, with almost 1000 client requests hitting the GEMINI website in the month of October alone. Furthermore, the number of requests sent to the Oracle database that houses all borehole information was over 56,000 in the same month. Direct correspondence with operators has provided positive feedback of the GEMINI programs, and indicates the growing demand and continued use of the software.

Commercial support for the proposed SIS tools is inherently built into the relationship of the KGS with the petroleum industry, as well as the regulatory framework of the data sharing required by Kansas law. Essentially, all new digital borehole data is legally required to be submitted to state regulatory agencies, and is then made publicly available after a given time period. Ultimately, these records are released to the KGS and integrated with the same database that runs the SIS tools. By definition, the KGS database will steadily grow and improve as operators drill and log wells with higher quality tools, and then submit their digital information as required by law. As the commercial industry expands, so too will the dataset by which the SIS tools operate, leading to better coverage, software performance, and accuracy of the analysis.